ONLINE
CONFERENCE
& SPECIAL
SYMPOSIA

AUGUST
29–31
2022

11th
MSAT

The 11th International Conference on Materials Science and Technology

Abstracts Book

Special Symposia

- Technology Frontiers in Well-Living
- Mega Trends in Future Mobility
- Materials Informatics: “Accelerating Materials Research using Artificial Intelligence”

www.mtec.or.th/msat-11

Co-organizers:

Supporters

Gold Sponsors

Exhibitor

DISCLAIMER

This book contains the abstracts of the papers presented at **The 11th International Conference on Materials Science and Technology (MSAT-11).** They reflect the authors' opinions and are published as received after revision by the authors.

The committee assumes no responsibility for the accuracy, completeness or usefulness of the disclosed information.

Unauthorized use might infringe on privately owned patents or publication rights. Please contact the individual author(s) for permission to reprint or make use of information from their papers.

Co-organizers:






Supporters


Gold Sponsors


Exhibitor

CONTENTS

PREFACE

Dear Colleagues,

On behalf of the Organizing Committee, I would like to welcome you all to the 11th International Conference on Materials Science and Technology (MSAT-11) be held during 29 – 31 August 2022 through a virtual conference because of the COVID-19 pandemic is still prevalent.

MSAT-11 be co-organized by the National Metal and Materials Technology Center (MTEC), the National Energy Technology Center (ENTEC), the Technology and Informatics Institute for Sustainability (TIIS), and the Rail and Modern Transports Research Center (RMT). The scope of this conference is to provide an overview of recent progress and R&D activities ranging from fundamental research to applied research in the fields of materials science, technology, and engineering. In this year's conference, the thematic field of "materials" includes the concepts in Biomedical and Devices, Ceramics, Design and Manufacturing, Energy, Environment, Metal, and Polymers. The series of MSAT could push forward research and development of materials science and its application by connecting scientists and experts through the disciplines at sessions and symposia such as Technology Frontiers in Well-Living, Mega Trends in Future Mobility and Materials Informatics: "Accelerating Materials Research using Artificial Intelligence"

Regarding the conference activities, we are honored to have 3 plenary and 44 invited lectures given by distinguished researchers around the world. The number of presentations received from Thailand and other countries is 80 presentations, including 49 oral research presentations from Japan, Germany, New Zealand, Singapore, Taiwan, Thailand, The Netherlands, United of Kingdom and USA.

Lastly, I would like to thank all of the sponsors who have contributed to the MSAT-11, without whom it would be difficult to organize a successful international conference. Their contributions are greatly appreciated.

Yours sincerely,

Dr. Julathep Kajornchaiyakul
Executive Director of MTEC
Chair of MSAT-11

COMMITTEES

Chair

Dr. Julathep Kajornchaiyakul	National Metal and Materials Technology Center

Vice Chair

Dr. Aree Thanaboonsombut	National Metal and Materials Technology Center
Dr. Kritsada Prapakorn	National Metal and Materials Technology Center
Ms. Siriwan Tantawechkit	National Metal and Materials Technology Center
Dr. Sumittra Charojrochkul	National Energy Technology Center

Scientific Committee

Dr. Asira Fuongfuchat	National Metal and Materials Technology Center
Mr. Bhanu Vetayanugul	National Metal and Materials Technology Center
Dr. Bralee Chayasombat	National Metal and Materials Technology Center
Asst. Prof. Dr. Chaiyasit Banjongprasert	Chiang Mai University
Dr. Chaiwut Gamonpilas	National Metal and Materials Technology Center
Dr. Chanchana Thanachayanont	National Metal and Materials Technology Center
Dr. Charusporn Mongkolkachit	National Metal and Materials Technology Center
Dr. Chayanoot Kositanont	National Metal and Materials Technology Center
Dr. Duangduen Atong	National Metal and Materials Technology Center
Asst. Prof. Dr. Dujreutai Pongkao Kashima	Chulalongkorn University
Assoc. Prof. Dr. Ekachai Chaichanasiri	Mahidol University
Dr. Ekkarut Viyanit	Rail and Modern Transports Research Center

Assoc. Prof. Dr. Jakrapong Kaewkhao	Nakhon Pathom Rajabhat University
Dr. Jintamai Suwanprateeb	National Metal and Materials Technology Center
Dr. Jitti Mungkalasiri	Technology and Informatics Institute for Sustainability
Dr. Kanit Soongprasit	National Metal and Materials Technology Center
Dr. Nirut Naksuk	National Metal and Materials Technology Center
Dr. Pacharapan Sonthithai	National Metal and Materials Technology Center
Dr. Panadda Sheppard	Rail and Modern Transports Research Center
Dr. Pasaree Laokijcharoen	National Metal and Materials Technology Center
Dr. Paweena Diloksumpan	National Metal and Materials Technology Center
Asst. Prof. Dr. Phromphong Pandee	King Mongkut's University of Technology Thonburi
Asst. Prof. Dr. Phornphop Naiyanetr	Mahidol University
Dr. Premrudee Kanchanapiya	National Metal and Materials Technology Center
Dr. Promsak Sa-nguanthammarong	National Metal and Materials Technology Center
Dr. Rathanakarn Sethayospongsa	National Metal and Materials Technology Center
Prof. Dr. Rattikorn Yimnirun	Vidyasirimedhi Institute of Science and Technology
Dr. Robert Molloy	Chiang Mai University
Dr. Samerkhae Jongthammanurak	National Metal and Materials Technology Center
Dr. Sedthawatt Sucharitpwatskul	National Metal and Materials Technology Center
Dr. Sinthu Chanthapan	Rail and Modern Transports Research Center
Asst. Prof. Dr. Sirirat Tubsungnoen Rattanachan	Suranaree University of Technology
Dr. Sitthisak Prasanphan	National Metal and Materials Technology Center
Dr. Somboon Otarawanna	National Metal and Materials Technology Center
Dr. Sorayot Chinkanjanarot	National Metal and Materials Technology Center

Dr. Sumittra Charojrochkul	National Energy Technology Center
Dr. Suparoek Henpraserttae	National Energy Technology Center
Dr. Surapich Loykulnant	National Metal and Materials Technology Center
Dr. Sutee Olarnrithinun	Rail and Modern Transports Research Center
Dr. Thanasat Sooksimuang	National Metal and Materials Technology Center
Prof. Dr. Thotsawat Sītawan	Sakon Nakhon Rajabhat University
Prof. Dr. Torranin Chairuangsri	Chiang Mai University
Ms. Umaporn Sanewirush	National Metal and Materials Technology Center
Dr. Ussadawut Patakham	National Metal and Materials Technology Center
Dr. Wanida Pongsaksawad	Rail and Modern Transports Research Center
Asst. Prof. Dr. Waraporn Piyawit	Suranaree University of Technology
Assoc. Prof. Dr. Wantanee Buggakupta	Chulalongkorn University
Dr. Witchuda Daud	National Metal and Materials Technology Center

TECHNICAL PROGRAM

Monday 29 August

09:00 - 09:15	15 min	Opening Ceremony		
09:15 - 09:55	40 min	PL-01 **3D Bioprinting: Technologies and Materials** Prof. dr. ir. Jos Malda, Ph.D *Head of Research at the Department of Orthopaedics, University Medical Center Utrecht, Utrecht, The Netherlands* *Appointment at the Department of Clinical Sciences, Faculty of Veterinary Medicine, Utrecht University*		
09:55 - 10:15	20 min	MC briefs		
Room		**Room 1**	**Room 2**	**Room 3**
Session		**Metal, Alloys and Intermetallic Compounds Session 1/2** (Corrosion and Non-corrosion)		**Biomedical Materials and Devices Session 1/2**
Session Chair(s)		Bhanu Vetayanugul, Dr. Phromphong Pandee		Dr. Paweena Diloksumpan, Dr. Nuttapol Risangud
10:15 - 10:30	15 min	MET-I-01 **Challenges in Aluminum Alloys for Elevated Temperature Applications** Assoc. Prof. Dr. Chaowalit Limmaneevichitr *King Mongkut's University of Technology Thonburi, Thailand*		
10:30 - 10:45	15 min			BIO-I-01 **Spatio-Temporal Control of 3D-Bioprinted Light Activated Hydrogels for Regenerative Medicine Applications** Assoc. Prof. Khoon Lim *University of Otago, Christchurch, New Zealand*
10:45 - 11:00	15 min	MET-I-02 **Current and Future of Research on Austempering Ductile Iron** Asst. Prof. Dr. Usanee Kitkamthorn *Suranaree University of Technology, Thailand*		
11:00 - 11:15	15 min			BIO-O-101 **Preparation and Physicochemical Properties of Soluble Starch/Na-AMPS Hydrogel for Wound Dressing** Kuntathee Chaimueng *Chiang Mai University, Thailand*
11:15 - 11:30	15 min	MET-O-127 **Study of Intergranular Corrosion in 617-Ni Alloy Using Electrochemical Technique** CANCELLED Noppakorn Phuraya *Mahidol University, Thailand*		BIO-O-075 **The Effects of Electropolishing Process Parameters on the Cobalt Chromium Surface Characteristics for Medical Device** Jitlada Sansatsadeekul *National Science and Technology Development Agency, Thailand*
11:30 - 11:45	15 min	MET-O-065 **Compact Field Exposure Test of Hot-Dip Galvanized Steel and Zn-Al-Mg Coated Steel with and without Organic Coating Under Tropical Climate** Pranpreeya Wangjina *Rail and Modern Transports Research Center, MTEC, Thailand*		BIO-O-087 **Finite Element Analysis of the Effects of Crown Design on Stent Recoil** Kavin Karunratanakul *National Science and Technology Development Agency, Thailand*
11:45 - 12:00	15 min	MET-O-060 **Railway Underfloor Chloride Deposition Rate Estimation from Atmospheric Corrosion Monitoring (ACM) Sensor and its Validation by ISO 16539 Accelerated Corrosion Test** Wanida Pongsaksawad *Rail and Modern Transports Research Center, MTEC, Thailand*		
12:00 - 13:00	60 min	Lunch Break		

Room		Room 1	Room 2	Room 3
Session		**Metal, Alloys and Intermetallic Compounds Session 2/2** (Corrosion and Non-corrosion)	**Computational Science & Engineering + Design & Manufacturing Session**	**Biomedical Materials and Devices Session 2/2**
Session Chair(s)		Dr. Sinthu Chanthapan	Dr. Somboon Otarawanna	Dr. Titinun Suannun
13:00 - 13:15	15 min	MET-O-041 **Effects of Multiple Repair Welds at Rail Head to Serviceability** Thiraphong Nakthong *King Mongkut's University of Technology Thonburi, Thailand*	COM-I-01 **Multi-Scale and Multi-Physics Modeling for Process-Structure-Property Relationships of Laser Powder-Based Additive Manufacturing** Asst.Prof. Patcharapit Promoppatum *King Mongkut's University of Technology Thonburi, Thailand*	BIO-I-02 **Metal Nanostructures Fabrication for Biomedical Application** Assoc. Prof. Benchaporn Lertanantawong, *Mahidol University, Thailand*
13:15 - 13:30	15 min	MET-O-098 **A Study for Influence of PWHT on Sensitization Microstructure of AISI 316Ti Stainless Steel Weld Joints** Jade Wongsakul *King Mongkut's University of Technology Thonburi, Thailand*		
13:30 - 13:45	15 min	MET-O-120 **Investigation of Surface Hardness and Roughness on Formability of Aluminum Alloy Sheet AA2024-T3 Subjected to the Shot Peening Process by Silica Shots** Jurarat Sawangpan *King Mongkut's University of Technology North Bangkok, Thailand*	COM-O-023 **Electricity and Resources Demand Long Term Forecast in Thailand by Using Polymath Software** CANCELLED Prachuab Peerapong *Bangkok Thonburi University, Thailand*	BIO-O-093 **Corrosion Fatigue Life of Magnetically Driven Components in Spinal Growth Rods in Artificial Cerebrospinal Fluid** Benjawan Saengwichian *Thailand Institute of Scientific and Technological Research, Thailand*
13:45 - 14:00	15 min	MET-O-028 **Effect of Heat Treatment and Equal Channel Angular Pressing on the Microstructure and Mechanical Properties of Al-Mg-Si Alloy with Erbium Addition** Mizuki Mikami *Chiang Mai University, Thailand*	COM-O-027 **Analysis of Rear Underrun Protective Device Using Real-Life Test and Finite Element Techniques** Narongrit Suebnunta *National Metal and Materials Technology Center, Thailand*	BIO-O-070 **The Optimized Design Mode of Exercise Bike for Rehabilitation after Suffering ICU Patients** Danu Prommin *National Metal and Materials Technology Center, Thailand*
14:00 - 14:15	15 min	MET-O-017 **Microstructure and Mechanical Properties of Sintered Fe-Cr-Mo-Si-C-(Ni) Alloys** Arisara Wanalerkngam *Suranaree University of Technology, Thailand*	DES-O-035 **Optimization Mechanical Angle Calculated for Gaylord Box Folding Machine in Industrial Scale by Solidworks** Banpot Meesa *Rajabhat Rajanagarindra University, Thailand*	
14:15 - 14:30	15 min	MET-O-034 **Mechanical Properties of Dual-Grained Cemented Tungsten Carbide** Chiraporn Auechalitanukul *King Mongkut's University of Technology Thonburi, Thailand*	DES-O-082 **Effects of Fused Deposition Process Parameters on Surface Quality and Mechanical Properties of 3D-Printed PLA Plastic Parts** Kittichai Sojiphan *Thai-German Graduate School of Engineering (TGGS), KMUTNB, Thailand*	
14:30 - 14:45	15 min		COM-O-113 **Fracture Prediction of Aluminum Alloy Sheet AA2024-T3 by Strain-Stress Based Failure Criteria** Jurarat Sawangpan *King Mongkut's University of Technology North Bangkok, Thailand*	
14:45 - 15:00	15 min			
15:00 - 15:15	15 min	MC briefs		
15:15 - 16:30	75 min	**Poster Session**		

Tuesday 30 August

09:00 - 09:40	40 min	PL-02 **RTRI's Initiatives in "Research 2025" for Addressing SDGs** Prof. Toru Miyauchi *Associate Director (International Affairs), Research and Development Promotion Division, Railway Technical Research Institute, Japan* **A Heavy Rainfall-Induced Disaster-Mitigation System for Railways Based on Precipitation Forecast Data** Mr. Takuya Urakoshi *Senior Researcher, Geology Laboratory, Disaster Prevention Technology Division, Railway Technical Research Institute, Japan*		
09:40 - 10:00	20 min	MC briefs		
Room		**Room 1**	**Room 2**	
Session		**Ceramics Session**	**Materials for Energy Session**	
Session Chair(s)		Dr. Charusporn Mongkolkachit, Dr. Sitthisak Prasanphan, Dr. Kanit Soongprasit, Dr. Khanthima Hemra	Dr. Thanya Phraewphiphat	
10:00 - 10:15	15 min	CER-I-01 **Efficacy of Biocompatible Phase Developed in Eggshell-Derived Porous Glass-Ceramic Orbital Implants** Assoc. Prof. Dr. Jiratchaya Ayawanna *Suranaree University of Technology, Thailand*	ENR-I-01 **Sulfur Tolerant Bimetallic Pd-Pt Catalysts for Aromatics Saturation of Diesel and O_2-Assisted H-FAME Production for Avoiding Sulfur Poisoning** Dr. Yuji Yoshimura *National Energy Technology Center, Thailand*	
10:15 - 10:30	15 min			
10:30 - 10:45	15 min	CER-I-02 **High-Entropy Titanate-Based Perovskite Oxides** Asst. Prof. Dr. Natthaphon Raengthon *Chulalongkorn University, Thailand*	ENR-O-049 **Exfoliated Graphite-Nickel Oxide Composite Electrode for Supercapacitor Application** Pyae Sone Soe *Sirindhorn International Institute of Technology, TU, Thailand*	
10:45 - 11:00	15 min		ENR-O-064 **Nitric Oxide Adsorption Diffuse Reflectance Fourier Transform Infrared Spectroscopy: A Complemantery Characterization for Hydrodearomatization Catalyst** Eumporn Buarod *National Energy Technology Center, Thailand*	
11:00 - 11:15	15 min	CER-O-013 **Study of Consistency and Density of Titanium Dioxide and Tungsten Trioxide Coatings on Conductive Glass from Dipping Process Affecting Light Absorption and Transmission** Kraiwut Rukkachat *Suranaree University of Technology, Thailand*	ENR-O-066 **Effect of Regenerative Braking System on State of Charge and Energy Consumption of Battery Electric Buses under Uncertainty Driving Condition** Sorawit Wanitanukul *King Mongkut's University of Technology Thonburi, Thailand*	
11:15 - 11:30	15 min	CER-O-025 **Geopolymers Derived From Waste Glass Powder, Fly Ash, and Calcium Carbide Residue** Chiraporn Auechalitanukul *King Mongkut's University of Technology Thonburi, Thailand*	ENR-O-072 **MnO_2/N-Doped Sugarcane Bagasse Derived Porous Carbon Nanocomposite as the Efficient Anode Material for Lithium-ion Battery** Krittaporn Pongpanyanate *Kasetsart University, Thailand*	
11:30 - 11:45	15 min	CER-O-044 **Improvement of Electrical Properties of ZnO Nanomaterials with Fe by Co-Precipitation Method** Pitchaporn Kingpho *Nakhon Ratchasima Rajabhat, Thailand*	ENR-O-124 **The Study of Zinc Oxide with Silicon Dots Thin Films Fabricated by Spin Coating Technique for Applying as Emitter Layer** Supanut Laohawiroj *Suranaree University of Technology, Thailand*	
11:45 - 12:00	15 min	CER-O-056 **Synthesis of Geopolymer/zeolite Composites from Lignite Fly Ash and Biomass Ash** Auekarn Chuwongwittaya *Chiang Mai University, Thailand*		

CANCELLED

Room		Room 1	Room 2	
Session		**Ceramics Session**		
12:00 - 12:15	15 min	CER-O-083 **Effect of Perlite on Properties of Porcelain Roofing Tiles Clay** Pasinee Siriprapa *Rajamangala University of Technology Lanna, Thailand*		
12:15 - 13:30	75 min	Lunch Break		
Session			**Materials Technology for Environment Session**	
Session Chair(s)			Umaporn Sanewirush, Dr. Premrudee Kanchanapiya, Dr. Samerkhae Jongthammanurak	
13:30 - 13:45	15 min		ENV-I-01 **Graphene Quantum Dot Based Nanomaterials for Environmental Sensing and Pollutant Photodegradation** Chair Prof. Ruey-An Doong *National Tsing Hua University, Taiwan*	
13:45 - 14:00	15 min			
14:00 - 14:15	15 min		ENV-I-02 **Development of Novel Water-Lean Solvent for CO_2 Capture Applications** Dr. Jak Tanthana *RTI International, USA*	
14:15 - 14:30	15 min			
14:30 - 14:45	15 min		ENV-I-03 **Flexible Thermoelectric Paper and its Thermoelectric Generator from Bacterial Cellulose/Ag_2Se Nanocomposites** Assoc. Prof. Supree Pinitsoontorn *Khon Kaen University, Thailand*	
14:45 - 15:00	15 min			
15:00 - 15:15	15 min		ENV-I-04 **An Electrochemical Journey from Screen-Printing to Additive Manufacturing (3D Printing): Towards Environment Protection** CANCELLED Prof. Craig E. Banks *Manchester Metropolitan University, United of Kingdom*	
15:15 - 15:30	15 min			
15:30 - 15:45	15 min		ENV-O-053 **Development Luminescence from Sm^{3+} of Barium Titanium Bismuth Borate Glass for Orange Emission Material Application** Thanapong Sareein *Rajamangala University of Technology Phra Nakhon , Thailand*	
15:45 - 16:00	15 min		ENV-O-110 **Synthesis and Characterizations of MXene ($Ti_3C_2T_x$) for Adsorption of an Enrofloxacin Antibiotic** Channarith Be *Sirindhorn International Institute of Technology, TU, Thailand*	
16:00 - 16:15	15 min		ENV-O-121 **Effects of Insulated Perlite Materials Addition on Lanna Traditional Clay Roof Tiles** Ampika Rachakom *Rajamangala University of Technology Lanna, Thailand*	
16:15 - 16:30	15 min		ENV-O-094 **Preliminaty Study of Perfluorooctanesulfonic Acid (PFOS) Removal by Electrocoagulation using Plackett-Burmann Design** Samerkhae Jongthammanurak *National Metal and Materials Technology Center, Thailand*	

Wednesday 31 August

Room		Room 1	Room 2	
Session		**Functional Polymeric Materials Session 1/2**	**Materials Testing and Reliability Session**	
Session Chair(s)		Dr. Witchuda Daud	Dr. Chanchana Thanachayanont, Asst. Prof. Dr. Waraporn Piyawit	
09:00 - 09:15	15 min	POL-I-01 **Polymeric Micellar Nanoreactors for Chemical Reactions in Water** Prof. Dr. Voravee P. Hoven *Chulalongkorn University, Thailand*	TES-I-01 **Nanoscale Stress Distribution and Crack Propagation in Rubber-Based Nano-Composites under Stretching** Prof. Hiroshi Jinnai *Tohoku University, Japan*	
09:15 - 09:30	15 min			
09:30 - 09:45	15 min	POL-O-024 **Polydiacetylene/Zn^{2+}/Zinc Oxide Nanocrystal for Volatile Organic Compound Sensing Applications** Kawinphob Phetnam *Chulalongkorn University, Thailand*	TES-I-02 **Probing Micro Nano and Atomic Structures of Material with Synchrotron X-Rays** Assoc. Prof. Dr. Supagorn Rugmai *Synchrotron Light Research Institute, Thailand*	
09:45 - 10:00	15 min	POL-O-063 **Development of The Organic Superhydrophobic Coating on Plastic Sheet for Food Packaging Applications** Pakjira Sirirutbunkajal *National Metal and Materials Technology Center, Thailand*		
10:00 - 10:15	15 min	POL-O-111 **Characterization of Nanocellulose Extracted from Used Papers** Weeradech Kiratitanavit *Prince of Songkla University, Thailand*	TES-O-010 **Optimizing Process Conditions and Ensuring End Product Requirements of Polymers with Rheological Analysis** Fabian Meyera [LMS] *ThermoScientific, Germany*	
10:15 - 10:30	15 min	POL-O-112 **Enhanced Mecchanical Properties and Improving Wetting Ability of Polypropylene/Cassava Pulp Composites** Natcha Prakymoramas *National Metal and Materials Technology Center, Thailand*	TES-O-054 **Synthesis and Characterization of Cesium Iodide Thin Film for Radiation Detection** Pariwat Limthanameteekul *Chulalongkorn University, Thailand*	
10:30 - 10:45	15 min	POL-O-097 **Study on Microperforated Biodegradable Films for Fresh Produce Packaging Applications** Charinee Winotapun *National Metal and Materials Technology Center, Thailand*	TES-O-011 **Introduction of JEOL Latest Ultrahigh Resolution FESEM and its capability of Chemical State Analysis** Tan Teck Siong [JEOL] *JEOL Asia Pte Ltd, Singapore*	
10:45 - 11:00	15 min		TES-O-050 **Characterization of 3D Printed-Part and AISI 316L Conventional Stainless Steel Pipe Jointed by TIG Welding** Niwat Kunawong *King Mongkut's University of Technology Thonburi, Thailand*	
11:00 - 11:15	15 min		TES-O-132 **Investigated Bond Strength of Welded Coatings using Scratch Test Technique** Hathaipat Koiprasert *Rail and Modern Transports Research Center, Thailand*	
11:15 - 11:30	15 min		TES-O-130 **Influence of Stabilization Heat Treatment on Sensitization Microstructure of ASTM A 312 TP316Ti Stainless Steel Welded Joints** Niwat Kunawong *King Mongkut's University of Technology Thonburi, Thailand*	
11:30 - 13:00	90 min	Lunch Break		

Room		Room 1		
Session		**Functional Polymeric Materials Session 2/2**		
Session Chair(s)		Dr. Pasaree Laokijcharoen, Dr. Promsak Sa-nguanthammarong		
13:00 - 13:15	15 min	POL-I-02 **Role of Chemistry in the Successful Development of Low Rolling Resistance Tires for Better Sustainability** Assoc. Prof. Dr. Kannika Sahakaro *Prince of Songkla University Pattani Campus, Thailand*		
13:15 - 13:30	15 min			
13:30 - 13:45	15 min	POL-O-129 **Improving Dispersion of Conductive Carbon Black in Natural Rubber Latex using Methyl Cellulose and Carboxymethyl Cellulose** Natsaporn Butsri *National Metal and Materials Technology Center, Thailand*		
13:45 - 14:00	15 min	POL-O-123 **Possibility Replacement of Epoxidized Natural Rubber in Acrylonitrile Butadiene Rubber Gasket** Karnda Sengloyluan *Prince of Songkla University, Thailand*		
14:00 - 14:15	15 min	POL-O-095 **Effect of Glucose as Pore Former on Physical and Morphological Properties of High Ammonia Natural Rubber Latex Film** Jedsada Rueangsen *Prince of Songkla University, Thailand*		
14:15 - 14:30	15 min	POL-O-078 **Development of an International Standard for Rubber Sheets for Livestock – Dairy Cattle – Specification** Chayapha Nimsuwan *National Metal and Materials Technology Center, Thailand*		
14:30 - 14:45	15 min			

LIST OF ORAL & POSTER PRESENTATIONS

PLENALY LECTURES

PL-01 **3D Bioprinting: Technologies and Materials**
Jos Malda
University Medical Center, Utrecht University, The Netherlands

PL-02 **RTRI's Initiatives in "Research 2025" for Addressing SDGs**
Toru Miyauchi
Research and Development Promotion Division, Railway Technical Research Institute, Japan

A Heavy Rainfall-Induced Disaster-Mitigation System for Railways Based on Precipitation Forecast Data
Takuya Urakoshi
Disaster Prevention Technology Division, Railway Technical Research Institute, Japan

BIOMEDICAL MATERIALS AND DEVICES

INVITED LECTURES

BIO-I-01 **Spatio-Temporal Control of 3D-Bioprinted Light Activated Hydrogels for Regenerative Medicine Applications**
Khoon Lim
University of Otago, Christchurch, New Zealand

BIO-I-02 **Metal Nanostructures Fabrication for Biomedical Application**
Benchaporn Lertanantawong,
Mahidol University, Thailand

ORAL PRESENTATIONS

BIO-O-070 **The Optimized Design Mode of Exercise Bike for Rehabilitation after Suffering ICU Patients**
Danu Prommin
National Metal and Materials Technology Center, Thailand

BIO-O-075 **The Effects of Electropolishing Process Parameters on the Cobalt Chromium Surface Characteristics for Medical Device**
Jitlada Sansatsadeekul
National Science and Technology Development Agency, Thailand

BIO-O-087 **Finite Element Analysis of the Effects of Crown Design on Stent Recoil**
Kavin Karunratanakul
National Science and Technology Development Agency, Thailand

BIO-O-093 **Corrosion Fatigue Life of Magnetically Driven Components in Spinal Growth Rods in Artificial Cerebrospinal Fluid**
Benjawan Saengwichian
Thailand Institute of Scientific and Technological Research, Thailand

BIO-O-101 **Preparation and Physicochemical Properties of Soluble Starch/Na-AMPS Hydrogel for Wound Dressing**
Kuntathee Chaimueng
Chiang Mai University, Thailand

POSTER PRESENTATIONS

BIO-P-020 **Heart Rate Monitor Prototype**
Kamonwan Thipprasert
Suranaree University of Technology, Thailand

BIO-P-090 **Bacterial Cellulose with Antimicrobial Properties From *Houttuynia cordata* Thunb. Powder Extract for Active Packaging**
Phimchanok Jaturapiree
Silpakorn University, Thailand

CERAMICS

INVITED LECTURES

CER-I-01 **Efficacy of Biocompatible Phase Developed in Eggshell-Derived Porous Glass-Ceramic Orbital Implants**
Jiratchaya Ayawanna
Suranaree University of Technology, Thailand

CER-I-02 **High-Entropy Titanate-Based Perovskite Oxides**
Natthaphon Raengthon
Chulalongkorn University, Thailand

ORAL PRESENTATIONS

CER-O-013 **Study of Consistency and Density of Titanium Dioxide and Tungsten Trioxide Coatings on Conductive Glass from Dipping Process Affecting Light Absorption and Transmission**
Kraiwut Rukkachat
Suranaree University of Technology, Thailand

CER-O-025 **Geopolymers Derived From Waste Glass Powder, Fly Ash, and Calcium Carbide Residue**
Chiraporn Auechalitanukul
King Mongkut's University of Technology Thonburi, Thailand

CER-O-044 **Improvement of Electrical Properties of ZnO Nanomaterials with Fe by Co-Precipitation Method**
CANCELLED
Pitchaporn Kingpho
Nakhon Ratchasima Rajabhat, Thailand

CER-O-056 **Synthesis of Geopolymer/zeolite Composites from Lignite Fly Ash and Biomass Ash**
Auekarn Chuwongwittaya
Chiang Mai University, Thailand

CER-O-083 **Effect of Perlite on Properties of Porcelain Roofing Tiles Clay**
Pasinee Siriprapa
Rajamangala University of Technology Lanna, Thailand

POSTER PRESENTATIONS

CER-P-030 **Synthesis and Characterization of MgF_2 Nanoparticles by Microwave Heating Method**
Warisara Suwandecha
Chulalongkorn University, Thailand

POSTER PRESENTATIONS

CER-P-031 **Utilization of Crude Glycerol in the Physical Properties of Expanded Foam Glasses**
Pat Sooksaen
Silpakorn University Sanam Chandra Palace Campus, Thailand

CER-P-032 **Synthesis and Characterization of Titanium-Doped Hydroxyapatite for Methylene Blue Dye Degradation**
Pimpitcha Bumrungsub
Chulalongkorn University, Thailand

CER-P-037 **Effects of Pottery Stone Feldspar and Quartz on Physical and Mechanical Properties of Porcelain Tableware**
Tamonwat Hiruncharta-Nan
Lampang Rajabhat University, Thailand

CER-P-043 **Effects of Curing Time on Physical Properties and Thermal Properties of Perlite-Based Composite**
Kattaliya Chaipisan
Chiang Mai University, Thailand

CER-P-061 **Diffuse Phase Transition and Electric Properties of Lead-Free $0.5Ba(Zr_{0.2}Ti_{0.8})O_3$-$0.5(Ba_{0.7}Ca_{0.3})TiO_3$ Ceramics by $Ba_{0.93}Ca_{0.04}La_{0.03}Sn_{0.1}Ti_{0.9}O_3$ Addition**
Nuttapon Pisitpipathsin
Rajamangala University of Technology Isan, Nakhon Ratchasima, Thailand

CER-P-104 **Effect of Firing Temperatures on Phase Structure and Electrical Properties of 0.9(BNT-BT)-0.1NT Ceramics with Synthesized via the Combustion Solid-State Technique**
Bhoowadol Thatawong
Naresuan University, Thailand

CER-P-106 **Effect of $(AlNb)^{4+}$ B-Sites Substitution on Phase Structure, Microstructure and Electrical Properties of $Bi_{0.47}Na_{0.47}Ba_{0.06}TiO_3$ Ceramics**
Wistsarut Chongsatan
Naresuan University, Thailand

CER-P-109 **Phase Formation, Microstructure and Electrical Properties of BST-BZN Ceramics Synthesized via the Solid-State Combustion Technique**
Widchaya Somsri
Naresuan University, Thailand

CER-P-131 **Study of Kinuta Glaez is Recycling Silica from Glass Beer Bottle**
Nattawut Ariyajinno
Loei Rajabhat University, Thailand

CER-P-133 **Synthesis of Zircon Pigments from Rice Husk Ash and Their Performance in Ceramic Glaze**
Niti Yongvanich
Silpakorn University, Thailand

COMPUTATIONAL SCIENCE & ENGINEERING

INVITED LECTURES

COM-I-01 **Multi-Scale and Multi-Physics Modeling for Process-Structure-Property Relationships of Laser Powder-Based Additive Manufacturing**
Patcharapit Promoppatum
King Mongkut's University of Technology Thonburi, Thailand

ORAL PRESENTATIONS

COM-O-023 **Electricity and Resources Demand Long Term Forecast in Thailand by Using Polymath Software** CANCELLED
Prachuab Peerapong
Bangkok Thonburi University, Thailand

COM-O-027 **Analysis of Rear Underrun Protective Device Using Real-Life Test and Finite Element Techniques**
Narongrit Suebnunta
National Metal and Materials Technology Center, Thailand

COM-O-113 **Fracture Prediction of Aluminum Alloy Sheet AA2024-T3 by Strain-Stress Based Failure Criteria**
Jurarat Sawangpan
King Mongkut's University of Technology North Bangkok, Thailand

POSTER PRESENTATIONS

COM-P-105 **3D Computational Fluid Dynamics (CFD) Analysis of a Solar Drying Room for Rubber Sheet Production and Experimental Validation** CANCELLED
Thipjak Na Lampang
National Metal and Materials Technology Center, Thailand

DESIGN & MANUFACTURING

ORAL PRESENTATIONS

DES-O-035 **Optimization Mechanical Angle Calculated for Gaylord Box Folding Machine in Industrial Scale by Solidworks**
Banpot Meesa
Rajabhat Rajanagarindra University, Thailand

DES-O-082 **Effects of Fused Deposition Process Parameters on Surface Quality and Mechanical Properties of 3D-Printed PLA Plastic Parts**
Kittichai Sojiphan
Thai-German Graduate School of Engineering (TGGS), KMUTNB, Thailand

MATERIALS FOR ENERGY

INVITED LECTURES

ENR-I-01 **Sulfur Tolerant Bimetallic Pd-Pt Catalysts for Aromatics Saturation of Diesel and O_2-Assisted H-FAME Production for Avoiding Sulfur Poisoning**
Yuji Yoshimura
National Energy Technology Center, Thailand

ORAL PRESENTATIONS

ENR-O-049 **Exfoliated Graphite-Nickel Oxide Composite Electrode for Supercapacitor Application**
Pyae Sone Soe
Sirindhorn International Institute of Technology, Thammasat University, Thailand

ENR-O-064 **Nitric Oxide Adsorption Diffuse Reflectance Fourier Transform Infrared Spectroscopy: A Complemantery Characterization for Hydrodearomatization Catalyst**
Eumporn Buarod
National Energy Technology Center, Thailand

ENR-O-066 **Effect of Regenerative Braking System on State of Charge and Energy Consumption of Battery Electric Buses under Uncertainty Driving Condition**
Sorawit Wanitanukul
King Mongkut's University of Technology Thonburi, Thailand

ENR-O-072 **MnO_2/N-Doped Sugarcane Bagasse Derived Porous Carbon Nanocomposite as the Efficient Anode Material for Lithium-Ion Battery**
Krittaporn Pongpanyanate
Kasetsart University, Thailand

ENR-O-124 **The Study of Zinc Oxide with Silicon Dots Thin Films Fabricated by Spin Coating Technique for Applying as Emitter Layer**
Supanut Laohawiroj
Suranaree University of Technology, Thailand

POSTER PRESENTATIONS

ENR-P-055 **Effect of Barium Iron Niobate Incorporation on Energy Storage Density, and Electrical Properties of Lead-Free Bismuth Sodium Titanate-Based Ceramics**
Pharatree Jaita
Chiang Mai University, Thailand

ENR-P-122 **Effect of Rapid Thermal Annealing Treatment on the Electrical Conductivity of Nanocrystalline Zinc Oxide Doped with Aluminum for Low Cost of Semiconductor Devices**
Peerawoot Rattanawichai
Suranaree University of Technology, Thailand

MATERIALS TECHNOLOGY FOR ENVIRONMENT

INVITED LECTURES

ENV-I-01 **Graphene Quantum Dot Based Nanomaterials for Environmental Sensing and Pollutant Photodegradation**
Ruey-An Doong
National Tsing Hua University, Taiwan

ENV-I-02 **Development of Novel Water-Lean Solvent for CO_2 Capture Applications**
Jak Tanthana
RTI International, USA

ENV-I-03 **Flexible Thermoelectric Paper and its Thermoelectric Generator from Bacterial Cellulose/Ag_2Se Nanocomposites**
Supree Pinitsoontorn
Khon Kaen University, Thailand

INVITED LECTURES

ENV-I-04 **An Electrochemical Journey from Screen-Printing to Additive Manufacturing (3D-Printing). Towards Environment Protection**
Craig E. Banks
Manchester Metropolitan University, United of Kingdom

ORAL PRESENTATIONS

ENV-O-053 **Development Luminescence from Sm^{3+} of Barium Titanium Bismuth Borate Glass for Orange Emission Material Application**
Thanapong Sareein
Rajamangala University of Technology Phra Nakhon, Thailand

ENV-O-094 **Preliminaty Study of Perfluorooctanesulfonic Acid (PFOS) Removal by Electrocoagulation using Plackett-Burmann Design**
Samerkhae Jongthammanurak
National Metal and Materials Technology Center, Thailand

ENV-O-110 **Synthesis and Characterizations of MXene ($Ti_3C_2T_x$) for Adsorption of an Enrofloxacin Antibiotic**
Channarith Be
Sirindhorn International Institute of Technology, Thammasat University, Thailand

ENV-O-121 **Effects of Insulated Perlite Materials Addition on Lanna Traditional Clay Roof Tiles**
Ampika Rachakom
Rajamangala University of Technology Lanna, Thailand

POSTER PRESENTATIONS

ENV-P-015 **The Behavior of Bismuth Oxide on Tellurite Borate Oxide Based Glass System for Ionizing Radiation Shielding**
Sunantasak Ravangvong
Phetchaburi Rajabhat University, Thailand

ENV-P-018 **Optical Properties Improvement of Steel Slag Glass and their Ionizing Radiation and Neutron Shielding Properties**
Kittisak Sriwongsa
Silpakorn University, Thailand

ENV-P-019 **The Effect of Nb_2O_3 for Gamma Rays, Fast and Thermal Neutrons Shielding on B_2O_3-TeO_2 Based Glasses**
Kittisak Sriwongsa
Silpakorn University, Thailand

ENV-P-051 **Characterization of Rubber Foam Added with Activated Carbon and Titanium Dioxide for Adsorption of White Rice Starch in Wastewater**
Ratana Sananmuang
Naresuan University, Thailand

ENV-P-052 **Removal Efficacy of C4 Adsorbent for Telon Yellow A3R Dye and Its Kinetic of Reactions**
Ratana Sananmuang
Naresuan University, Thailand

ENV-P-080 **Dye Removal from the Fabric Dyeing Process Wastewater by Municipal Solid Waste Fly Ash Blended with Nano-TiO_2**
Yongthanat Bunroong
Phranakhon Rajabhat University, Thailand

POSTER PRESENTATIONS

ENV-P-086 **Development of Nano-TiO_2 Coated Koh Kret Pottery Surface for Dye Removal from the Dyeing Process Wastewater by the Photocatalytic**
Kanthanat Chullasupya
Phranakhon Rajabhat University, Thailand

ENV-P-103 **Degradation of Natural Rubber and Tire Sidewall under Thermophilic Aerobic Conditions**
Chomnutcha Boonmee
National Metal and Materials Technology Center, Thailand

METAL, ALLOYS AND INTERMETALLIC COMPOUNDS

INVITED LECTURES

MET-I-01 **Challenges in Aluminum Alloys for Elevated Temperature Applications**
Chaowalit Limmaneevichitr
King Mongkut's University of Technology Thonburi, Thailand

MET-I-02 **Current and Future of Research on Austempering Ductile Iron**
Usanee Kitkamthorn
Suranaree University of Technology, Thailand

ORAL PRESENTATIONS

MET-O-017 **Microstructure and Mechanical Properties of Sintered Fe-Cr-Mo-Si-C-(Ni) Alloys**
Arisara Wanalerkngam
Suranaree University of Technology, Thailand

MET-O-028 **Effect of Heat Treatment and Equal Channel Angular Pressing on the Microstructure and Mechanical Properties of Al-Mg-Si Alloy with Erbium Addition**
Mizuki Mikami
Chiang Mai University, Thailand

MET-O-034 **Mechanical Properties of Dual-Grained Cemented Tungsten Carbide**
Chiraporn Auechalitanukul
King Mongkut's University of Technology Thonburi, Thailand

MET-O-041 **Effects of Multiple Repair Welds at Rail Head to Serviceability**
Thiraphong Nakthong
King Mongkut's University of Technology Thonburi, Thailand

MET-O-060 **Railway Underfloor Chloride Deposition Rate Estimation from Atmospheric Corrosion Monitoring (ACM) Sensor and its Validation by ISO 16539 Accelerated Corrosion Test**
Wanida Pongsaksawad
Rail and Modern Transports Research Center, Thailand

MET-O-065 **Compact Field Exposure Test of Hot-Dip Galvanized Steel and Zn-Al-Mg Coated Steel with and without Organic Coating Under Tropical Climate**
Pranpreeya Wangjina
Rail and Modern Transports Research Center, Thailand

MET-O-098 **A Study for Influence of PWHT on Sensitization Microstructure of AISI 316Ti Stainless Steel Weld Joints**
Jade Wongsakul
King Mongkut's University of Technology Thonburi, Thailand

ORAL PRESENTATIONS

MET-O-120 **Investigation of Surface Hardness and Roughness on Formability of Aluminum Alloy Sheet AA2024-T3 Subjected to the Shot Peening Process by Silica Shots**
Jurarat Sawangpan
King Mongkut's University of Technology North Bangkok, Thailand

MET-O-127 **Study of Intergranular Corrosion in 617-Ni Alloy Using Electrochemical Technique**
CANCELLED
Noppakorn Phuraya
Mahidol University, Thailand

POSTER PRESENTATIONS

MET-P-062 **Zn-Al Coatings Produced by Low Velocity Oxy-Fuel Technique with Different Powder Feed Rates**
Duangrada Yuttakamthon
Chiang Mai University, Thailand

MET-P-068 **Identification of Martensitic Structures in Plastically Deformed 316L Stainless Steel by AFM/MFM**
Pimsiri Rattanasopa
Suranaree University of Technology, Thailand

MET-P-092 **Thermal Stability of Al-Ni-Sc Alloy Fabricated by Equal Channel Angular Pressing**
Sirinapa Shuecamlue
Chiang Mai University, Thailand

FUNCTIONAL POLYMERIC MATERIALS

INVITED LECTURES

POL-I-01 **Polymeric Micellar Nanoreactors for Chemical Reactions in Water**
Voravee P. Hoven
Chulalongkorn University, Thailand

POL-I-02 **Role of Chemistry in the Successful Development of Low Rolling Resistance Tires for Better Sustainability**
Kannika Sahakaro
Prince of Songkla University Pattani Campus, Thailand

ORAL PRESENTATIONS

POL-O-024 **Polydiacetylene/Zn^{2+}/Zinc Oxide Nanocrystal for Volatile Organic Compound Sensing Applications**
Kawinphob Phetnam
Chulalongkorn University, Thailand

POL-O-063 **Development of the Organic Superhydrophobic Coating on Plastic Sheet for Food Packaging Applications**
Pakjira Sirirutbunkajal
National Metal and Materials Technology Center, Thailand

POL-O-078 **Development of an International Standard for Rubber Sheets for Livestock – Dairy Cattle – Specification**
Chayapha Nimsuwan
National Metal and Materials Technology Center, Thailand

ORAL PRESENTATIONS

POL-O-095 **Effect of Glucose as Pore Former on Physical and Morphological Properties of High Ammonia Natural Rubber Latex Film**
Jedsada Rueangsen
Prince of Songkla University, Thailand

POL-O-097 **Study on Microperforated Biodegradable Films for Fresh Produce Packaging Applications**
Charinee Winotapun
National Metal and Materials Technology Center, Thailand

POL-O-111 **Characterization of Nanocellulose Extracted from Used Papers**
Weeradech Kiratitanavit
Prince of Songkla University, Thailand

POL-O-112 **Enhanced Mecchanical Properties and Improving Wetting Ability of Polypropylene/Cassava Pulp Composites**
Natcha Prakymoramas
National Metal and Materials Technology Center, Thailand

POL-O-123 **Possibility Replacement of Epoxidized Natural Rubber in Acrylonitrile Butadiene Rubber Gasket**
Karnda Sengloyluan
Prince of Songkla University, Thailand

POL-O-129 **Improving Dispersion of Conductive Carbon Black in Natural Rubber Latex using Methyl Cellulose and Carboxymethyl Cellulose**
Natsaporn Butsri
National Metal and Materials Technology Center, Thailand

POSTER PRESENTATIONS

POL-P-071 **Fabrication of Thermo-Responsive Rhodamine Derivatives/Polymer Blend Films for Optical Temperature Indicator Label Applications**
Sanguansak Sriphalang
Chiang Mai University, Thailand

POL-P-076 **Development of a National Standard for Tactile Rubber Flooring for Visually Impaired Persons**
Chayapha Nimsuwan
National Metal and Materials Technology Center, Thailand

POL-P-079 **Assessment of Fresh Natural Rubber Latex Putrefaction Using Resazurin Reduction Test**
Chayanoot Kositanont
National Metal and Materials Technology Center, Thailand

POL-P-084 **Effect of Crosslinking Agents on Properties and Oil-painting Cleaning Efficacy of Poly(vinyl alcohol) Gel**
Watsachon Leksomboon
Chulalongkorn University, Thailand

MATERIALS TESTING AND RELIABILITY

INVITED LECTURES

TES-I-01 **Nanoscale Stress Distribution and Crack Propagation in Rubber-Based Nano-Composites under Stretching**
Hiroshi Jinnai
Tohoku University, Japan

TES-I-02 **Probing Micro Nano and Atomic Structures of Material with Synchrotron X-Rays**
Supagorn Rugmai
Synchrotron Light Research Institute, Thailand

ORAL PRESENTATIONS

TES-O-010 **Optimizing Process Conditions and Ensuring End Product Requirements of Polymers with Rheological Analysis**
Fabian Meyer
ThermoScientific, Germany

TES-O-011 **Introduction of JEOL Latest Ultrahigh Resolution FESEM and Its Capability of Chemical State Analysis**
Tan Teck Siong
JEOL Asia Pte Ltd, Singapore

TES-O-050 **Characterization of 3D Printed-Part and AISI 316L Conventional Stainless Steel Pipe Jointed by TIG Welding**
Niwat Kunawong
King Mongkut's University of Technology Thonburi, Thailand

TES-O-054 **Synthesis and Characterization of Cesium Iodide Thin Film for Radiation Detection**
Pariwat Limthanameteekul
Chulalongkorn University, Thailand

TES-O-130 **Influence of Stabilization Heat Treatment on Sensitization Microstructure of ASTM A 312 TP316Ti Stainless Steel Welded Joints**
Niwat Kunawong
King Mongkut's University of Technology Thonburi, Thailand

TES-O-132 **Investigated Bond Strength of Welded Coatings using Scratch Test Technique**
Hathaipat Koiprasert
Rail and Modern Transports Research Center, Thailand

PLENALY LECTURES

PL-01

3D Bioprinting: Technologies and Materials

Prof. dr. ir. Jos Malda, Ph.D
Head of Research at the Department of Orthopaedics, University Medical Center Utrecht, Utrecht, The Netherlands
Appointment at the Department of Clinical Sciences, Faculty of Veterinary Medicine, Utrecht University, The Netherlands

Three-dimensional (3D) printing is already routinely used in the clinic, e.g. for pre-operative models or intra-operative guides. However, this does not involve the generation of living 3D structures, i.e., biofabrication of tissues and organs. This automated approach holds potential to advance the field of regenerative medicine as outer shapes can be personalised and organised constructs can be produced when printing with multiple bio-inks. Recent developments have now resulted in the availability of a plethora of bioinks, new printing approaches, and the technological advancement of established techniques. Nevertheless, mimicking the functional properties of the tissues and clinical translation of the technology are two important remaining challenges. In order to achieve this, we urge that the field now shifts its focus from materials and technologies towards the biological development of the resulting constructs. Moreover, there is an urgent need for more specialized production facilities to move this technology towards the patient.

PL-02

RTRI's Initiatives in "Research 2025" for Addressing SDGs

Toru Miyauchi
Research and Development Promotion Division,
Railway Technical Research Institute, Japan

The Sustainable Development Goals (SDGs) were adopted by the United Nations in 2025 as a universal call to action to end poverty, protect the planet, and ensure that by 2030 all people enjoy peace and prosperity.
The Railway Technical Research Institute (RTRI) will be communicating how its research and development activities are contributing to the achievement of the SDGs through its periodicals and website.

A Heavy Rainfall-Induced Disaster-Mitigation System for Railways Based on Precipitation Forecast Data

Takuya Urakoshi
Disaster Prevention Technology Division, Railway Technical Research Institute, Japan

Natural disasters, excluding earthquakes, on railways in Japan has been decreasing to less than 1,000 times a year with effective measures. Train operation control regulation under rain is one of the measures, and it requires a train operation commander to order train drivers to stop trains if the amount of precipitation exceeds predefined threshold. Remained issues of this regulation are preventing detection omission of localized heavy rainfall and optimization of the stopping position of trains.
To solve the remained issues and to improve railway operational safety, a prototype system to mitigate disasters due to heavy rain has been newly developed. This system conducts following four analyses: (1) calculation of rainfall indices using precipitation forecast data from a third-party provider, (2) runoff and inundation analysis, (3) large-scale landslide analysis, and (4) train operation analysis to prevent trains from approaching hazardous area. This system is currently undergoing improvement for practical use.

BIOMEDICAL MATERIALS AND DEVICES

BIO-I-01

Spatio-Temporal Control of 3D-Bioprinted Light Activated Hydrogels for Regenerative Medicine Applications

Khoon S. Lim[1]

[1]*Light Activated Biomaterials Research Group, Department of Orthopaedic Surgery and MusculoskeletalMedicine, University of Otago, New Zealand*

Keywords: Hydrogel, 3D bioprinting, photopolymerization, tissue engineering

Engineering multi-scalar vascular network is the key to fabricate functional tissues/organs. Although current bioprinting approaches have demonstrated promise in recapitulating the macro-scale (100-1000µm) regions of vascular network, spatial-patterning of the microscale (5-10µm) aspects remains an unmet challenge [1]. Microscale vasculogenesis, which is typically driven through cell-directed capillary-like network formation, requires a cell-permissive environment, typically provided by hydrogels exhibiting low-stiffness properties. This is however problematic as current low-stiffness bioink formulations inherently possess low viscosity, which is not compatible with most biofabrication approaches [2]. Therefore, the aim of this study is to develop vascular bioinks that simultaneously allow spatial patterning of macroscale vessels, as well as capillary-like vessel formation. Physicochemical (mass-loss) and mechanical (compressive modulus) properties were screened in allylated-gelatin (Gel-AGE, 3-5wt%) hydrogels (Ø5mm, 1mm height), photo-polymerised (5.4 kJ/cm2) with initiators ruthenium (0.2-1mM) and sodium persulfate (5-10mM). Thiolated crosslinkers used were dithiothreitol (DTT) or 8-arm thiol- functionalized poly(ethylene glycol) (PEG-8-SH). Rheological properties were measured and bioinks were directly printed through extrusion-based bioprinting (Bioscaffolder, Sys+Eng, 19-23G, speed 300-700 mms-1). Cell viability (Live/Dead®), capillary formation and macroscale vessel lining (CD31/F-actin) were investigated in a co-culture of human umbilical cord endothelial cells ($5x10^6$mL-1) and mesenchymal stromal cells (1x106mL- 1), after 7-14 days culture in endothelial growth media. Gel-AGE hydrogels of low stiffness (5-20kPa) were tailorable through crosslinker size and concentration. Rheological assessment revealed favorable viscosity (3-4Pa·s) and shear-thinning behavior for extrusion-based bioprinting. High cell viability (80-90%) and subsequent capillary-like networks were obtained within the bioprinted constructs. Moreover, macroscale channels were successfully included in engineered constructs and long-term shape stability was observed. Thiol-ene clickable bioinks allowed a wide window of physicochemical properties and provided flexibility in flow properties for various biofabrication methods. This was successfully leveraged towards vasculogenesis, demonstrating that thiol- ene bioinks hold great potential for micro- and macroscale vasculogenesis for tissue engineering.

References

1.Kolesky D et al. PNAS. 2016;113(12). 2. Datta P et al. Acta Biomater. 2017;15(51). 3. Bertlein S et.al. AdvMater. 2017;29(44)

BIO-I-02

Metal Nanostructures Fabrication for Biomedical Application

Benchaporn Lertanantawong
Mahidol University, Thailand

Nanobiosensors are an attractive approach in biomedical application in order to develop assays, diagnostic platforms and devices. We aim to create point of care testing that can be applied with clinical samples and field used. Nanomaterials such as gold nanoparticles and silica-dye nanoparticles have been prepared in our group to use as the label or signaling elements in order to enhance sensitivity of the sensors. In the other area of interest, we fabricate new biosensors materials such as gold nanostructure coated light-weight flexible substrate, colloidal semiconductor nanomaterials, quantum dots and liquid metal gallium andits nanoparticles, gallium oxyhydroxide (GaOOH). In this talk, the fabrication of these nanostructure materials and their application will be presented.

References:

1. Lertanantawong B, J. Riches, O'Mullane A, Room temperature electrochemical synthesis of crystalline GaOOH nanoparticles from expanding liquid metals. Langmuir. 2018, 34 (26), 7604-7611.
2. Lertanantawong B, Lertsathitphong P, O'Mullane A, Chemical reactivity of Ga based liquidmetals with redox active species and its influence on electrochemical processes. Electrochem. Comm. 2018;93;15-19.
3. Thanyarat Chaibun, Jiratchaya Puenpa, Tatchanun Ngamdee, Nimaradee Boonapatcharoen, Pornpat Athamanolap, Anthony Peter O'Mullane, Sompong Vongpunsawad, Yong Poovorawan, Lee Su Yin, Benchaporn Lertanantawong*, Rapid Electrochemical Detection of Coronavirus SARS-CoV-2 (2020), Nature Communication, 12,802 (2021).
4. Cheryl S.Y. Yeap, Thanyarat Chaibun, Su Yin Lee, Bin Zhao, Yuan Jan, Chan La-o-vorakiat, Werasak Surareungchai, Shiping Song and Benchaporn Lertanantawong*, Ultrasensitive pathogen detection with a rolling circle amplification-empowered multiplex electrochemicalDNA sensor, Chemical Communications, 2021,57, 12155-12158.
5. Tatchanun Ngamdee; Su Yin Lee; Sompong Vongpunsawad; Yong Poovorawan; WerasakSurareungchai; Benchaporn Lertanantawong*, (2020), Target Induced-DNA Strand Displacement Reaction Using Gold Nanoparticle Labeling for Hepatitis E Virus Detection, Analytica Chimica Acta, Volume 1134, Pages 10-17.
6. Pringkasemchai, A., Hoshyargar, F. , Lertanantawong, B*. and O'Mullane, A. P. (2019),Lightweight ITO Electrodes Decorated with Gold Nanostructures for Electrochemical Applications. Electroanalysis (2019) Volume 31, Issue 11, pages 2095 2102. doi:10.1002/elan.201900152
7. B. Lertanantawong, F. Hoshyargar and A. P. O'Mullane, Directing nanostructure formationof gold via the in situ under potential deposition of a secondary metal for the detection of nitrite ions, 2018, ChemElectroChem, Volume 5, Issue 6, Pages 911-916.

BIO-O-070

The Optimized Design Mode of Exercise Bike for Rehabilitation after Suffering ICU Patients

Ornin Srihakulung[a], Parinya Junhunee[a], Duanggamon Vorakasemsak[a], Noppawan Charususin[b], Danu Prommin[a,*]

[a] Biofunctional Materials and Devices Research Group (BMDRG), National Metal and Materials Technology Center (MTEC), Pathumthani, 12120, Thailand

[b] Department of Physical Therapy, Faculty of Allied Health Sciences, Thammasat University, Pathumthani, 12120, Thailand

* danup@mtec.or.th

Keywords: Atrophy, Muscular dystrophy, Exercise bike, Rehabilitation

Background: Mobility problems commonly become muscle atrophy due to lack of movement or exercise for a long time. The exercise program for the muscle atrophy depends on various factors. One of them is the type of exercise. From some studies, the routine care with in-bed cycling for ICU patients is feasible and safe.

Objective: To investigate three different movement modes of the exercise bike that provided support to relevant muscles.

Materials and Methods: Two participant's movements were recorded by using an eight-infrared camera. Tracking was set at a frame rate of 50 Hz with the 3D position of 36 reflective markers. For the testing position, the participant's lower back leaned on the back cushion of a hospital bed. Two feet were placed on two pedals of the exercise bike. They were cycling with three different modes of exercise bike. There were mode A, two speeds were set at 15 and 35 rpm; mode B, the participants cycled the bike until reaching the set speed at 35 rpm. If participants cycled at a higher speed, the motor can be damped to the set speed; mode C, the participants cycled a bike at 35 rpm, then the clutch provided the friction with 50% from participant speed.

Results and Discussion: The VL muscle of both samples was the most active. Sample 1 utilized the VM as the maximal muscle, which worked in tandem with the VL muscle according to the simulation. Contrarily, sample 2 applied the VM muscles with SM. The EMG comparison results between the 5 seconds time interval with three muscle activation. At a mode of 15 rpm, muscle activation of the VL, SOL, and RF muscles exhibited a single peak revealing only one rotation of the pedal. Contrarily, as the higher speed as 35 rpm of mode A, B, and C, the movement of the pedal took place approximately 3 cycles with a similar amplitude of muscle activation. Preliminary, the speed of the ride directly affected peak muscle activation. The VM for sample 1 was the main muscle, unlike the VL for sample 2, used for cycling. Both samples used different muscles during the same movement and mode C, for pushing the force during the cycling, the muscle activation shifted in different degrees.

Conclusion: Three main results showed that in mode A, the motor drove the legs through the machine speed which assisted patient muscle activation with the frequency of the amplitude following the configured speed; second, for mode A with the higher speed, the muscle activated faster and a little higher similar to mode B with 35 rpm; and for mode C, the patient was required to push more force to drive the motor causing the muscle activation to shift to a different sequence (out of phase), and some muscles, such as VM, were obliged to work harder. Finally, for the same movement and same speed both lay down and cycling in the same machine, each of the samples utilized a different muscle group for biking in one cycle.

BIO-O-075

The Effects of Electropolishing Process Parameters on the Cobalt Chromium Surface Characteristics for Medical Device

Jitlada Sansatsadeekul[a,*], Kharittha Joonlapak[a], Kavin Karunratanakul[a], Sedthawatt Sucharitpwatskul[b], Kriskrai Sitthiseripratip[a], Sarocha Kamolrungsriporn[a], Pisist Kumnorkaew[c], Anusit Kaewprajak[c]

[a]*Assistive Technology and Medical Devices Research Center (A-MED), National Science and Technology Development Agency (NSTDA), Khlong Nueng, Khlong Luang, Pathum Thani 12120, Thailand*

[b]*National Metal and Materials Technology Center (MTEC), National Science and Technology Development Agency (NSTDA), Khlong Nueng, Khlong Luang, Pathum Thani 12120, Thailand*

[c]*National Nanotechnology Center, National Science and Technology Development Agency (NSTDA), Khlong Nueng, Khlong Luang, Pathum Thani 12120, Thailand*

*jitlada.san@nstda.or.th

Keywords: ELECTROPOLISHING, SURFACE, MEDICAL DEVICE

When blood flow to the heart is decreasing due to plaque builds up on the inner walls of coronary arteries, coronary stents are used to help widen the clogged artery and restore blood flow. Surface roughness of stent is one of the important parameters to ensure blood and tissue compatibility. A Smooth surface can help reduce restenosis. Electropolishing process is an effective way to remove roughness due to laser cutting process and improve surface smoothness. In the present work, the electropolishing process on cobalt chromium (CoCr) metal surface was developed. CoCr tubes are used as raw materials for the manufacturing of stents due to its biocompatibility, good mechanical strength, and an ability to be easily seen under Fluoroscopy or x-ray images. Therefore, the aim of this work is focused on the study of surface treatment factors of CoCr tube by electropolishing process. The workpiece (anode) material was the CoCr tube which was hold with titanium wire. The cathode material under study was copper. The electrolyte was composed of sulfuric acid, phosphoric acid, hydrogen fluoride, glycerin, and deionized water. The purpose of this study is to determine optimal electric current parameters and time required for conducting electropolishing process from the perspective of changes of microgeometry of surface. The values of electric current (DC) were applied in the range of 0-2.0 amperes. The time was taken in the process at 0, 0.5, 1, 3 and 6 minutes, and the voltage source provides 22 volts. These parameters were adjusted in the electropolishing process to provide an electrochemical polishing method for CoCr tube surface with a smoothness equivalent to that of the commercial stent and suitable for application in the stent manufacturing process.

BIO-O-087

Finite Element Analysis of the Effects of Crown Design on Stent Recoil

Kavin Karunratanakul[a,*], Jitlada Sansatsadeekul[a], Sarocha Kamolrungsriporn[a], Sedthawatt Sucharitpwatskul[b], Kriskrai Sitthiseripratip[a], Kharittha Joonlapak[a], Muenpetch Muenkaew[c], Dilok Piyayotai[c]

[a]Assistive Technology and Medical Devices Research Center (A-MED), National Science and Technology Development Agency (NSTDA), Khlong Nueng, Khlong Luang, Pathum Thani 12120, Thailand

[b]National Metal and Materials Technology Center (MTEC), National Science and Technology Development Agency (NSTDA), Khlong Nueng, Khlong Luang, Pathum Thani 12120, Thailand

[c]Faculty of Medicine, Thammasat University, Khlong Nueng, Khlong Luang, Pathum Thani 12120, Thailand

*kavin.kar@nstda.or.th

Keywords: FINITE ELEMENT ANALYSIS, STENT DESIGN, MEDICAL DEVICE

Coronary stents are used to help widen the clogged artery and provide vessel wall scaffolding to restore blood flow. Acute stent recoil results in inadequate stent expansion and decreased final stent area leading to subsequent restenosis. The crown of the stent is an important part of the stent design that effect the ability of the stent to retain its shape. In this study, several parameters related to crown design including crown thickness, inner radius and crown angle are discussed. The 3-dimensional (3D) model of one stent ring was created. The parameters were varied from 0.08 to 0.12 mm for crown thickness, 0.04 to 0.08 mm for inner radius and -10.6 degree to 10.6 degree for crown angle. Other parameters such as strut thickness and strut length were kept constant. The linear hexahedral elements were assigned to the model. Convergent study was performed to ensure the sufficient element size. Material properties of cobalt chromium (CoCr) alloy obtained from manufacturer were assigned to all elements. Boundary conditions were applied to simulate stent crimping to diameter of 1 mm. Then, the stent was release and allow for elastic recoil. After that it was expanded to diameter of 2.75 mm. Finally, the stent was released again to recoil to final diameter. The recoil percentage was measured as the different between final diameter and expanded diameter. The final design that provides the smallest recoil was presented and discussed.

BIO-O-093

Corrosion Fatigue Life of Magnetically Driven Components in Spinal Growth Rods in Artificial Cerebrospinal Fluid

Benjawan Saengwichian[a,*], Edward. A. Charles[b], Philip. J. Hyde[b]

[a]*Thailand Institute of Scientific and Technological Research (TISTR), Pathum Thani, 12120, Thailand*

[b]*Newcastle University, Newcastle upon Tyne, NE1 7RU, UK*

*benjawan@tistr.or.th

Keywords: Cerebrospinal fluid, Intergranular corrosion fatigue, Magnetically controlled growth rods, Non-invasive treatment, Scoliosis

Magnetically controlled growing rods (MCGRs) are designed to treat early-onset scoliosis. The magnetically driven mechanism is encapsulated in MCGRs casings to serve non-invasive spine lengthening periodically until reaching skeletal maturity. However, premature failure of MCGRs related to corrosion, fatigue and wear *in vivo* has been observed. In this study, *in vitro* immersion and corrosion fatigue test setups were designed to simulate corrosion and fatigue of the driving components with couples of 440C stainless steel (SS) and Ti6Al4V in 37 °C artificial cerebrospinal fluid(ACSF). The 440C alloy was hardened and tempered at 200 and 500 °C to study the effect of heat treatment on intergranular corrosion (IGC). The S-N curves of tempered 440C rods in air and ACSF were determined so that the premature fracture could be predicted and more clearly understood.

After a 2-day soaking, incipient IGC formed on 440C was revealed. The results showed chromium ions released to 90 μg/L approximately after two months of immersion, exceeding the MHRA criterion. Despite lack of wear and corrosion indications on Ti6Al4V, Titanium was dissolved up to 6 μg/L. The fatigue test results suggest that 440C drive pins in 'dry' encapsulation are resistant to fatigue. On the other hand, the fatigue life at the corresponding load in 37 °C ACSF decreased 25 times, from 10 million cycles (2.6-year implantation) to 0.4 MC (1.3-month implantation). The fatigue crack propagated when it reached the threshold length with a stress intensity range (ΔK_{th}) of 6 - 9 MPa-$m^{1/2}$. It is recommended that the performance of MCGRs seals should be improved to prevent the ingress of body fluids. The likelihood of IGC *in vivo* can be avoided by using low-carbon alloys with appropriate heat treatment.

BIO-O-101

Preparation and Physicochemical Properties of Soluble Starch/Na-AMPS Hydrogel for Wound Dressing

Kuntathee Chaimueng[a], Amlika Rungrod[b], Waewploy Sukmongkolwongs[a], Runglawan Somsunan[b] *

[a]*Master's Degree Program in Chemistry, Department of Chemistry, Faculty of Science, Chiang Mai University, Chiang Mai, 50200, Thailand*

[b] *Department of Chemistry, Faculty of Science, Chiang Mai University, Chiang Mai,50200, Thailand*

E-mail: runglawan.s@cmu.ac.th

Keywords: Hydrogel, Na-AMPS, Soluble starch, Wound dressing

The soluble starch reinforced sodium salt of 2-acrylamido-2-methylpropane sulfonic acid (Na-AMPS) – based hydrogel was synthesized by UV-photo polymerization using 2-hydroxy-4′-(2-hydroxyethoxy)-2-methylpropiophenone as an initiator. The different concentrations of trimethylolpropane ethoxylate triacrylate (average M_n 575) crosslinker (0.05, 0.10, 0.15, 0.20 wt%) and soluble starch (1, 2, 3 %w/v) were studied. The results indicated that the synthesized hydrogels gave 97- 99 % gel fraction, which was not significantly different when varying the concentration of crosslinker and soluble starch. Furthermore, the swelling capacity was in the range of 9180 to 27600 %, depending on the concentration of crosslinker and soluble starch. For the mechanical property test, the percentage strain decreased with an increase of crosslinker concentrations, while Young's modulus increased. Considering the difference in soluble starch concentrations, the maximum percentage strain was found to be at 2 %w/v of the starch but it showed the minimum Young's modulus. The water vapour transmission rate (WVTR) was 1416-1608 g m^{-2} day^{-1} and an increasing crosslinker concentration resulted in a slight increase in WVTR. Moreover, WVTR showed similar results in all concentrations of soluble starch. As described above, the synthesized hydrogels show high gel fraction, and high swelling capacity, which can help an excess exudate absorption and good mechanical properties without easy rupture while moving. It also showed that WVTR value suitable for second-degree burn wounds. It could be concluded that the synthesized starch/Na-AMPS hydrogels in this work have the potential to be used as a wound dressing.

BIO-P-020

Heart Rate Monitor Prototype

Kamonwan Thipprasert[a], Settawit Poochaya [b], Sukasem Watcharamaisakul [c], Jantakarn Kanjanawetang[d], Siriwan Chokkha[e*]

[a]Biomedical Innovation Engineering, Institute of Engineering
Suranaree University of Technology, Nakhon Ratchasima, 30000, Thailand
[b]School of Telecommunication Engineering, Institute of Engineering
Suranaree University of Technology, Nakhon Ratchasima, 30000, Thailand
[c]School of Ceramic Engineering, Institute of Engineering
Suranaree University of Technology, Nakhon Ratchasima, 30000, Thailand
[d]School of Family Health and Midwifery Nursing, Institute of Nursing
Suranaree University of Technology, Nakhon Ratchasima, 30000, Thailand
[e]School of Ceramic Engineering, Institute of Engineering
Suranaree University of Technology, Nakhon Ratchasima, 30000, Thailand
*E-mail address corresponding author: Siriwan@sut.ac.th

Keywords: Heart rate (HR), Fetal Heart Rate (FHR), Microphone Sensor, Arduino

Heart rate measurement is an important indication of the initial health of an organism. The development of a heart rate monitor can lead the development of home fetal heart rate monitor. This will be important helping to monitor the health of the fetus and reduce the infant mortality rate. Therefore, this work develops a heart rate monitor prototype, leading to the development of home fetal heart rate monitors with high accuracy. KY 037 sensor was selected for heart sound data collection. The sensor acquires the data then undergoes pre-processing and sending the signal to the microcontroller for the transmission of data by developing an algorithm, effecting to signal reading of computer. Finally, the output data of heart rate was showed on LED display. Comparison method was selected for measurement calibration. The proposed fetal heart prototype was calibrated with standard fetal heart sound device. Percentage of measurement error is investigated. Comparison method was selected for measurement calibration. LifeDop-250 model was chosen for standard fetal heart sound devices. The measurement error was 23.26% before calibration. Measurement error reduced to 1.62% when using comparison method. This is highly efficient because the measurement error results is in the range 3-5% measurement error according to medical standard. .Moreover, cost of the proposed system is 96 % less than a standard instrument. The production cost is 810 baht.. Such a preliminary test was confirmed that this home heart rate prototype could be developed into a home fetal heart rate monitor. In addition to reducing the mortality rate of the fetus but it can also reduce the cost of device and import of the tools from abroad, resulting to increasing of easily to use as well.

BIO-P-090

Bacterial Cellulose with Antimicrobial Properties from *Houttuynia cordata* Thunb. Powder Extract for Active Packaging

Narumol Promniyomchai and Phimchanok Jaturapiree*
Department of Biotechnology, Faculty of Industrial Technology and Engineering, Silpakorn University, Muang / Nakhon Pathom, 73000, Thailand
*jaturapiree_p@su.ac.th

Keywords: Active packaging Antimicrobial Bacterial cellulose (BC)

As a response to the significant environmental impact caused by plastic packaging materials, biodegradable active packaging materials must be developed. Bacterial cellulose has gained interest as a result of its edibility, biodegradability, environmentally-friendly, and shows promise as a dependable carrier of a range of antimicrobial agents. The objective of the current work is to synthesize bacterial cellulose from *Acetobacter xylinum* TISTR 975 containing antimicrobial properties from *Houttuynia cordata* Thunb. powder extract. The membranes of BC immobilized with *Houttuynia cordata* Thunb. extract showed a good potential for antimicrobial activity against both Gram-negative and Gram-positive bacteria, with tested strains of *Escherichia coli*, *Staphylococcus aureus*, and *Bacillus cereus* by agar disc diffusion test. These findings imply that the active bacterial cellulose films used in this work might be a potential material in food applications for extending the shelf life and improving food safety.

CERAMICS

CER-I-01

Efficacy of Biocompatible Phase Developed in Eggshell-Derived Porous Glass-Ceramic Orbital Implants

Jiratchaya Ayawanna[a,*], Thanyapon Wanpen[a], Namthip Kingnoi

[a]School of Ceramic Engineering, Institute of Engineering, Suranaree University of Technology, Muang, Nakhon Ratchasima 30000, Thailand.

Keywords: Glass-ceramic, Calcium silicate, Eggshell, Orbital implants.

When the patients have suffered an eye ailment or accident. Orbital implants are typically used to fill the anophthalmic socket and maintain surrounding tissues after the removal of the eyeball in surgery. Calcium silicate porous glass-ceramic materials were used to form an orbital implant due to their biocompatible property with an abundance of pores for ingrowth of fibrovascular tissue to fasten the implants to orbital tissues. In this research, less expensive CaCO3 from eggshells was used to produce calcium silicate porous glass-ceramic material. The key morphological features of the porous glass-ceramic product were evaluated, and its ability to endure in body fluid was investigated. The porous glass-ceramic orbital implants were prepared by fabricating X mol% CaCO3 (or eggshell) - 10mol% Na2O - 60mol% SiO2 glass systems with varying eggshell contents (X = 30 - 50 mol%). After heating at 870°C and 1000°C, the microstructure, mineral composition, and porosity of glass-ceramic orbital implants were comparatively studied. By soaking in simulated body fluid, the efficacy of the bio-compatible phase developed in eggshell-derived calcium-silicate porous glass- ceramic orbital implants was investigated. The compatibility of porous glass-ceramic with simulated human body fluid was reported in the form of weight change and bio- phase formation after the test for 2 weeks to 3 months. The maximum contents of eggshell in making the calcium silicate glass was 40 mol%, in which a pure amorphous structure was formed for fabrication of glass-ceramic orbital implants. A pure biocompatible wollastonite (CaSiO3) phase was obtained after heat treatment at 1000ºC. In comparison to glass-ceramic orbital implants made from commercial CaCO3, those made from eggshells had an open-macropore network with porosity over 30% that allowed fibrovascular tissue to grow. The glass-ceramic implants made from eggshells demonstrated good chemical stability in simulated body fluids (90-days *in vitro* test). This innovative porous glass-ceramic material is therefore a promising alternative low- cost biomedical implant for ocular prosthesis applications.

CER-I-02

High-Entropy Titanate-Based Perovskite Oxides

Ketkaeo Bunpang[a, b, c], Chanatta Kolaka[a], Kornkawat Suksamran[a], Natthaphon Raengthon[a, b, c, *]

[a]*Department of Materials Science, Faculty of Science, Chulalongkorn University, Bangkok, 10330, Thailand*

[b]*Center of Excellence on Advanced Materials for Energy Storage, Chulalongkorn University, Bangkok 10330, Thailand*

[c]*Center of Excellence in Physics of Energy Materials (CE:PEM), Department of Physics, Faculty of Science, Chulalongkorn University, Bangkok, 10330, Thailand*

*Natthaphon.R@chula.ac.th

Keywords: High-Entropy Oxides, Titanate-Based, Perovskite, Dielectric

High-entropy oxides (HEOs), also known as entropy-stabilized oxides, have recently been widely investigated by scientific communities due to their unique characteristics providing promising properties. This group of materials was firstly explored in alloy families as high-entropy-alloy (HEAs), which high configurational entropy is a key factor in governing stabilization of single-phase multi-cations compound. Recent studies have shown that HEOs can be successfully synthesized by well-known techniques and stabilized in various structures such as rocksalt, pyrochlore, perovskite, spinel, and fluorite. In this study, we focus on HEOs that are stabilized in the perovskite structure based on $ATiO_3$, which A is cations (5 or more) persisting similar ionic radii. Phase identification and crystal structure analysis revealed that a single-phase perovskite could be obtained by a conventional mixed oxide method. A-site modification by cation substitution could alter dielectric properties of the compound. Similarly, B-site doping with homo- and heterovalent cations could be achieved with limited doping concentration to maintain the single-phase perovskite. However, structural distortion was found to be more prominence in B-site modification than that of A-site modification. Based on this study, it should be noted that HEOs with perovskite structure need further investigation due to its flexibility in chemical manipulation and structural modification which can lead to promising electrical properties.

CER-O-013

Study of Consistency and Density of Titanium Dioxide and Tungsten Trioxide Coatings on Conductive Glass from Dipping Process Affecting Light Absorption and Transmission

Anurat Poowancum[1], Kraiwut Rukkachat[1], Phakkhananan Pakawanit[2], Chatchai Ponchio[3], Sakhob Khumkoa[4], Siriwan Chokkha[1]*

[1]School of Ceramic Engineering, Institute of Engineering, Suranaree University of Technology

[2]Synchrotron Light Research Institute (Public Organization),111 University Avenue, Muang District Nakhon Ratchasima, 30000, Thailand

[3]Department of chemistry, Faculty of science and technology, Rajamangala University of Technology Thunyaburi

[4]School of Metallurgical Engineering, Institute of Engineering, Suranaree University of Technology

*E-mail address corresponding author: Siriwan@sut.ac.th

Keywords: Solar cell, Photocatalysis, Photovoltaic application, Synchrotron X-ray tomographic microscopy

Light property is a crucial factor in photovoltaic power generation. Therefore, the study of light absorption and transmission of materials is important for developing of solar cell coating material. Titanium dioxide (TiO_2) and tungsten trioxide (WO_3) are the important candidates for use as the solar cell coating material. Because TiO_2 and WO_3 have a narrow energy band gap and have photocatalytic properties which are the essential properties for the solar cell application. The aim of this work is to investigate the light absorbance ability of the TiO_2 and WO_3 coating layer. The gel of TiO_2 and WO_3 was synthesized by the sol-gel method. The synthesized gel of TiO_2 and WO_3 was coated on the conductive glass (FTO) by using the dip-coating technique. The light absorbance of the coated surface was examined by the UV-Visible Spectrophotometer technique (UV-Vis). The surface of coating homogeneity and the coating density were evaluated by 3D imaging which was investigated by 3D reconstruction of the samples by Synchrotron X-ray tomographic microscopy (SR-XTM) technique. The results show the light absorption ability of the conductive glass coated by WO_3 is higher than that of TiO_2. However, the coating homogeneity and the coating density of the WO_3 coated layer are lower than that of the TiO_2 coated layer. The unevenness of the WO_3 coated layer is the cause of non-uniform light absorption. The homogeneity of the coating layer is decreased with increasing the coating layer number because the coating is unevenly distributed resulting in some areas are denser than others. From all the experimental results, it is concluded that even the TiO_2 coated layer has a tendency to increase the absorbance less than WO_3 coated layer, but it is acceptable considering of uniformity coated layer. Consequently, TiO_2 is suitable for applying to solar cells because of its increasing of absorbance capacity and reducing of light reflection.

CER-O-025

Geopolymers Derived from Waste Glass Powder, Fly Ash, and Calcium Carbide Residue

Chiraporn Auechalitanukul[a,*], Ryan McCuiston[a], Daruneenuch Chankasem[a], Kasinee Chankong[a], Natanan Seeplee[a], Weerachart Tangchirapat[a]

[a]King Mongkut's University of Tehnology Thonburi, Thungkru, Bangkok, 10140, Thailand

*chiraporn.aue@kmutt.ac.th

Keywords: Geopolymer, Waste glass powder, Fly Ash, Calcium carbide residue

Due to the limits of natural resources needed for cement manufacturing, coupled with ever increasing amounts of industrial waste and growing environmental consciousness, alternatives such as geopolymers are becoming attractive building materials. Particularly with the use of compatible wastes to make geopolymers at room temperature. This study investigated five formulated geopolymers, prepared from waste glass powder, fly ash, and calcium carbide residue. The ratio of glass powder, fly ash and calcium carbide residue was varied, while the amounts of sodium hydroxide solution, superplasticizer, sand (as aggregate) and short glass fiber (as reinforcement) were fixed. The specimens were mixed, cast and cured at room temperature for 7, 14 and 28 days, after which the compressive strengths were measured. The results suggest that the rate of strength development was different between the waste glass powder and the fly ash. The longer cure-time strength was increased with an increased amount of fly ash (i.e. a reduced amount of glass powder). This was despite the glass powder being fully amorphous, compared to the less amorphous fly ash. This could be due to the differences in the physical characteristics of the powders. The fly ash is a fragile, shell-like particle, while the glass powder is a harder, dense particle, which could decrease the reaction rate. From the XRD results, geo-polymerization potentially occurred more in the specimens with higher strength and could be responsible for the observed increase in strength.

CER-O-044

Improvement of Electrical Properties of ZnO Nanomaterials with Fe by Co-Precipitation Method

Pitchaporn Kingpho[a], Buppachat Toboonsung[a,b,*]
[a]Program of Science Education, Graduate School, Nakhon Ratchasima Rajabhat University, Nakhon Ratchasima, 30000, Thailand
[b]Program of Physics, Faculty of Science and Technology, Nakhon Ratchasima Rajabhat University, Nakhon Ratchasima, 30000, Thailand
*buppachat.t@nrru.ac.th

Keywords: Co-precipitation method, Fe-doped ZnO, Optical properties, Electrical properties

In the present study, improvement of electrical properties of ZnO nanomaterials with Fe by co-precipitation method. The experiments were used a solution of 0.5 M, $ZnCl_2$ as a precursor and doped $FeSO_4$ have compositions 0%, 1%, 3% and 5% with magnetic stirrer with dropping a NaOH of 1 M and the product of precipitation were calcinated at of 550 ^oC for 3 h. UV-Vis spectroscopy has been used to optical and electrical properties of the samples. The results showed that the wavelength was shown in the range of 373-413 nm. The electrical studies had shown the energy band gap for ZnO nanomaterials were determined using Tauc plot. The crystal structure of ZnO nanomaterials was investigated using X-ray diffraction (XRD) and the morphological feature of the ZnO nanomaterials was identified by using scanning electron microscopic (SEM).

CER-O-056

Synthesis of Geopolymer/zeolite Composites from Lignite Fly Ash and Biomass Ash

Auekarn Chuwongwittaya[a], Adisak Siyasukh[a], Kedsarin Pimraksa[a, b, *]

[a]*Department of Industrial Chemistry, Faculty of Science, Chiang Mai University, 50200, Thailand*

[b]*Center of Excellence in Materials Science and Technology, Faculty of Science, Chiang Mai University, 50200, Thailand*

*kedsarin.p@cmu.ac.th

Keywords: Geopolymer, Zeolite, Hydrothermal method, Waste circulation

This research paper investigated the synthesis of geopolymer/zeolite composites from lignite fly ash and biomass ash using combined reactions of geopolymerization and zeolitization under hydrothermal treatment. The initial molar ratios of SiO_2/Al_2O_3 were designed in the range of 3.0-6.0 using different hydrothermal alkalinities, hydrothermal temperature and time, and specimen preparation in hydrothermal system. At low SiO_2/Al_2O_3 molar ratio (3.0-5.0), sodalite zeolite could be obtained incorporating with geopolymeric phase. Tobermorite binder was also formed in this range. Zeolite P was found at higher SiO_2/Al_2O_3 molar ratio (4.0-5.0). The formation of zeolitic materials in geopolymeric matrix affected a mechanical strength of the hardened composite materials. Before hydrothermal treatment, geopolymeric gel was mainly formed reaching the highest compressive strength about 43.5 MPa at SiO_2/Al_2O_3 molar ratio of 5.0. The strength degraded over 50% to be 19.0 MPa after hydrothermal treatment owning to the formation of geopolymeric/zeolite composite.

CER-O-083

Effect of Perlite on Properties of Porcelain Roofing Tiles Clay

Pasinee Siriprapa[a], Ampika Rachakom[b], Kattaliya Chaipisanc[c], Pimpilai Wannasut[c], Nittaya Keawprak[e], Anucha Watcharapasorn[c,f,*]

[a]*Faculty of Art and Architecture, Rajamangala University of Technology Lanna, Chiang Mai 50300, Thailand*

[b]*Faculty of Science and Agricultural Technology, Rajamangala University of Technology Lanna, Chiang Mai 50300, Thailand*

[c]*Department of Physics and Materials Science, Faculty of Science, Chiang Mai University, Chiang Mai 50200, Thailand*

[e]*Thailand Institute of Scientific and Technological Research, Pathum Thani 12120, Thailand*

[f]*Center of Excellence in Materials Science and Technology, Materials ScienceResearch Center*

Keywords: Porcelain Clay, Roofing tiles, Perlite, Thermal insulating

Nowadays stricter energy regulations are compelling us to further improve the thermal insulation performance of current building materials. In this study we investigated the possibility of improving the thermal insulating performance of fired clay roof tile. The effect of perlite on the physical mechanical and thermal properties of ceramic tile bodies was investigated. The phases present in the raw materials were measured by X-ray diffraction while chemical analysis of the raw materials were determined by X-ray fluorescence. The effect of perlite on firing shrinkage (%), water absorption (%), density (g/cm^3), bending strength and colour values (L, a, b) were studied and resultant microstructures were characterized by scanning electron microscope studies (SEM). It was clearly observed that perlite improves sinter ability of the tile bodies but increases the firing shrinkage due to the presence of water in its structure. The low thermal expansion values of the sintered bodies containing perlite makes it a visible raw material for porcelain stoneware tiles.

CER-P-030

Synthesis and Characterization of MgF_2 Nanoparticles by Microwave Heating Method

Warisara Suwandecha[a], Noppakhate Jiraborvornpongsa[b], Pornapa Sujaridworakul[a,c]*

[a]*Department of Materials Science, Faculty of Science, Chulalongkorn University, Bangkok, 10330, Thailand*

[b]*Metallurgy and Materials Science Research Institute, Chulalongkorn University, Bangkok, 10330, Thailand*

[c]*Center of Excellence on Petrochemical and Materials Technology, Chulalongkorn University, Bangkok, 10330, Thailand*

* pornapa.s@chula.ac.th

Keywords: MgF2, Nanoparticles, Microwave, Hollow structure

Anti-reflective coating plays an important role in developing the efficiency of photovoltaics. One of the substances that received attention in this field is magnesium fluoride (MgF2) due to its low refractive index (RI). In this work, we use a rapid route, microwave heating, to synthesize MgF2 nanoparticles. The MgF2 nanoparticles were prepared from magnesium acetate, hydrofluoric acid, and hydrochloric acid. The sol was heated in microwave oven at 700 watts for 5, 10, 15 and 20 minutes. After heated, the sol was rinsed with acetone and centrifuged to separated nanoparticles from the sol. Finally, the samples were dried at 60^{o}C. The effects of different heating time on the synthesized MgF2 nanoparticles were investigated. The crystalline phase was characterized by X-ray diffractometer (XRD). The morphology and particles size were measured by transmission electron microscopy (TEM). The pore size distribution, pore structure and surface area were also determined using Brunauer, Emmett, and Teller (BET) method with N2 adsorption. The XRD results confirmed that crystalline MgF2 phase having tetragonal structure was obtained from all samples. The crystallite size calculated from Scherer equation and BET surface area of MgF2 were increased from 8.13 to 9.29 nm, and 109.75 to 123.13 m^2/g, respectively as increasing heating time. The TEM images showed that all synthesized MgF2 nanoparticles have the hollow asymmetrical shape. Finally, the refractive index also investigated by %R follow Fresnel's law. This can be proven that MgF2 nanoparticles can be rapidly synthesized by microwave heating and suitable to be used as anti-reflective materials.

CER-P-031

Utilization of Crude Glycerol in the Physical Properties of Expanded Foam Glasses

Pat Sooksaen [a, b *], Tanin Unnapan [a], Suphahud Pintasiri [a] and Puttarapapa Meetongpun [a]

[a] *Department of Materials Science and Engineering, Faculty of Engineering and Industrial Technology, Silpakorn University, Nakhon Pathom 73000 Thailand*

[b] *Center of Excellence for Petroleum, Petrochemicals and Advanced Materials, Chulalongkorn University, Bangkok, 10330, Thailand*

*E-mail address corresponding author: sooksaen_p@silpakorn.edu

Keywords: Crude glycerol, Decomposition, Foam glass, Microstructure

Expanded foam glasses were fabricated from a clear color soda-lime silicate glass. Crude glycerol obtained from biodiesel production was used as the foaming agent. This research focused on the effect of crude glycerol content on the expanding behavior and physical properties of foam glasses. The role of crude glycerol was to promote small closed cell pores. The expanding behavior relied on the decomposition mechanism of the foaming agent and fluxing effect occurred in the mixture with glass powder. Overall, foam glasses fabricated at 850°C showed best uniform pore size distribution within the bulk structures compared to other fabricated temperatures. Pore size of foam glasses increased with increasing firing temperature. The evidence of black color in some areas in the samples fired at 800°C occurred due to incomplete combustion of crude glycerol within the bulk structure. Samples produced at above 850°C gave complete combustion of carbonaceous compound which resulted in white color shading. Samples fired at 900˚C showed some structure distortion caused by high temperature firing leading to glass melting and foam glass structure collapsed. Large holes or pores within the foam glass were caused by the sweeping and combining of gas bubbles (CO_2) within the samples.

CER-P-032

Synthesis and Characterization of Titanium-Doped Hydroxyapatite for Methylene Blue Dye Degradation

Pimpitcha Bumrungsub[a], Noppakhate Jiraborvornpongsa[b], Pornapa Sujaridworakun[c,*]

[a]*Department of Materials Science, Faculty of Science, Chulalongkorn University, Bangkok 10330, Thailand*

[b]*Metallurgy and Materials Science Research Institute, Chulalongkorn University, Bangkok 10330, Thailand*

[c]*Center of Excellence on Petrochemical and Materials Technology, Chulalongkorn University, Bangkok 10330, Thailand*

*E-mail address corresponding author: pornapa.s@chula.ac.th

Keywords: Dye degradation, Hydroxyapatite, Photocatalyst, Titanium doped

The adsorption properties are a critical factor in developing materials for environmental remediation technologies via photocatalytic reaction. So, the adsorbent materials could be used for the removal of pollutants by retaining them on their surfaces. Hydroxyapatite (HAP) is biocompatible, mechanical stable, and non-toxicity. Moreover, it presents great adsorption capability for adsorbing the retention of contaminants such as heavy metals, dyes, hydrocarbon, and other pollutants. The synthesis of HAP with other metal ions or compounds has been studied in the catalyst field to improve the properties of HAP. In this study, Hydroxyapatite (HAP) and Titanium-doped hydroxyapatite (TiHAP) were synthesized by hydrothermal method using 100 ºC for 6 h, followed by heated treatment at 650 ºC for 1 h. The heat-treated HAP and TiHAP were referred as HAP_HT and TiHAP_HT respectively. The amount of doping Ti (IV) ions to HAP was kept at 0.1 by atomic ratio between Ti and Ca (Ti/Ca). The effect of Ti-doping and the heat treatment were studied. The HAP and TiHAP powder showed a hexagonal apatite structure by X-ray diffraction (XRD). In addition, the morphology of the particles were analyzed by using scanning electron microscopy (SEM). The specific surface area (S_{BET}) was determined by Brunauer-Emmett-Teller (BET) method with N_2 adsorption. The S_{BET} value of TiHAP, HAP, TiHAP_HT, and HAP_HT were 141.22, 79.28, 59.97 and 46.34 m^2/g, respectively. The photocatalytic activity was carried out by using 0.05 g of photocatalysts in 100 mL of the 10 mg/L methylene blue (MB) aqueous solution under UV light irradiation for 4 h. The adsorption capability under the dark indicated that TiHAP showed the highest adsorption, which corresponds to its highest S_{BET} value (141.22 m^2/g). After UV irradiation, the photodegradation of MB is found to be effectivewith TiHAP, TiHAP_HT, HAP, and HAP_HT respectively. From the results, it can be summarized that Ti-doping affected the adsorption capability of HAP which corresponds to the performance of the photocatalytic activity. In case of the effect of heat treatment, it was found to decrease the surface area, so the adsorption and degradation ability of the heat-treated samples were reduced accordingly.

CER-P-037

Effects of Pottery Stone Feldspar and Quartz on Physical and Mechanical Properties of Porcelain Tableware

Soravich Mulinta[a,*] Thitima Khunyotying[a], Tamonwat Hirunchata-nan[a], Pincha Tolkidtikul[b]

[a] *Department of Production Innovation and Ceramic Design, Faculty of Industrial Technology, Lampang Rajabhat University, Thailand, 52100*

[b] *Department of Civil Technology, Faculty of Industrial Technology, Lampang Rajabhat University, Thailand, 52100*

*E-mail; Soravich@lpru.ac.th

Keywords: Pottery Stone, Feldspar, Quartz, Mechanical strength, Shrinkage.

The objective of this research was to study and investigate the effect of raw materials for porcelain tableware in Lampang province, Thailand. The raw materials used in the study were from local sources comprising Lampang pottery stone, feldspar, and quartz. The characterization of the raw materials was analyzed by a particle analyzer, X-ray fluorescence (XRF) and X-ray diffraction (XRD). The mixing ratio of the porcelain tableware body was designed as following in wt% of 60-70 of Lampang pottery stone, 0-15 feldspar, and 0-40% for quartz in seven component ratios. The properties of the porcelain tableware body after firing at a temperature of 1,200°C and firing time of 8 hours in an oxidation atmosphere were studied, and the shrinkage, water absorption, bulk density, apparent porosity, whiteness index, crazing and bending strength of the porcelain tableware body were also tested. The results showed that Formula 7 components of 50% Lampang pottery stone, 10% of feldspar and 40% of quartz had optimum properties. Formula 7 had shrinkage of 13.1%, water absorption of 3.08%, bulk density of 2.04 g/cm^3, appearance porosity of 9.1 %, non-crazing and resistance to the bending strength at 760 kg/cm^2. The porcelain tableware body improved the requirements of the Thai industrial standard (TIS 564-2546).

CER-P-043

Effects of Curing Time on Physical Properties and Thermal Properties of Perlite-Based Composite

Kattaliya Chaipisan[1,2], Paitoon Boonsong[1], Pimpilai Wannasut[1,3], Ampika Rachakom[5], Pasinee Siriprapa[6], Nittaya Keawprak[7], Panya Suriyachay[8], Anucha Watcharapasorn[*1,4]

[1] Department of Physics and Materials Science, Faculty of Science, Chiang Mai University, Chiang Mai 50200, Thailand

[2] Graduate School, Chiang Mai University, Chiang Mai 50200, Thailand

[3] Office of Research Administration, Chiang Mai University, Chiang Mai 50200, Thailand

[4] Center of Excellence in Materials Science and Technology, Materials Science Research Center,
Faculty of Science, Chiang Mai University, Chiang Mai 50200, Thailand

[5] Faculty of Science and Agricultural Technology, Rajamangala University of Technology Lanna, Chiang Mai 50300, Thailand

[6] Faculty of Art and Architecture, Rajamangala University of Technology Lanna, Chiang Mai 50300, Thailand

[7] Thailand Institute of Scientific and Technological Research, Pathum Thani 12120, Thailand

[8] Khlong Yang Limited Partnership, Bangkok 10170, Thailand

Corresponding author: anucha@stanfordalumni.org

Keywords: Perlite, Mortar, Physical Properties, Thermal Conductivity.

This work studied the phase, microstructure, water absorption, mechanical and thermal properties of (1-*x*)mortar-(*x*)perlite composites, where x = 0, 2, 4, 6, 8, 10 weight fraction, and their dependence on curing time. The X-ray diffraction (XRD) analysis revealed the amorphous structure of perlite. The distribution of perlite in the specimen is uniform. The scanning electron microscope (SEM) images indicated that the perlite particle size range was around 11.1-12.2 μm. The compressive strength of the composite was found to decrease when the perlite fraction increased, corresponding to the change in sample density. The near zero percentage of water absorption was similarly observed for both perlite-added mortar and pure mortar. The differential scanning calorimetric (DSC) data indicated several exothermic peaks, corresponding to some reaction/decomposition of chemical species. The thermal conductivity at room temperature was found to decrease with increasing perlite content with the value range of 0.0507-0.0584 W/m•K. The longer curing time also showed apparent changes in the physical and thermal properties of perlite. This study suggested that the perlite particles could be used as a good insulation material for industrial and household applications.

CER-P-061

Diffuse Phase Transition and Electric Properties of Lead-Free $0.5Ba(Zr_{0.2}Ti_{0.8})O_3$-$0.5(Ba_{0.7}Ca_{0.3})TiO_3$ Ceramics by $Ba_{0.93}Ca_{0.04}La_{0.03}Sn_{0.1}Ti_{0.9}O_3$ Addition

Nuttapon Pisitpipathsin[a,b,*], Tawee Tunkasiri[c]

[a]*Department of Applied Physics, Faculty of Sciences and Liberal Arts, Rajamangala University of Technology Isan, Nakhon Ratchasima 30000, Thailand*

[b]*Advanced Materials and Renewable Energy Research Unit, Faculty of Sciences and LiberalArts, Rajamangala University of Technology Isan, Nakhon Ratchasima 30000, Thailand*

[c]*Department of Physics and Materials Science, Faculty of Science, Chiang Mai University, Chiang Mai 50202, Thailand*

* Email: nuttapon.pi@rmuti.ac.th

Keywords: Dielectric properties, Phase transition, BCZT, Ferroelectric properties

Lead-free piezoelectric ceramics from $0.5Ba(Zr_{0.2}Ti_{0.8})O_3$-$0.5(Ba_{0.7}Ca_{0.3})TiO_3$ (BCZT) and $Ba_{0.93}Ca_{0.04}La_{0.03}Sn_{0.1}Ti_{0.9}O_3$ (BCLST) systems were prepared by a modified two-step mixed oxide method. BCLST powder was added to BCZT powder with the desired compositions of (1-x)BCZT-xBCLST, where x = 0.00, 0.01, 0.03, 0.05 and 0.07. Effects of BCLST content on the structure, diffuse phase transition and dielectric properties of BCZT-BCLST ceramics were investigated. The global structure was investigated by X-ray diffraction (XRD). The XRD results of ceramics indicated a tetragonal perovskite crystal structure. The dielectric property investigation indicated that the degree of the diffuseness of phase transition was maximum at x = 0.01 and thendecreased with increasing BCLST content for $x \geq 0.03$. The dielectric constant at room temperature increased with the addition of BCLST at x = 0.03 (ε_r ~2552) which is ~81% higher than that of the unadded sample.

CER-P-104

Effect of Firing Temperatures on Phase Structure and Electrical Properties of 0.9(BNT-BT)-0.1NT Ceramics with Synthesized via the Combustion Solid-State Technique

Bhoowadol Thatawong[a], Kanyanut Tagerd [a], Naratip Vittayakorn[b], Thanya Udeye[a,c*] and Theerachai Bongkarn[a,c]

[a]*Department of Physics, Faculty of Science, Naresuan University, Phitsanulok, 65000, Thailand*

[b]*Advanced Material Research Unit, Faculty of Science, King Mongkut's Institute of Technology Ladkrabang, Bangkok 10520, Thailand*

[c]*Research Center for Academic Excellence in Applied Physics, Faculty of Science, Naresuan University, Phitsanulok, 65000, Thailand*

*Corresponding Author: Thanyau@nu.ac.th

Keywords: 0.9(BNT-BT)-0.1NT, combustion, dielectric, energy-storage

Lead-free ferroelectric ceramics of $0.9(0.92Bi_{0.5}Na_{0.5}TiO_3–0.08BaTiO_3)$-$0.1NaTaO_3$ or 0.9(BNT-BT)-0.1NT were prepared by the combustion solid-state technique using glycine as fuel. Effect of firing temperatures (calcination temperature of 600-800^{o}C for 2 h and sintering temperature of 1075-1175^{o}C for 2 h) on phase structure, microstructure, electrical and energy-storage properties of 0.9(BNT-BT)-0.1NT ceramics were investigated. The perovskite phase was observed in all powder samples. 0.9(BNT-BT)-0.1NT powder calcined at the temperature of 750^{o}C for 2 h showed the pure perovskite phase of 100%. The particles exhibited spherical shape and wide distribution morphology. The average particle size increased from 340 to 370 nm by increase of calcination temperature. The 0.9(BNT-BT)-0.1NT ceramics exhibited a single perovskite structure with coexistence phases of rhombohedral (R), tetragonal (T) and cubic (C), as found by Rietveld refinement. The average grain size increased from 0.85 to 2.66 μm by increase of sintering temperature, while the maximum dielectric constant (ε_m), remanent polarization (P_r) and coercive field (E_c) decreased. At a sintering temperature of 1150^{o}C for 2 h, the ceramic showed the highest dielectric constant ($\varepsilon_m \sim 1840$), high density of 5.83 g/cm^3 and the highest energy-storage density of 0.71 J/cm^3 at electric field of 70 *k*V/cm.

CER-P-106

Effect of $(AlNb)^{4+}$ B-Sites Substitution on Phase Structure, Microstructure and Electrical Properties of $Bi_{0.47}Na_{0.47}Ba_{0.06}TiO_3$ Ceramics

Anupong Luangpangai[a], Wistsarut Chongsatan[a], Nipaphat Charoenthai[b,c], Naratip Vittayakorn[d] and Theerachai Bongkarn[a,c*]

[a]*Department of Physics, Faculty of Science, Naresuan University, Phitsanulok, 65000, Thailand*

[b]*Department of Chemistry and Center for Innovation in Chemistry, Faculty of Science, Naresuan University, Phitsanulok, 65000, Thailand*

[c]*Research Center for Academic Excellence in Applied Physics, Faculty of Science, Naresuan University, Phitsanulok, 65000, Thailand*

[d]*Advanced Material Research Unit, Faculty of Science, King Mongkut's Institute of Technology Ladkabang, Bangkok, 10520, Thailand*

*E-mail address corresponding author: researchcmu@yahoo.com

Keywords: $BNBT_{1-x}AN_x$, phase structure, dielectric, ferroelectric.

The $Bi_{0.47}Na_{0.47}Ba_{0.06}Ti_{1-x}(AlNb)_x$ (abbreviated as $BNBT_{1-x}AN_x$) lead-free ceramics (x=0-0.05) have been synthesized by the solid-state combustion technique. The effect of $(AlNb)^{4+}$ content on phase structure, microstructure and electrical properties were investigated. A pure perovskite structure was obtained from all specimens. Rietveld refinement revealed coexisting rhombohedral and tetragonal phases in all samples and tetragonal phase increased with increasing x. The morphology of $BNBT_{1-x}AN_x$ displayed nearly-roundness grain shape and anisotropic grain growth. Average grain size decreased from 1.8 to 0.7 μm when x increased from 0 to 0.05. By increasing x, the grain size distribution became narrower. Density, maximum dielectric constant and remnant polarization rapidly decreased with increasing x. The deterioration of electrical properties induced by $(AlNb)^{4+}$ substitution due to shifting from morphotropic phase boundary (MPB), poor microstructure and low density.

CER-P-109

Phase Formation, Microstructure and Electrical Properties of BST-BZN Ceramics Synthesized via the Solid-State Combustion Technique

Widchaya Somsri[a], Panadda Duangkeaw[a], Rattiphorn Sumang[b], Phieraya Pulphol[c], Naratip Vittayakorn[d], Nipaphat Charoenthai[e,f,*] and Theerachai Bongkarn[a,f]

[a]*Department of Physics, Faculty of Science, Naresuan University, Phitsanulok, 65000, Thailand*

[b]*Program of Physics, Faculty of Science and Technology, Pibulsongkram Rajabhat University, Phitsanulok, 65000, Thailand*

[c]*Department of Materials Science, Faculty of Science, Srinakharinwirot University, Bangkok, 10110, Thailand*

[d]*Advanced Materials Research Unit, Faculty of Science, King Mongkut's Institute of Technology Ladkrabang, Bangkok, 10110, Thailand*

[e]*Department of Chemistry, Faculty of Science, Naresuan University, Phitsanulok, 65000, Thailand*

[f]*Research Center for Academic Excellence in Applied Physics, Faculty of Science, Naresuan University, Phitsanulok, 65000, Thailand*

*E-mail: nipaphatc@nu.ac.th

Keywords: BST-BZN, Combustion technique, Ferroelectric, Dielectric

Lead-free ceramics of $0.84Ba_{0.8}Sr_{0.2}TiO_3$-$0.16Bi(Zn_{2/3}Nb_{1/3})O_3$ (BST-BZN) were prepared by the solid-state combustion technique using glycine as fuel. The BST-BZN powders and ceramics were calcined between 950-1150 ^oC for 2 h and sintered between 1300-1400 ^oC for 2 h. The pure perovskite phase with pseudo-cubic structure was observed by XRD and confirmed by Rietveld refinement technique. The average particle and grain size tended to increase with increases of calcination and sintering temperatures. The measured density was in range of 5.52-5.88 g/cm^3. The dielectric constant (ε_r) and dielectric loss (tan δ_r) decreased with increase sintering temperatures up to 1350 ^oC and thereafter increased. The energy storage density (W_{total}) and energy storage efficiency (η) of the ceramics were 0.488 J/cm^3 and 94.10% measured at 100 kV/cm, respectively, obtained by the sample sintered at 1375 ^oC.

CER-P-131

Study of Kinuta Glaez is Recycling Silica from Glass Beer Bottle

Nattawut Ariyajinno[1, 2, *]

[1] *Nattawut Ariyajinno (Department of Management Engineering, Faculty of Industrial, Loei Rajabath University, Loei 42000, Thailand)*

[2] *Nattawut Ariyajinno (Department of Ceramics Technology, Industrial Faculty of Technology, Loei Rajabhat University, Loei 42000, Thailand)*

*Email: Nattawut.ari@lru.ac.th

Keyword: Ceramic Glaze, Kinuta glaze, Cracking, Glass Beer Bottle, Recycling..

These research study Kinuta glaze is cracking from glass beer bottle select two samples of the beer bottle Blue is green and brown by observing the results after burning study the physical properties of Kinuta glaze temperature 1250 ºC reduction and study the changing physical properties of the broken glass can be observed with the naked eye after burning for use in decorating ceramics products From the experimental results, it was found that In the temperature range 1250 ºC The glass scraps melting well and glaze is cracking from glass beer bottle Blue is green and brown The experimental results of using glass scraps from beer bottles As a result, it can be used to decorate ceramics products, Recycling silica especially in the form of cracking glazed cracking for the Japanese glaze Kinuta glaze.

CER-P-133

Synthesis of Zircon Pigments from Rice Husk Ash and Their Performance in Ceramic Glaze

Niti Yongvanich*, Peerapat Soysom, Worachet Ratkasemsak
Department of Materials Science and Engineering, Faculty of Engineering and Industrial Technology, Silpakorn University, Nakornpathom, 73000,
*niti.yongvanich@gmail.com

Keywords: Zircon, Pigment, Rice husk ash, Glaze.

$ZrSiO_4$-based pigments have been known to be very stable in ceramic glazes. However, their main drawback is a high firing temperature required for phase formation due to refractoriness of both ZrO_2 and SiO_2 as precursors. Fluxes are usually used to facilitate such enduring process. Another way is to utilize a starting precursor with a low degree of crystallinity in order to enhance chemical reactivity. This study examined the feasibility of using rice husk as a substitute for crystalline silicon dioxide (SiO_2) in synthesizing zircon pigments. The amorphous form of silica with some impurities was obtained by calcining the rice husk at 800°C. No further complicated chemical treatment on the obtained rice husk ash (RHA) was included as this study aims to apply this process in local ceramic enterprises. The general chemical formula were $(Zr_{0.9}M_{0.1})SiO_4$, where M = V, Pr, Fe and Cr. The conventional solid-state processing was achieved by firing at 1200°C for 12 hours with NaF addition of 5 wt%. X-ray Diffraction (XRD) revealed a lower relative fraction between ZrO_2 (secondary phase) and $ZrSiO_4$ (major phase) in the RHA systems compared to the oxide (crystalline SiO_2) system for all dopants. These results suggested that amorphousness of RHA did help enhance phase formability. Infrared spectroscopy also displayed zircon as major peaks. The particle sizes of all pigments were in the 2 – 10 micron range as examined by Scanning electron microscopy. Elemental analysis revealed some areas with intense signals of zirconium, indicating the presence of unreacted ZrO_2 particles which is in agreement with the XRD results. Colorations in the CIELab system appeared to be blue, yellow, brown and green for dopants of V, Pr, Fe and Cr, respectively. No significant difference in the color parameters was observed between the RHA and oxide systems. Technological performance was tested in a practical ceramic glaze (transparent) fired at its maturation point (1200°C). Their colors still appeared close to those of the pigments. The results of this study hold huge potential for using rice husks to substitute for industrial-grade SiO_2. In addition, utilization of this agricultural waste would be a good example for BCG economy for sustainable future.

COMPUTATIONAL SCIENCE & ENGINEERING

COM-I-01

Multi-Scale and Multi-Physics Modeling for Process-Structure-Property Relationships of Laser Powder-Based Additive Manufacturing

Patcharapit Promoppatum[a,*]
[a]*Department of Mechanical Engineering, Faculty of Engineering, King Mongkut's University of Technology Thonburi (KMUTT), Bangkok, 10140, Thailand*
*E-mail address: patcharapit.pro@kmutt.ac.th

Keywords: Laser powder bed fusion process, Additive manufacturing, Process-structure-property relationship, Multi-scale and multi-physics modeling

A laser powder bed fusion (LPBF) process has emerged as a promising manufacturing technology for various industries such as medical, automotive, aerospace, and offshore. However, the technology is still facing a great challenge due to the processing complexity. The process contains more than 100 adjustable parameters. As a result, the comprehensive experiments that can reveal the process-structure-property relationship are practically unachievable. For this reason, computational modeling becomes essential for attaining a fundamental understanding of the process. However, developing high-fidelity modeling is not an easy task owing to the multi-scale nature of the LPBF system. For an instance, the melting and solidification can occur within a fraction of milliseconds while the total build time could take up to several hours. Linking multiple physics at multiple spatial and temporal scales has been a target of this community. Therefore, I aim to provide an overview of the modeling works for the LPBF process from laser-material interaction, defect formation, microstructural development, mechanical properties, and damage initiation. Integration between different numerical strategies to gain a better understanding of a complex phenomenon and achieve a printed component with high build quality will be presented. I will also demonstrate how we can utilize different process strategies to modulate desirable mechanical properties through processing-mediated mesostructured. Finally, this talk hopes to describe the challenges, opportunities, and future research direction of the LPBF additive manufacturing process.

COM-O-023

Electricity and Resources Demand Long Term Forecast in Thailandby Using Polymath Software

Prachuab Peerapong[a,*]

[a]*Bangkokthonburi University, Taweewatana sub-district, Taweewatana district, Bangkok, 10170, Thailand.*
*prachuab.pee2@gmail.com.

Keywords: Electricity generation, Resources demand, Long term forecast, Polymath modeling.

The electricity generation and resources demand forecast for a long-term period in Thailand are based on two important parameters. The first one is the population growth rate, and the second one is the growth rate of the gross domestic product, GDP. This research uses two input parameters to forecast electricity and resource demand for a long-term period in Thailand. These resources demand electricity generation such as coal, natural gas, hydropower, and other renewable energy resources, and import electricity is needed. This research uses polymath software as a tool to forecast electricity and resource demand. The polynomial linear regression in this research by polymath software uses input data from the Energy Policy and Planning Office, the Ministry of Energy. Polynomial linear regression in this research by using Polymath V6.1 to forecast the electricity and resources demand in Thailand in the future. Polymath program is a powerful tool as a mathematical model to solve optimization problems, other complex problems, and polynomial linear regression.

COM-O-027

Analysis of Rear Underrun Protective Device Using Real-Life Test and Finite Element Techniques

Narongrit Suebnunta[a,b*], Sarawut Lerspalungsanti[b], Preechar Karin[a] and Kazuaki Inaba[c]

[a]*Department of Mechanical Engineering, School of Engineering, King Mongkut's Institute of Technology Ladkrabang, Bangkok, 10520, Thailand*

[b]*National Metal and Material Technology Center, National Science and Technology Department Agency, Pathum Thani, 12120, Thailand*

[c]*School of Engineering, Tokyo Institute of Technology, Tokyo 152-8550, Japan*

*E-mail address corresponding author: Narongrit.sue@mtec.ot.th

Keywords: RUPD (Rear Underrun Protective Device); UN R58 (Economic Commission for Europe Regulation 58); Heavy Truck; Finite Element Analysis

One of the most fatal accidents on the road occurs due to the rear underrun, i.e., a passenger car crashing into the rear of a truck. To reduce injury and death from this type of accident, one solution is to install a rear underrun protective device (RUPD) on the truck, which should meet the safety standards. The aim of this research is to establish a design guideline to validate the structural strength analysis method of the RUPD using a quasi-static test and finite element analysis according to the UN R58 standard, in which the minimum required forces applied at a cross-section of the protective beam and the corresponding deformation limits are given. The significant design parameter such as the cross-sectional area, section height, and thickness are investigated. As an example, a benchmark study of two models of commercial RUPDs satisfied the UN R58 regulation and the proposed RUPD design was carried out following the presented design guideline which all models were based on domestically available materials, such as SS400. The finite element analysis to demonstrate the structural strength of all RUPD models is achieved using RADIOSS. These findings provide performances of all models and can be used as guidelines for other RUPD types, such as foldable or slidable RUPD.

COM-O-113

Fracture Prediction of Aluminum Alloy Sheet AA2024-T3 by Strain-Stress Based Failure Criteria

Jurarat Sawangpan[a], Sansot Panich[a,*], Tanakorn Jantarasricha[b]
[a]King Mongkut's University of Technology North Bangkok, Bangsue, Bangkok, 10800, Thailand
[b]Pibulsongkram Rajabhat University, Amphoe Mueang, Phitsanulok, 65000, Thailand
*sansot.p@eng.kmutnb.ac.th

Keywords: Fracture Prediction, Fracture Forming Limit Curve, Fracture Forming Limit Stress Curve, AA2024-T3

Nowadays, the forming parts have various complex shapes to respond to the requirements of the market. In the meantime, new materials have been made that are stronger and lighter to help the industrial world move forward. As a result of this effort, an aluminum alloy sheet (AA2024-T3) is a material commonly used in the aerospace industry. AA2024-T3 sheet aluminum-alloy has an attractive base material for lightweight aerospace components. Unfortunately, its formability is relatively low, and more importantly, it abruptly cracks shortly after the ultimate loading point. Generally, the Finite Element Method (FEM) has been generally applied to simulate the forming processes of this material to reduce production costs and time of trial tests. The strain-based conventional fracture forming limit curve (FFLC) is a well-accepted tool for predicting the formability limit of material in sheet metal forming processes. Based on the stress limit, the Fracture Forming Limit Stress Curve (FFLSC) is numerically calculated using the experimental FFLC data for complex forming parts prediction.

This research aims to investigate the sheet metal formability of AA2024-T3 sheet, having 1.2 mm of thickness, by the Fukui conical cup test and three-point bending test, including numerical simulation using ABAQUS 2017. Sheet metal formability was evaluated by utilizing FFLC as experimentally determined with the help of the standard Nakajima stretching forming test. Furthermore, the FFLSC was numerically developed using combined flow rule theory, Swift hardening law, and the Hill'48 anisotropic yield criterion with the experimental FFLC data. To validate the use of FFLC and FFLSC as failure criteria, two forming parts are used: a classic Fukui conical cup test and a three-point bending test. The criteria are put into service via the element-deletion feature in ABAQUS 2017, by which any element whose failure value reaches a certain limit is removed. The results showed that FFLSC could be used to predict the location of the fracture point, and these results were consistent with the experimental forming test. Thus, it was found that the stress paths were dragged through the FFLSC corresponding to the elements that were deleted in the simulation model. On the other hand, the FFLC has failed to predict the fracture behavior of the Fukui conical cup test, which is an exceptional result for a three-point bending test. The validation of the reference point, the stress path, and the strain path were considered damage to the material after forming the test. To compare validation between simulation and experiment testing, force versus displacement, drawing depth, and accuracy dimension at fracture state were certainly accepted. From this study, it can be concluded that the FFLSC is a more accurate failure criterion for the formability prediction of sheet material.

COM-P-105

3D Computational Fluid Dynamics (CFD) Analysis of a Solar Drying Room for Rubber Sheet Production and Experimental Validation

Thipjak Na Lampang*, Sedthawatt Sucharitpwatskul, Chayanoot Kositanont, Satit Siriruk *National Metal and Materials Technology Center (MTEC), National Science and Technology Development Agency (NSTDA), Pathum Thani 12120, Thailand*
* thipjak.nal@mtec.or.th

Keywords: Solar drying, Rubber sheet, CFD, Energy Saving

In traditional smoked rubber sheet production, most of the energy is consumed during the drying process in the smoking room. To save energy costs, a new drying process was developed using only solar energy. After the proper design of a solar drying room, a 3D computational fluid dynamics (CFD) analysis was used to investigate the velocity and temperature distributions of the air in the drying room. Measurements of air velocity and air temperature at various positions were also carried out to validate the CFD model. It was found that the results from the CFD simulation and experiments were in good agreement. The CFD simulation was later used to predict the temperature and moisture content of the rubber sheets in the solar drying room. The application of this solar drying room can save energy costs by approximately 0.5-0.8 THB/sheet.

DESIGN & MANUFACTURING

DES-O-035

Optimization Mechanical Angle Calculated for Gaylord Box Folding Machine in Industrial Scale by Solidworks

Sanphasit Chonlaphan[a], Banpot Meesa[b*]

[a]*Automotive Engineering, Industrial Technology faculty, Rajabhat Rajanagarindra University*

[b]*Industrial Management Engineering, Faculty of Industrial Technology, Rajabhat Rajanagarindra University*

*E-mail address corresponding author : banpotmeesa@gmail.com

Keywords: Optimization, CAE, Machine design, Solidworks.

From previous paper in cooperated between Rajabhat Rajanagarindra university and TPCC company for create Gaylord box folding machine prototype. To solved worker back injury problem. The result has showed increasing angles will decrease operated machine force. But the angle of machine arm cannot be 180◦ because this angle must separate mechanism of machine to 2 steps of work. Analysis result showed 120◦ is the best angle because more than 130◦. Because this angle will affect the mechanism of prototype machine. Then this paper has purpose to analyzes mechanic arm angle of Gaylord box folding machine prototype in fine angle. Previous paper presented as explained above the suitable angle between 120 -130. Then with optimization and motion analysis by Solidworks simulation. The result shows the same trend as last paper in fine detail. Suitable angle was selected by condition from TPCC company. The criteria of selected use cycles time and switch time to consider. Result presented the suitable angles is between 122◦-124◦.

DES-O-082

Effects of Fused Deposition Process Parameters on Surface Quality and Mechanical Properties of 3D-Printed PLA Plastic Parts

Kittichai Sojiphan[a,*]

[a]*The Sirindhorn International Thai-German Graduate School of Engineering, King Mongkut's University of Technology North Bangkok, Bangkok, 10800, Thailand*

*kittichai.s@tggs.kmutnb.ac.th

Keywords: Fused Deposition Modeling, Additive Manufacturing, Polylactic Acid, Mechanical Property

3D-Printing technology or additive manufacturing using fused deposition modeling (FDM) technique is widely used in commercial 3D printers nowadays. Polylactic acid (PLA) is most common material used for 3D printing application by FDM. This research is aimed to study the effect of 3D-printing process parameters on the surface quality and mechanical property of PLA 3D-printed parts as well as to find the optimum parameter for printing PLA 3D-parts with complex shapes, sizes, and geometries. In this research, commercial 3D Printer is used with PLA as filling filaments. The 3D CAD files was generated using SolidWorks software. The 3D printed parts are measured and characterized using Vernier caliper, 3D-scanner, optical microscope, and tensile testing machine. Investigated parameters include raster angle, infill density, nozzle temperature, stage temperature, print speed, and types of PLA filaments. Total of three samples were made for each set of process parameters. The results of the present work can be used to further optimize the process parameters and 3D part design to create parts with optimal structure and mechanical property for design performance.

MATERIALS FOR ENERGY

ENR-I-01

Sulfur Tolerant Bimetallic Pd-Pt Catalysts for Aromatics Saturation of Diesel and O_2-Assisted H-FAME Production for Avoiding Sulfur Poisoning

Yuji Yoshimura[a],*, **Nuwong Chollacoop**[a], **Shih-Yuan Chen**[b], **Takehisa Mochizuki**[b]
[a]*National Energy Technology Center (ENTEC), National Science and Technology Development Agency (NSTDA), Pathum Thani 12120, Thailand*
[b]*National Institute of Advanced Industrial Science and Technology (AIST), Tsukuba305-8569, Japan*
*E-mail address: y.yoshimura@opal.ocn.ne.jp

Keywords: Low-aromatics diesel, H-FAME, Noble metal catalyst, Sulfur tolerance

Diesel vehicles are core commercial vehicles in the transportation sectors, and many measures for reducing their emissions have been taken from both of the automobile and fuel sides. For EURO 5 diesel vehicles with Diesel Particulate Filter (DPF) systems, sulfur reduction of diesel (EURO 5 diesel with sulfur amounts of 10 ppm or less) will be very effective to minimize sulfur-poisoning of the exhaust gas treatment catalysts. However, aromatics reduction of diesel (total aromatics<5-10 vol%) will be more effective for EURO 4 vehicles without DPF systems, because PM amounts in the engine out gas are reported to have a positive correlation with the amounts of aromatics in diesel. Total aromatics in diesel can be successfully reduced over sulfur tolerant noble metal catalysts, which are used in the 2nd stage reactor coupled with the 1st stage HDS oriented reactor. These diesel aromatics saturation processes have been commercialized as a SynSat process and a SMDH process, etc. and contribute to the "City diesel" production. We have improved sulfur tolerance of noble metal catalysts and developed the Pd-Pt/Yb-USY-Al_2O_3 catalyst. This catalyst could reduce the total aromatics amounts to 5 vol% or less from EURO 5 diesel (S<10 ppm) as well as from EURO 3 diesel (S<500 ppm). We also confirmed its stability over 2,700 h during the aromatics saturation of EURO 3 diesel. Thermodynamic analysis using a chemical potential diagram contributed to taking improvement measures for sulfur tolerance.

Fatty Acid Methyl Ester (FAME) has been used as a diesel alternative fuel to contribute to reducing the CO_2 emission, increased energy security and promoting agricultural industry, etc., but there are concerns on FAME over B20 blend due to its limited thermal and oxidative stability. Partially hydrogenated FAME (H-FAME) can solve these issues because of its low content of polyunsaturated FAME, e.g. about 1 wt% or less for Palm H-FAME and less than 4 wt% for Jatropha H-FAME. Oxidation stability of Palm H-FAME improved to 80 h (Rancimat) within 16 ºC of cloud point. H-FAME can be produced over Pd catalyst at the mild reaction conations, e.g. T<150 ºC, and P_{H2}<0.5 MPa, but Pd catalyst still faced S-poisoning during the low temperature hydrogenation. We have developed an innovative hydrogenation method assisted with trace amounts of coexisting oxygen for avoiding S-poisoning of Pd catalysts. Thermodynamic analysis indicated that sulfur species chemisorbed over Pd surfaces were more stable as SO_2 and its formation renewed the Pd surfaces as metallic. We confirmed the SO_2 formation experimentally during the O_2-assited hydrogenation of FAME. This O_2-assisted hydrogenation can avoid S-poisoning of noble metal catalysts, so we can expect a wide application of this method to prolong the noble metal catalyst life and to lead to cost reduction of the hydrotreating processes.

ENR-O-049

Exfoliated Graphite-Nickel Oxide Composite Electrode for Supercapacitor Application

Pyae Sone Soe[a*], Jedsada Manyam[b], Paiboon Sreearunothai[c*]

[a]*TAIST-Tokyo Tech & Sirindhorn International Institute of Technology, Thammasat University, Bangkok, Pathum Thani, 12120, Thailand*

[b]*National Nanotechnology Center (NANOTECH), National Science and Technology Development Agency, Bangkok, Pathum Thani, 12120, Thailand* [c]*School of Bio-Chemical Engineering and Technology, Sirindhorn InternationalInstitute of Technology, Thammasat University, Bangkok, Pathum Thani, 12120, Thailand*

* pyaesonesoe.putu.meteve@gmail.com

Keywords: Nickel oxide, Exfoliated graphite, Composite electrode, Supercapacitor

Typical metal oxides such as Ru_2O, MnO_2, NiO, Co_3O_4, V_2O_5 with carbon-based composite electrodes can offer several benefits such as combined modes of charge storage through the faradaic pseudo-capacitance as well as the electrical double layer charge storage and are promising for high specific capacitance. In this study, NiO nanoparticles on exfoliated graphite (EG) composite were prepared with various Ni ions to EG ratios and different calcination temperatures. It is aimed to study the effects of metal oxide concentrations and crystallinity on the performance of the NiO/EG supercapacitors. The graphite has been electrochemically exfoliated from graphite rods in poly(sodium-p-styrenesulfonate) electrolyte. The solution of nickel precursor, $Ni(NO_3)_2.6H_2O$, and EG were mixed, and added with NaOH to produce $Ni(OH)_2$/EG colloidal solution. The $Ni(OH)_2$/EG was converted to NiO/EG by calcination at 300℃ and 500℃. The electrode composed of NiO/EG and CMC were prepared on stainless steel substrate for electrochemical measurement. The FE-SEM with EDS results of NiO/EG confirmed that NiO nanoparticles were successfully dispersed on the EG. XRD phase determination of NiO/EG was found to be bulk graphite and NiO. Furthermore, the XRD peak of NiO/EG-500℃ has a stronger peak value at ($2\theta = 44^o$) than that of NiO/EG-300℃ which shows high crystallinity of NiO. The electrical resistance of the EG electrode increased with the addition of NiO nanoparticles. Cyclic voltammogram of NiO/EG electrodes in 1 M KOH showed redox peaks of NiO with the capacitive background. It was found that NiO/G-500℃ had the specific capacitance of 2.3 F/g and that of NiO/G-300℃ was 0.7 F/g at the scan rate of 10 mV/s. The results suggest that crystallinity of NiO particles strongly affects the electrochemical activity. Specific capacitance of the NiO/EG electrode could be further improved by tuning the exfoliation process to achieve few-layer graphene flakes which is expected to have larger specific surface area and support the greater load of NiO than graphite.

ENR-O-064

Nitric Oxide Adsorption Diffuse Reflectance Fourier Transform Infrared Spectroscopy: A Complemantery Characterization for Hydrodearomatization Catalyst

Eumporn Buarod[a], Pennapa Muthitamongkol[b], Vituruch Goodwin[a], Boonyawan Yoosuk[a], and Suparoek Henpraserttae[a]*

[a]National Energy Technology Center (ENTEC), National Science and Technology Development Agency (NSTDA), Khlong Luang, Pathum Thani 12120, Thailand

[b]National Metal and Materials Technology Center (MTEC), National Science and Technology Development Agency (NSTDA), Khlong Luang, Pathum Thani 12120, Thailand

*E-mail address corresponding author: suparoek.hen@entec.or.th

Keywords: NO adsorption; DRIFT; Catalyst characterization; HDA catalyst

Diffuse Reflectance Infrared Fourier Transform (DRIFT) spectroscopy can be used as in-situ technique to investigate adsorption of nitric oxide (NO) on Nickel Molybdenum sulfide (NiMoS) catalysts. The in-situ NO-DRIFT technique is more sensitive to surface species than NO Chemisorption Pulse Titration technique (NO-Pulse). The NO-Pulse data indicates three important information; 1) number of coordinatively unsaturated sites (CUS) on the edge sites of MoS_2, 2) number of CUS on the NiS_X sites which are not formed as the NiMoS phases (segregated NiS_X) and 3) number of CUS on the NiS_X phaseswell decorated the MoS_2 edges and forms the NiMoS phases. Among the three information, the third data is the most important to correlate the NO-Pulse data with HDA activity. The in-situ NO-DRIFT was utilized as a complementary technique to individually investigate NO adsorption on CUS of NiS_X and MoS_2 on the catalysts. NiMoS catalysts have been generally used in Hydrodearomatization (HDA) process to reduce polycyclic aromatic hydrocarbons (PAHs) in diesel fuel. The PAHs in diesel increases toxicity of PM 2.5 from exhaust gases of diesel engine. NiMoS catalysts were prepared with 0.45, 0.5, 0.57 and 0.6 Ni/Mo molar ratio to investigate effect of Ni amount toward HDA activity of catalysts. The NiMoS catalyst, prepared with 0.57 Ni/Mo molar ratio, exhibits the highest HDA activity among the catalysts in this study. The in-situ NO-DRIFT shows informative data along with other characterization techniques for catalytic performance explanation. This study shows that the in-situ NO-DRIFT could be used as a complementary characterization for HDA catalysts.

ENR-O-066

Effect of Regenerative Braking System on State of Charge and Energy Consumption of Battery Electric Buses under Uncertainty Driving Condition

Sorawit Wanitanukul[a,*], Kuskana Kubaha[a], Roongrojana Songprakorp[b]

[a]*Energy Management Technology Program, School of Energy, Environment and Materials, King Mongkut's University of Technology Thonburi, 26 Pracha-utid Rd., Bangmod, Toongkru, Bangkok 10140, Thailand.*

[b]*School of Energy, Environment and Materials, King Mongkut's University of Technology Thonburi, 26 Pracha-utid Rd., Bangmod, Toongkru, Bangkok 10140, Thailand.*

*E-mail: Sorawit.w@hotmail.com

Keywords: Battery Electric Buses (BEBs), Electric Vehicle (EV), Energy consumption, Real-world operation data, Regenerative Braking System (RBS), State of Charge (SOC)

An Electric Vehicle (EV) is coming by the topic of an environmental and energy efficiency solution, especially for a mass transit system. The EV still provides some technical limitations, such as driving range per charge, availability of charging stations, battery aging, charging time, and charging cost. Battery Electric Buses (BEBs) will be the initiative in public transportation. Because of the feasibility of the economy. The energy consumption of the BEBs is a key for vehicle and fleet designs. Most of the energy BEBs are consumed by the propulsion system, which is influenced by a driving condition, Heating, Ventilation, Air conditioning (HVAC), and auxiliary, respectively. The energy consumption from the propulsion system is the focus of this study. The real-world BEBs operation data, which are velocity and GPS profile, is built andinvestigated in MATLAB/Simulink. State of Charge (SOC) comes from the CAN-BUS and is used for the evaluation. The Regenerative Braking System (RBS) is used as the BEBs operating condition. These are the experimental design. The results are shown in this study. There are speed profile, power profile, energy profile, SOC evaluation, and energy consumption of the driving without RBS and the driving with RBS conditions. The results were highlighted and shown the Regenerative Breaking System (RBS) was suitable and worthy to use in battery electric buses. The electric motor and drive of the BEBs were 70% of regenerative braking efficiency. There are 6.31 kWh of RBS energy harvesting or 22% of the total energy propulsion consumed in the travel cycle. There are 17% savings on total energy consumption, which will affect the economic feasibility of BEBs operating. The energy consumption with RBS condition is approximately 1.23 kWh/km. There is slightly lower than the typical value.

ENR-O-072

MnO_2/N-doped Sugarcane Bagasse Derived Porous Carbon Nanocomposite as the Efficient Anode Material for Lithium-ion Battery

Krittaporn Pongpanyanate [a], Supacharee Roddecha[a,*], Chanita Piyanirund[a], and Panitat Hasin[b]

[a] *Department Chemical Engineering, Faculty of Engineering, Kasetsart University, Thailand*

[b] *Department Chemistry and Center of Excellence for Innovation in Chemistry (PERCH-CIC), Ministry of Higher Education, Science, Research and Innovation, Faculty of Science, Kasetsart University, Thailand*

krittaporn.po@ku.th, *fengsrro@ku.ac.th, chanita.pi@ku.th, fscipths@ku.ac.th

Keywords: bagasse, bagasse derived carbon material, lithium-ion battery, and manganese dioxide

Lithium-ion batteries (LIBs) have become the important electrical storage and conversion device, owing to their high energy density, excellent cyclic stability and low self-discharge. Nonetheless, the current commercial LIBs with graphite anode, whose specific capacity is limited to about 370 $mAhg^{-1}$, may be insufficient to meet the future human demand for high energy and high-power density devices. Sugarcane bagasse is the majority waste from sugarcane industries. Regarding to the high density of xylem and phloem in its bark, the bagasse is considered as a promising carbon precursor to prepare a porous carbon material with abundant transport channels. In addition, doping carbon electrode material with nitrogen functional group has been reported to improve the electrode's ionic conduction and capacity. Manganese dioxide (MnO_2) is currently the attractive anode material for LIBs according to its high capacity, low cost, and eco-friendliness. However, it is dimensionally unstable under long cycling runs. Hence, this work is aimed to sustainably develop the bagasse derived carbon electrode thereby doping with nitrogen functional group and compositing with MnO_2 nano-particles (MnO_2/N-BGC). The N-doped bagasse-based porous carbon substrate was also expected to improve the dimensional stability of the deposited MnO_2 nano-particles. The MnO_2/N-BGC was prepared by depositing the MnO_2 nano-particle onto the N-doped bagasse derived porous carbon substrate via the reduction of $KMnO_4$. Different initial loading concentration of $KMnO_4$ (i.e. 10, 40 and 60 mM) were applied to optimize the composite morphology and the corresponding electrochemical performance. Various characterization techniques, including XRD, and SEM equipped with EDS confirmed the deposition of the MnO_2 nano-particles onto the carbon meso-porous structure. The composite achieved by loading initial $KMnO_4$ concentration of 10 mM (10-MnO_2/NBGC) exhibited the highest electrochemical performance for the reversible capacity of 705 $mAh.g^{-1}$ at 0.5 C after 50 cycles, with Coulombic efficiency nearly 100%.

ENR-O-124

The Study of Zinc Oxide with Silicon Dots Thin Films Fabricated by Spin Coating Technique for Applying as Emitter Layer

Supanut Laohawiroj[a], Thipwan Fangsuwannarak[a,*], Peerawoot Rattanawichai[a], Warakorn Limsiri[a], Rungrueang Phatthanakun[b]

[a]School of Electrical Engineering, Institute of Engineering, Suranaree University of Technology, Nakhon Ratchasima, 30000, Thailand

[b]BL6a: Deep X-ray Lithography, Synchrotron Light Research Institute (Public Organization), Nakhon Ratchasima, 30000, Thailand

*thipwan@g.sut.ac.th

Keywords: Zinc oxide, Silicon powder, Thin film

A low-cost spin coating technique and rapid thermal annealing method have been utilized for the preparation of zinc oxide doped aluminum with Si dots thin film on the quartz substrates compared with zinc oxide doped bismuth thin film with low-temperature annealing. The dispersed Si dots particle in the film showed that these additional Si dots can be tunable material for light absorption applied in photovoltaic work. X-ray diffraction was used to study the nanocrystalline silicon and zinc oxide with the crystal grain size of ~100 and ~20 nm presented in the films, respectively. The optical result of the thin films shows that <20% of reflectance and >80% transmittance were presented in the film. The absorption edge of thin films that have occupied Si dots was expanded from the original zinc oxide which strongly absorbs UV wavelength (~380 nm) to near-infrared wavelength (~800 nm) depending on the amount of Si dots layer. For the electrical properties of the film, the two-probe method was used to observe the photocurrent gain under the illumination compared with the dark test and showed that the film can greatly respond to the light and provided a higher current density. Additionally, the increase in annealing temperature and amount of zinc oxide layer leads to the enchantment of the current density. Hence, these zinc oxide thin films can be an alternative candidate for the tunable absorption emitter layer of solar cells and can be applied for other optoelectronic devices.

ENR-P-055

Effect of Barium Iron Niobate Incorporation on Energy Storage Density, and Electrical Properties of Lead-Free Bismuth Sodium Titanate-Based Ceramics

Pharatree Jaita[1,2,*], Kamonporn Saenkam[2,3], and Gobwute Rujijanagul[2,4,5,6]

[1]*Office of Research Administration, Chiang Mai University, Chiang Mai 50200, Thailand*

[2]*Department of Physics and Materials Science, Faculty of Science, Chiang Mai University, Chiang Mai 50200, Thailand*

[3]*Graduate School, Chiang Mai University, Chiang Mai 50200, Thailand*

[4] *Science and Technology Research Institute, Chiang Mai University, Chiang Mai 50200, Thailand*

[5]*Research Center in Physics and Astronomy, Faculty of Science, Chiang Mai University, Chiang Mai 50200, Thailand*

[6]*Materials Science Research Center, Faculty of Science, Chiang Mai University, Chiang Mai 50200, Thailand*

*E-mail address corresponding author: pharatree@gmail.com (P. Jaita)

Keywords: Recoverable Energy Storage Density, Energy Storage Efficiency, Dielectric, Ferroelectric

In this research, the (1-x)($Bi_{0.485}Na_{0.388}K_{0.097}Ba_{0.021}Sr_{0.09}$)$TiO_3$-$x$Ba($Fe_{0.5}Nb_{0.5}$)$TiO_3$ or (1-x)BNKBST-xBFNb were fabricated by a solid-state mixed oxide. The effects of BFNb adding on phase evolution, microstructure, dielectric, ferroelectric, and energy storage density properties of the BNKBST ceramics (with x = 0, 0.01, 0.02, and 0.03 mol fraction) were investigated. X-ray diffraction analysis showed that all samples exhibited a single perovskite phase. With increasing BFNb content, a phase transition from mixed rhombohedral-tetragonal to more tetragonal phase was observed. The density value increased with increasing the additive content, which resulted in the improvement of the dielectric properties. In addition, the incorporation of BFNb into the BNKBST ceramic significantly affects the ferroelectric properties. The x = 0.03 ceramic showed high energy storage properties, *i.e.* it had a high recoverable energy storage density (W_{rec} = 1.25 J/cm^3) and good energy storage efficiency (η = 86.55%) at 120 ^{o}C and E = 75 kV. These results indicated that the (1-x)BNKBST-xBFNb system can be designed for high recoverable energy storage density value via a substitution induced relaxor state and developed this material for an electric power pulse energy storage applications.

ENR-P-122

Effect of Rapid Thermal Annealing Treatment on the Electrical Conductivity of Nanocrystalline Zinc Oxide Doped with Aluminum for Low Cost of Semiconductor Devices

Peerawoot Rattanawichai[a], Thipwan Fangsuwannarak[a,*], Karoon Fangsuwannarak[b], Supanut Laohawiroj[a], Warakorn Limsiri[a], DuangkamonPrasertdee[a], Sukamai Rattanatham[a], Rungrueang Phatthanakun[c]

[a]*School of Electrical Engineering, Institute of Engineering, Suranaree University of Technology, Nakhon Ratchasima, 30000, Thailand*

[b]*School of Mechanical Engineering, Institute of Engineering, Suranaree University of Technology, Nakhon Ratchasima, 30000, Thailand*

[c]*BL6a: Deep X-ray Lithography, Synchrotron Light Research Institute (Public Organization), Nakhon Ratchasima 30000, Thailand*

* thipwan@g.sut.ac.th

Keywords: AZO, rapid thermal annealing, electron transport layer, conductive improvement

In this work, spherical nanocrystalline zinc oxide doped with aluminum (nc-AZO) spin-coated on quartz substrates exhibited the improvement of conductivity and optical properties under the rapid thermal annealing (RTA) treatment. The nc-AZO nanostructure was prepared by varying atom percent of aluminum doped from 0.0at.%, 0.4at.%, 0.8at.%, 1.0at.%, 1.2at.%, 1.6at.%, and 2.0at% with the number of the layer from 1layer to 5layer. The nc-AZO films were formed at 500°C for 1 hr. annealing temperature provides low electrical conductivity and low photocurrent. RTA treatment at 930°C for 20 seconds in the ambient atmosphere condition was applied to nc-AZO film coated on a quartz substrate to perform the good spherical nc-AZO properties high transmittance and low resistivity, concomitantly which results in significant improvement of electrical and optical properties of nc-AZO on a quartz substrate. It is noticeable that the RTA can obtain nc-AZO nanostructure, good optical property, and high conductivity existence, simultaneously. The nano-spherical nc-AZO around 10-30nm diameter size at the film surface morphology provides the reflectance of 10%, and the transmittance of above 85% in the light wavelength between 250-850 nm. In addition, the energy band gap (Eg) of nc-AZO on quartz substrate provides 3.2-3.4eV and optical absorbance evaluated by Tauc plot is a crucial attribute to apply in a promising photonic device. Thus, the high electrical and optical qualities of such nc-AZO films could be used to produce an electron transport layer (ETL) for further emerging solar cells and transparent contact electrodes for low-cost semiconductor devices.

MATERIALS TECHNOLOGY FOR ENVIRONMENT

ENV-I-01

Graphene Quantum Dot Based Nanomaterials for Environmental Sensing and Pollutant Photodegradation

Hai Linh Tran[a]; Van Dien Dang[b]; Ruey-an Doong[c,*]

[a] 101, Sec. 2, Kuang Fu Road, Department of Biomedical Engineering and Environmental Sciences, National Tsing Hua University, Hsinchu, 30013, Taiwan.
b Faculty of Environment-Natural Resources and Climate Change, Ho Chi Minh City University of Food Industry, Ho Chi Minh City, 700000, Vietnam.
c 101, Sec. 2, Kuang Fu Road, Institute of Analytical and Environmental Sciences, National Tsing Hua University, Hsinchu, 30013, Taiwan.
*E-mail address: radoong@mx.nthu.edu.tw

Keywords: Graphene quantum dots (QGD); environmental sensing; photodegradation; pharmaceutical chemicals.

Carbon based nanomaterials such as graphene family and graphitic carbon nitride (g-C_3N_4) are novel materials which can not only serve as a photoelectrochemical catalyst but also act as optical and electrochemical electrode materials for sensing purposes because of their suitable band gap, high surface area, large pore size/volume, and good electrical conductivity. Herein, we report the possible fabrication and application of 0-dimensional graphene quantum dots (GQDs) for sensing, environmental and energy application. GQDs can be fabricated from naturally occurring carbon products like passion fruit juice and citric acid under hydrothermal conditions. The homogeneous and well distributed 5 – 10 nm GQDs can provide both strong fluorescent property as well as accessible electroactive sites and low resistance to accelerate the electrons and electrolyte ions transport, resulting in the excellent performance on optical and electrochemical detection of a wide variety of chemicals like Fe^{3+}, Hg^{2+}, nitrophenols, antibiotics and cancer cells. The combination of GQDs with g-C_3N_4 and Bi_2MoO_6 (NCD@BMCN) exhibits advanced advantages on high photocurrent density and low impedance to facilitate the excellent charge transfer efficiency for the enhanced photodegradation of ciprofloxacin (CIP) via indirect Z-scheme mechanism with GQD as a mediator to transfer electrons from the conduction band of Bi_2MoO_6 to the valence band of g-C_3N_4. Moreover, the influence of environmental parameters like pH, co-ion, and initial concentration on the photocatalytic degradation efficiency was investigated. The possible reaction mechanism as well as degradation pathways was also proposed. Results clearly signify that GQD-based nanomaterial is a promising carbon material with a great application potential in sensing, environmental and energy areas.

ENV-I-02

Development of Novel Water-Lean Solvent for CO_2 Capture Applications

Jak Tanthana*, Paul Mobley, Vijay Gupta, and Marty Lail
RTI International, Durham, North Carolina, 27709, USA
*jtanthana@rti.org

Keywords: CO_2 capture, water-lean solvent, gas absorption, technology demonstration

The most effective approach to reduce global carbon emissions is capturing CO_2 from large, point-source emitter such as power plants. Approximately one-third of the annual CO_2 emission is generated from the power industry. Research and development efforts have been made to scaleup CO_2 capture technologies which can be used at scale and reasonable cost. In near-term, solvents are the most promising technology for large-scale CO_2 capture in terms of technology maturity. The first-generation of solvent technologies, developed more than 40 years ago, such as aqueous monoethanolamine (MEA) are not commercially suitable due to their high energy consumption and high equipment cost. The high energy consumption stems from the vaporization of water to be used as the CO_2-stripping agent during the regeneration process. The high equipment cost is attributed to the low CO_2 absorption capacity combined with corrosive nature of these solvents requiring higher grade steel as materials of construction for the process equipment.

Recently, water-lean solvents (WLS) have emerged as an advanced solvent technology with reduced energy requirements. The low energy consumption is realized by replacement of the water by an organic diluent. RTI's WLS eCO_2Sol^{TM} has demonstrated low energy requirement, achieving as low as 2.1 GJ/ton-CO_2, a 42% reduction compared to that of MEA. eCO_2Sol^{TM} has shown to perform more than 90% CO_2 removal from gas streams containing 1-20 vol% CO_2. In addition, eCO_2Sol^{TM} displays significant performance improvements over MEA such as 4X CO_2 working capacity, 7X faster absorption kinetics, and 100X lower corrosivity. These performance results have been consistently observed from lab- to pilot-scale demonstration at various third-party testing sites around the globe. The improved solvent properties of eCO_2Sol^{TM} results in smaller process equipment with lower-cost materials of construction than that of MEA thereby lowering the equipment cost. A technoeconomic assessment of the eCO_2Sol^{TM} has shown ~25% improvement in cost of capture compared to MEA.

The eCO_2Sol^{TM} CO_2 capture process design differs only slightly from a conventional gas absorption process thus likely to be quickly adopted by industries. The process can be retrofitted to existing power plants or green-field installation. The combination of eCO_2Sol^{TM} formulation and process improvements has resulted in the low-cost CO_2 capture solvent technology that could be implemented at scale across various industries.

ENV-I-03

Flexible Thermoelectric Paper and Its Thermoelectric Generator from Bacterial Cellulose/Ag_2Se Nanocomposites

Supree Pinitsoontorn[a,*], Dulyawich Palaporn[a], Wiyada Mongkolthanaruk[b], Kajornsak Faungnawakij[c], Sora-at Tanusilp[d], Ken Kurosaki[d]

[a]*Institute of Nanomaterials Research and Innovation for Energy (IN-RIE), Department of Physics, Faculty of Science, Khon Kaen University, Khon Kaen 40002, Thailand.*

[b]*Department of Microbiology, Faculty of Science, Khon Kaen University, Khon Kaen 40002, Thailand.*

[c] *National Nanotechnology Center, National Science and Technology Development Agency, 111 Thailand Science Park, Pathum Thani, 12120, Thailand.*

[d] *Institute for Integrated Radiation and Nuclear Science, Kyoto University, 2, Asashiro-Nishi, Kumatori-cho, Sennan-gun, Osaka 590-0494, Japan.*

*E-mail address corresponding author: psupree@kku.ac.th

Keywords: flexible thermoelectric; Ag_2Se; bacterial cellulose; nanocomposite;

In this research, a flexible thermoelectric paper was fabricated from bacterial cellulose/silver selenide (BC/Ag_2Se) nanocomposites. Ag_2Se particles were *in situ* synthesized in the network of BC nanofibers. Several synthesis parameters that crucially affect the formation of Ag_2Se particles in the BC structure were investigated to understand the phase formation mechanism. Under the optimized conditions, the BC/Ag_2Se paper with a large proportion of Ag_2Se up to 75 wt.% was successfully obtained. The *in situ* synthesis limits the Ag_2Se formation within the nanopores of the BC structure. As a result, the sub-micro size Ag_2Se particles with narrow size distribution were homogeneously dispersed in the BC nanofiber network. The microstructure was further improved by hot-pressing, which increase the density of the BC/Ag_2Se paper and make the BC layered structure more compacted. These contributed to a significant enhancement of the thermoelectric properties, with the electrical conductivity of 23000 S/m and the Seebeck coefficient of -167 μV/K at 400 K. The power factor was 642 $\mu W/mK^2$ at 400 K, a very high value compared to other flexible thermoelectric research. The measurement of thermal conductivity yielded the κ value of 0.36 W/mK at 400 K, which led to the maximum *ZT* of 0.70 at 400 K. To demonstrate the thermoelectric conversion, five BC/Ag2Se paper pieces were connected in series to construct a thermoelectric module. The module is very flexible and can be curved to attach to any arbitrary shape of the hot/cold surfaces. In addition, the process for fabricating the BC/Ag_2Se paper is scalable without any use of advanced or expensive instruments. This makes it a very attractive choice as a flexible TEG.

ENV-I-04

An Electrochemical Journey from Screen-Printing to Additive Manufacturing (3D Printing): Towards Environment Protection

Craig E. Banks

Manchester Metropolitan University, United Kingdom

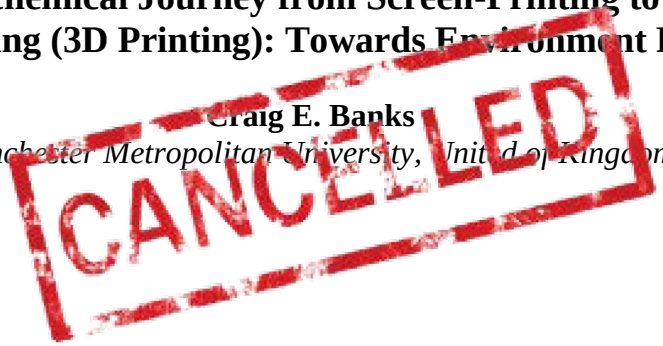

ENV-O-053

Development Luminescence from Sm^{3+} of Barium Titanium Bismuth Borate Glass for Orange Emission Material Application

Nawarut Jarucha[1,2], Yotsakit Ruangtaweep[1,2], Pichet Limsuwan[3], Hong Joo Kim[4],Jakrapong Kaewkhao[1,2] and Thanapong Sareein[5,*]

[1]Physics Program, Faculty of Science and Technology, Nakhon Pathom Rajabhat University, Nakhon Pathom 73000, Thailand

[2]Center of Excellence in Glass Technology and Materials Science (CEGM), Nakhon Pathom Rajabhat University, Nakhon Pathom 73000, Thailand

[3]Department of physics, Faculty of Science, King Mongkut's Institute of Technology Ladkrabang, Bangkok, Thailand

[4]Department of Physics, Kyungpook National University, Daegu, 41566, Republic of Korea

[5]Division of Industrial Materials Science, Faculty of Science and Technology, Rajamangala University of Technology Phra Nakhon, Bangkok 10800, Thailand

*thanapong.s@rmutp.ac.th

Keywords: Borate glass, Orange emission material, Samarium, Judd-Ofelt

Barium titanium bismuth borate doped with Sm^{3+} ions were prepared by using the melt quenching technique. Optical spectroscopy and Judd–Ofelt analysis were performed on the Sm^{3+} spectroscopic properties. It was found that the glass density was significantly increased with an increase in the doping concentration of Sm_2O_3. Moreover, it can absorb more photons in the visible light near the infrared region. The intense orange emission at approximately 600 nm wavelength via the $^4G_{5/2} \rightarrow {}^6H_{7/2}$ transition of Sm^{3+} occurs under various types of excitation, not only ultraviolet but also visible light and X-ray. The emission intensity of Sm^{3+} increases as the Sm_2O_3 concentration increases to 0.50 mol%. On the other hand, the decay time decreased as the Sm_2O_3 concentration increased. A color inspection from the Commission Internationale de l'Éclairage (CIE) defined in 1931 chromaticity diagram apparently that the Sm^{3+} doped glass emits an orange light. Thus, these response behaviors can be improved and developed for orangephotonic applications.

ENV-O-094

Preliminaty Study of Perfluorooctanesulfonic Acid (PFOS) Removal by Electrocoagulation using Plackett-Burmann Design

Samerkhae Jongthammanurak[a,*], Chabaiporn Junin[a], Chanchana Thanachayanont[a]

[a]National Metal and Materials Technology Center (MTEC), Pathum Thani, 12120, Thailand

*E-mail address samerkhj@mtec.or.th

Keywords: Electrocoagulation, PFOS Removal, Plackett-Burmann Design

Perfluorooctanesulfonic acid (PFOS) was listed persistent organic pollutant (POPs) under the Stockholm Convention and found in wastewater at ppb level. An electro-coagulation (EC) technique using steel electrodes (SS 400) was studied to investigate the removal efficiency of perfluorooctanesulfonic acid (PFOS) in sodium chloride solution.

A two-level Plackett-Burmann Design was used to estimate the effects of EC variables, i.e., PFOS concentrations (500 ppt and 8 ppb), current density (10 and 100 mA/sq.cm), NaCl concentrations (1 and 2 g/l), initial pH values (3 and 9), time (1.5 and 3 hours), stirring speed and electrode gaps (1 and 2 cm). Experiments were carried out in duplicates. Aqueous samples were filtered, diluted in methanol with 0.1% v/v acetic acid prior to the liquid chromatography tandem mass spectrometer (LCMS) analysis. Internal standard was used to minimize the matrix effects. PFOS removal efficiency was estimated by comparing the peaks areas of samples before and after the EC experiments.

Removal efficiency was estimated in a range of 1%-91% for 8 ppb PFOS concentrated samples. Time, stirring speed and initial pH value significantly affected the PFOS removal. At the high current level, stirring speed decreased the PFOS removal efficiency from approximately 60% to 10%. High current and dissolved oxygen, introduced by stirring, may favor any other reactions beside Fe(II,III)hydroxide formation. Characterization results of EC electrodes and flocs using Scanning Electron Microscope and Energy-Dispersive X-ray Spectrometer (SEM-EDS), X-ray diffraction (XRD) technique and Fourier Transform infrared spectroscopy (FTIR) will be presented.

ENV-O-110

Synthesis and Characterizations of MXene ($Ti_3C_2T_x$) for Adsorption of an Enrofloxacin Antibiotic

Channarith Be[a], Thilina R. Katugampalage [b], Paiboon Sreearunothai [c*], Pakorn Opaprakasit [d], Chamorn Chawengkijwanich[e]

[a] TAIST Tokyo Tech program, Sirindhorn International Institute of Technology, Thammasat University, Pathum Thani, 12120, Thailand

[b,c,d] School of Bio-Chemical Engineering and Technology, Sirindhorn International Institute of Technology, Thammasat University, Pathum Thani, 12120, Thailand*

[e] National Nanotechnology Center (NANOTEC), NSDTA, 111 Thailand Science Park, Khlong Luang, Pathum Thani, 12120, Thailand

*E-mail address Paiboon_sree@siit.tu.ac.th

Keywords: MXene; in-situ-HF etching; ion-exchange; adsorption

Two dimensional materials of titanium carbides or nitrides have sparked significant interest in many applications due to their distinct properties such as electrical conductivity, hydrophilicity, abundant functional group, and ion-intercalability. In this work, we report the preparation of Ti_3C_2 MXene using direct HF etchant and hydrochloric acid with lithium fluoride in order to form in-situ HF etchant. In addition, sodium chloride was added in the mixture of in-situ HF etchant in order to obtain sodium intercalated MXene. The simultaneous intercalation of Li or Na cations causes the obtained MXene to have larger interlayer space compared to that prepared using direct HF etchant. The morphology and elements presence were evaluated by using field emission scanning electron microscope (FESEM) and energy dispersion X-ray (EDX) spectroscopy analyses, respectively. The analysis shows that the MXene synthesized through the direct HF method and in-situ HF method have a multilayer accordion-like structure. EDX results suggest that Al element has decreased when comparing to the MAX phase (Ti_3AlC_2) precursor. The XRD revealed the MXene peaks at 8.70°, 6.49° and 7.02° corresponding to the d-spacing 10.02Å, 13.6Å and 12.55Å for sample etched using direct HF (50%HF MXene), in-situ HF (Li-Ti_3C_2) and in-situ HF with sodium intercalation (Na-Ti_3C_2), respectively. The direct HF-Ti_3C_2, Li-Ti_3C_2 and Na-Ti_3C_2 showed different enrofloxacin adsorption capacity of 2.0, 9.9 and 7.1 mg ENR/g MXene, respectively for the ENR initial concentration of 10 mg/L. The adsorption kinetic was further studied and was well fitted to the pseudo-second-order model. The Li and Na cations intercalated inside the MXene structure facilitate the ENR uptake greatly indicating important role of ion intercalations inside the MXene structure.

ENV-O-121

Effects of Insulated Perlite Materials Addition on Lanna Traditional Clay Roof Tiles

Ampika Rachakom[a] ,Pasinee Siriprapa[b] , Nittaya Keawprak[e], Anucha Watcharapasorn[c,f,*]

[a]Faculty of Science and Agricultural Technology, Rajamangala University of Technology Lanna, Chiang Mai 50300, Thailand

[b]Faculty of Art and Architecture, Rajamangala University of Technology Lanna, Chiang Mai 50300, Thailand

[c]Department of Physics and Materials Science, Faculty of Science, Chiang Mai University, Chiang Mai 50200, Thailand

[e]Thailand Institute of Scientific and Technological Research, Pathum Thani 12120, Thailand

[f]Center of Excellence in Materials Science and Technology, Materials Science Research Center

* anucha@stanfordalumni.org

Keywords: Lanna Traditional Clay Roof Tiles, Perlite, Insulation materials,

Trend of construction materials are focus on green living and concerns about carbon footprint in processing method. Especially, insulated perlite materials have attracted the attention in construction industry and agriculture due to lightweight, water retention, sound and heat insulation. Therefore, this research was investigated an effect of perlite on Lanna traditional clay roof tiles by varying perlite containing at 0, 10, 20, 30, 40 and 50 wt%. Fired clay/perlite composites were heated at 1100 °C for 15 minutes. Chemical composition and microstructure were determined by X-ray fluorescence (XRF), X-ray diffraction (XRD) and scanning electron microscope (SEM) techniques, respectively. In term of physical properties were investigated a firing shrinkage (%), water absorption (%), density (g/cm^3), bending strength and color values (L, a, b). Thermal conductivity was measured of all samples. Furthermore, these resulted can be useful to contribute to the production of more sustainable construction materials.

ENV-P-015

The Behavior of Bismuth Oxide on Tellurite Borate Oxide Based Glass System for Ionizing Radiation Shielding

S. Ravangvong[a,*], K. Pinnak[a], P. Glumglomchit[b], P. Lertlimpiyarat[b], B. Panwong[b], T. Keawkrid[b], K. Sriwongsa[c,d], J. Kaewkhao[e,f]

[a]*Division of Science and Technology, Faculty of Science and Technology, Phetchaburi Rajabhat University, Phetchaburi, 76000, Thailand*

[b]*Huahin Vitthayalai School, Hua–Hin, Prachuap Khiri Khan, 77110, Thailand*

[c]*Lecturers responsible for Bachelor of Education Program in Physics, Faculty of Education, Silpakorn University, Nakhon Pathom, 73000, Thailand*

[d]*The demonstration school of Silpakorn University, Nakhon Pathom, 73000, Thailand*

[e]*5Physics Program, Faculty of Science and Technology, Nakhon Pathom Rajabhat University, Nakhon Pathom, 73000, Thailand*

[f]*Center of Excellence in Glass Technology and Materials Science (CEGM), Nakhon Pathom Rajabhat University, Nakhon Pathom, 73000, Thailand*

* Corresponding Author: sunantasak.rav@mail.pbru.ac.th

Keywords: Ionizing radiation shielding, Telluroborate glass, Build-up factors

This research, the photons shielding parameters such as mass attenuation coefficients (μ_m), effective atomic number (Z_{eff}) and Kerma relative to air (K_a) for Bi_2O_3 based TeO_2-B_2O_3-Bi_2O_3 glass system have been simulated by WinXCom software program at energies of 10^{-3}–10^5 MeV. Also, buildup factors (BFs) have been estimated in wide energy ranging 15 keV–15 MeV for penetration depths (PD) until 40 mean free path (mfp). The results of glass system in formula (70–x)TeO_2–30B_2O_3–xBi_2O_3 at x = 10, 20, 30, 40 and 50 mol% exhibited that Bi_2O_3 partial replacement of TeO_2 adjust photons attenuation behaviors for get better. In addition, charged particles (proton: H^{+1} and alpha particles: He^{+2}) shielding parameters such as mass sopping power (MSP) and projected range (PR) were evaluated using SRIM software program at kinetic energy ranging 10 keV–10 MeV. The results may be inferred that glass sample with high Bi_2O_3 content is superb for photons attenuation while low Bi_2O_3 content is excellent H^{+1} and He^{+2} shielding glass. The results of this research may be useful in enhancing optimization of ionizing radiation shielding materials.

ENV-P-018

Optical Properties Improvement of Steel Slag Glass and their Ionizing Radiation and Neutron Shielding Properties

K. Sriwongsa[a,b,*], S. Neawhengtham[b], C. Tuncharoen[b], N. Anuntabundit[b], P. Intasan[b], P. Glumglomchit[c], K. Nameung[c], S. Ravangvong[d], W.Chaiphaksa[e,f] and J. kaewkhao[e,f]

[a]Lecturers responsible for Bachelor of Education Program in Physics, Faculty of Education, Silpakorn University, Nakhon Pathom, 73000, Thailand

[b]The demonstration school of Silpakorn University, Nakhon Pathom, 73000, Thailand

[c]Huahin Vitthayalai School, Hua-Hin, Prachuapkhirikhan, 77110, Thailand

[d]Division of Science and Technology, Faculty of Science and Technology, Phetchaburi Rajabhat University, Phetchaburi, 76000, Thailand

[e]Physics Program, Faculty of Science and Technology, Nakhon Pathom Rajabhat University, Nakhon Pathom, 73000, Thailand

[f]Center of Excellence in Glass Technology and Materials Science (CEGM) Nakhon Pathom Rajabhat University, Nakhon Pathom, 73000, Thailand

*e-mail: sriwongsa_k@silpakorn.edu

Keywords: steel slag glass system, gamma-ray shielding, neutron shielding.

This research, steel slag glass (SSG) system in formula (70-x)steel slag: $20Na_2O$: 10CaO: xB_2O_3 where x = 0, 10, 20, 30, 40, and 50 w% were prepared by using conventional melt quenching method at 1,200 °C and investigated physical, optical, ionizing radiation (uncharged and charged particles) and neutron shielding properties. Experimental on shielding properties of uncharged particles (γ-rays) were carried out with ^{22}Ba, ^{137}Cs and ^{60}Co sources at photon energies from 80-1332 keV while theoretical calculations were carried out with the WinXCom program. The results of γ-rays shielding for both processes are good agreements and 70steel slag: $20Na_2O$: 10CaO glass sample is excellent shielding compared with in glass system. In addition, all glass samples are better γ-rays shielding compared to some standard shielding materials. While charged particles (proton: H^+, alpha particles: He^{2+}) shielding properties of SSG system have been evaluated using SRIM program while electron particles were using ESTAR program. The results found that mass stopping power (MSP) and project range (PR) of proton and alpha particles while electron total stopping power (TSP) and Continues Slowing Down Approximation (CSDA) for 70steel slag: $20Na_2O$: 10CaO glass sample was excellent charged particles shielding glass. Also, fast and thermal neutron shielding of SSG have been evaluated and discussed. The results indicated that SSG system had potential to develop transparent and Pb-free shielding material.

ENV-P-019

The Effect of Nb_2O_5 for Gamma Rays, Fast and Thermal Neutrons Shielding on B_2O_3-TeO_2 Based Glasses

K. Sriwongsa[a,b,*], S. Makornkijwiboon[b], P. Glumglomchit[c], N. Suphakan[c], I. Tantiwatcharakultorn[c], R. Chetri[c], S. Ravangvong[d], J. Kaewkhao[e,f]

[a]*Lecturers responsible for Bachelor of Education Program in Physics, Faculty of Education, Silpakorn University, Nakhon Pathom, 73000, Thailand*

[b]*The demonstration school of Silpakorn University, Nakhon Pathom, 73000, Thailand*

[c]*Huahin Vitthayalai School, Hua–Hin, Prachuap Khiri Khan, 77110, Thailand*

[d]*Division of Science and Technology, Faculty of Science and Technology, Phetchaburi Rajabhat University, Phetchaburi, 76000, Thailand*

[e]*Physics Program, Faculty of Science and Technology, Nakhon Pathom Rajabhat University, Nakhon Pathom, 73000, Thailand*

[f]*Center of Excellence in Glass Technology and Materials Science (CEGM), Nakhon Pathom Rajabhat University, Nakhon Pathom, 73000, Thailand*

* Corresponding Author: sriwongsa_k@silpakorn.edu

Keywords: Gamma Rays Shielding, Fast and Thermal Neutrons Shielding, Glasses

This work, the glass system in formula (70-x)B_2O_3-30TeO_2-xNb_2O_5 at x = 0, 10, 20, 30, 40 and 50 mol% were determined gamma rays, fast and thermal neutrons shielding properties. The gamma rays shielding properties have been explained by some parameters such as mass attenuation coefficients (μ_m), effective atomic number (Z_{eff}) and half value layer (HVL). These parameters were evaluated by WinXCom software program at energies of 10^{-3}–10^5 MeV. While fast and thermal neutrons were calculated based on the macroscopic neutron capture cross-section. The results found that the addition of Nb_2O_5 by replacing B_2O_3 improved gamma rays shielding characteristic better. This event also improved fast neutron shielding. Whereas the result the opposite effect of thermal neutron was observed. These results reflected that glass sample with high Nb_2O_5 content is excellent for gamma rays and fast neutron attenuation while low Nb_2O_5 content is excellent thermal neutron shielding glass. The results of this study are useful in enhancing the efficiency of materials for shielding gamma rays, fast and thermal neutrons.

ENV-P-051

Characterization of Rubber Foam Added with Activated Carbon and Titanium Dioxide for Adsorption of White Rice Starch in Wastewater

Ratana Sananmuang [a,b*], and Doungdao Channei [a,b]

[a] *Department of Chemistry, Faculty of Science, Naresuan University, Phitsanulok, 65000, Thailand*

[b] *Center of Academic Excellence for Petroleum, Petrochemical, and Advanced Materials, Naresuan University, Phitsanulok, 65000, Thailand*

*E-mail address: ratana_s6@hotmail.com

Keywords: Rubber foam, Adsorption, Rice starch, Titanium dioxide

The white rice starch is the major ingredient of many kinds of food. So, these rice starch may be discarded and caused of wastewater. The objective of this study was to developed the rubber foam (RF) added with activated carbon (AC) and Titanium dioxide (TD) for removal of white rice starch from wastewater. There were 5 types of rubber foam prepared by adding AC and TD at the ratio of 4:1, 1:4, 5:0, 2.5:2.5, and 0:5. The surface characteristics of adsorbent was determined by SEM with EDAX. The adsorption of rice starch in synthetic wastewater was determined by batch experiment. The residues of rice starch were analyzed by COD technique. The studied parameters were pH (2-9), temperatures (30ºC,35ºC and 40ºC), initial concentration (100,300,500,1000 and 2000 mg L^{-1}), and adsorption isotherms. The results indicated that the SEM morphology of RF adsorbent showed a lot of porous characteristics. The percentages of adsorption (at 30ºC, pH 9) of rice starch onto adsorbents RF added with AC:TD at ratio of 4:1, 1:4, 5:0, 2.5:2.5, and 0:5 were 100, 98-100, 76-100, 74-100, and 74-100, respectively. In addition, the adsorption models were fitted to both Langmuir and Freundlich models.

ENV-P-052

Removal Efficacy of C4 Adsorbent for Telon Yellow A3R Dye and Its Kinetic of Reactions

Ratana Sananmuang [a,b*], Sorachon Yoriya[c], Wipharat Chuachuad Chaiyasith [a,b] Yuthapong Ud-nan [a,b], and Keswaree Kerdmongkhon [a,b]

[a] *Department of Chemistry, Faculty of Science, Naresuan University, Phitsanulok, 65000, Thailand*

[b] *Center of Academic Excellence for Petroleum, Petrochemical, and Advanced Materials, Naresuan University, Phitsanulok, 65000, Thailand*

[c] *National Metal and Materials Technology Centre (MTEC) 114, Paholyothin Rd., Klong 1, Klong Luang, Pathumthani 12120, Thailand*

*E-mail address: ratana_s6@hotmail.com

Keywords: Removal; C4 adsorbent; Kinetics; Talon Yellow A3R

The wastewater contaminated with dyes is still to be a serious problem of the textile industry. So, this study was to investigate the efficacy of C4 adsorbent for removal the Talon Yellow A3R dye from the solution using batch adsorption technique. The characteristics of C4 adsorbent was determined by SEM, FTIR, and BET. The dye concentration was measured by a UV-VIS Spectrophotometer at the wavelength 380 nm. The studied parameters were pH (4-10), temperatures (20ºC,30ºC and 40ºC), initial concentration (50, 100,200,300,400 and 500 mg L^{-1}), Contact time (30 -240 min) and equilibrium study (1-10 h). The results revealed that the SEM morphology of C4 adsorbent showed less porous characteristics. The EDAX analysis indicated some trace elements including carbon, oxygen, sodium, magnesium, silicon, aluminium, potassium and iron. The BET surface area, pore volume and average pore size were 0.6574 $m^2 g^{-1}$, 0.000145 $cm^3 g^{-1}$, and 0.8815 nm, respectively. The optimum pH of adsorption was 8. The effect of initial concentration showed the increasing of dye removal as the dye concentration increase. The dye removal at 30ºC and 40ºC was better than that of 20ºC. The equilibrium of dye adsorption was found to be reached at 6 h for all adsorption temperatures. When the contact time increased, the removal efficiency was slightly increase. In addition, the adsorption models were fitted to both Langmuir and Freundlich models. Based on the study of adsorption kinetics, it was found to be consistent with the pseudo-second order reaction equation model. Moreover, the negative ΔG^o value indicated the spontaneous reaction. The positive ΔH^o value represented the endothermic process.

ENV-P-080

Dye Removal from the Fabric Dyeing Process Wastewater by Municipal Solid Waste Fly Ash blended with Nano-TiO_2

Cholnikarn Thawinkarn[a], Kaweesin Sukkasem[a], Nutthawadee Kaewkumnerd[a], Yanisa Chinsot[a], Yongthanat Bunroong[a], and Pheeraphong Bunroek[a,*]

[a]Wat Phrasrimahadhat Secondary Demonstration School
Phranakhon Rajabhat University, Bangkok, 10220, Thailand
*pheeraphong@pnru.ac.th

Keywords: Dye Removal, Fly Ash, Nano-TiO_2, Photocatalytic

The objective of this research were to 1) blend nano-TiO_2 (P25) photocatalyst with municipal solid waste (MSW) fly ash from PTTGC and 2) study dye degradation efficiency by MSW fly ash blended with nano-TiO_2 (P25) photocatalyst. The sample was blended by mechanical method. The 0.02 mM methylene blue concentration was used to study dye degradation efficiency under UV light in the UV box for 60, 120, and 180 min. The samples were measured for absorbance at a wavelength of 663 nm with a Microplate reader. The results were found that nano-TiO_2 (P25) photocatalyst blended with municipal solid waste (MSW) fly ash from PTTGC in contents of 0%, 5%, 10%, and 15% nano-TiO_2 by weight. The study of dye degradation efficiency found that 60 min of reaction time, the percent removal of 0%, 5%, 10%, and 15% nano-TiO_2 samples were 77.00%, 82.46%, 84.88%, and 88.06% respectively. When the reaction time was 120 min, the percent removal of 0%, 5%, 10%, and 15% nano-TiO_2 samples were 81.00%, 85.96%, 89.07%, and 93.05% respectively. Finally, when the reaction time was 180 min, the percent removal of 0%, 5%, 10%, and 15% nano-TiO_2 samples were 87.13%, 90.29%, 91.74%, and 99.42% respectively. Therefore, by increasing the nano-TiO_2 (P25) photocatalyst, the percentage of dye removal can be increased. The MSW fly ash blended with nano-TiO_2 (P25) photocatalyst could be used in the treatment of wastewater from the dyeing process.

ENV-P-086

Development of Nano-TiO_2 Coated Koh Kret Pottery Surface for Dye Removal from the Dyeing Process Wastewater by the Photocatalytic

Sutasinee Srihong[a], Kanthanat Chullasupya[a], Palath Ruenchit[a], Ratchapol Saodang[a], and Pheeraphong Bunroek[a,*]

[a]Wat Phrasrimahadhat Secondary Demonstration School
Phranakhon Rajabhat University, Bangkok, 10220, Thailand
*pheeraphong@pnru.ac.th

Keywords: Dye Removal, Koh Kret pottery, Nano-TiO_2, Photocatalytic

The objectives of this study were 1) to develop TiO_2 nanoparticles coated on Koh Kret pottery surface and 2) to study the dye removal from dyeing process wastewater by the Photocatalytic. In this study, the nano-TiO_2 (P25) was sprayed on the surface of Koh Kret pottery with Air Brush. Then, the microscope confirmed it. The sample size was 5-6 mm in diameter. The concentration of nano-TiO_2 were 0.5%, 1.0%, and 1.5% W/V using ethanol as the solvent. The 0.02 mM methylene blue concentration was used to study dye removal from dyeing process wastewater under UV light in the UV box for 3 and 18 hours. The samples were measured for absorbance at a wavelength of 664 nm with a Microplate reader. The results revealed that the absorbance decreased from 0.83 to 0.50, 0.46, and 0.35 respectively at 3 hours of reaction time. After 18 hours, the absorbance decreased from 0.83 to 0.39, 0.15, and 0.11 respectively, which was greater than the decrease at 3 hours. It was ensured that the nano-TiO_2 could decompose dye by the Photocatalytic and apply them effectively to dye removal from dyeing process wastewater.

ENV-P-103

Degradation of Natural Rubber and Tire Sidewall under Thermophilic Aerobic Conditions

Chomnutcha Boonmee[a,*], Peeraphong Pokphat[a], Thanawadee Leejarkpai[a]
[a] *National Metal and Materials Technology Center, Pathum Thani 12120, Thailand*
* chomnutcha.boo@mtec.or.th

Keywords: Degradation, Air dried sheet, Weigh loss

In this study, the degradation behavior of natural rubber sheet (NRS), air dried rubber sheet (ADS) and tire sidewall (SW) under aerobic conditions at 52 ± 2 °C was investigated. NRS displayed 61.73% weight loss after test for 270 days and small fragile fragments were found after 360 days. The weight of ADS was reduced to 47.65% at the end of degradation test, whereas no degradation of tire sidewall was observed under test conditions. SEM micrographs revealed that irregular roughness with cracks and holes presented on both NRS and ADS surface, while the surface morphology of tire sidewall seems unchanged. Fourier Transform Infrared Spectroscopy (FTIR) revealed that change in the chemical structure during the degradation process. Details will be discussed.

METAL, ALLOYS AND INTERMETALLIC COMPOUNDS

MET-I-01

Challenges in Aluminum Alloys for Elevated Temperature Applications

Chaowalit Limmaneevichitr
Department of Production Engineering, Faculty of Engineering, King Mongkut's University of Technology Thonburi, Bangkok 10140, Thailand
*chaowalit.lim@mail.kmutt.ac.th (C. Limmaneevichitr).

Keywords: Al-Ni-Sc alloys/ Nanoparticles/ Elevated-temperature applications

Al-Si-based alloys are the most widely used among aluminum casting alloys because of their good castability, high corrosion resistance, and good weldability. However, their mechanical properties rapidly decrease when they are exposed to high temperature. Two main reasons causing the alloys to lose their mechanical properties are the coarsening of precipitates because of high diffusivity of Cu and Mg in aluminum and the dissolution of the eutectic silicon phase due to its low eutectic temperature. Many studies have attempted to find new aluminum-based alloys having a eutectic temperature higher than Al-Si (577 °C), which are more suitable for high-temperature applications. It was reported that eutectic aluminum-nickel alloys (Al-Ni) can fulfill these requirements. The Al-Ni alloy contains very fine rod-like Al3Ni eutectic structure, which has good chemical stability and excellent thermal properties up to 500 °C. In spite of these, the mechanical properties of Al-Ni are not good enough to apply to high-temperature engineering structures. The matrix of eutectic Al-Ni is relatively weak because the solubility limit of Ni in Al is low. Therefore, alloying addition to Al-Ni plays an essential role not only in improving the mechanical properties of the alloys by the precipitation mechanism but also in preserving the thermal stability and structure of eutectic Al_3Ni. Moreover, precipitates that result from the alloying elements should have high thermal stability to improve the high-temperature properties of the Al-Ni alloy as well.

Scandium (Sc) is one of the alloying elements having high thermal stability. Eutectic Al-Ni alloys with Sc additions were studied through the microstructure, resultant hardness after elevated temperature exposure, high-temperature tensile properties, fracture behavior, and TEM micrographs. We found that the hardness increases with increasing amount of Sc and remains high when the temperature reaches 300 °C, which is a result of precipitation hardening of Al3Sc precipitates. The hardness then decreases because of coarsening of the precipitates. The tensile properties at high temperature of Al-6Ni alloys with Sc additions are better than those of Al-6Ni alloy without Sc addition. This can also be explained by the occurrence of Al3Sc precipitates. The fracture behavior of the alloys has the same trend as the tensile properties. Therefore, Al-6Ni-0.4Sc is a new candidate for high-temperature engineering applications.

We furthered our study on the simultaneous addition of zirconium (Zr) and scandium (Sc) in Al. Dilute, binary Al–Sc and Al–Zr alloys form, upon aging, a high number density of coherent, stable Al_3Sc and metastable Al_3Zr L12-nanoprecipitates, respectively, providing a sizeable precipitation strengthening effect at ambient and elevated temperatures. Although the volume fraction of these nanoprecipitates is below 1 vol.% (based on the equilibrium phase diagram), they have high thermal stability and excellent coarsening resistance up to 300 ◦C for Al_3Sc and 450 ◦C for Al_3Zr. This is because of the slow diffusivity of Sc and Zr in Al. We found that simultaneous Zr and Sc addition provides a combination of rapid L12-precipitation from Sc and slow L12-coarsening from Zr, achieving better coarsening- and creep resistance than if equivalent amounts of Sc and Zr are added separately. Partial replacement of Sc with Zr also reduces the cost of the alloy, while maintaining good mechanical properties at both room and elevated temperature. We will briefly discuss the mechanism of simultaneous addition of Zr and Sc in Al that will lead to the potential of new aluminum alloy with increased creep resistance for the new challenging applications.

MET-I-02

Current and Future of Research on Austempering Ductile Iron

Usanee Kitkamthorn
[a]*School of Metallurgical Engineering, Institute of Engineering,Suranaree University of Technology, Nakhon Ratchsima, 30000 THAILAND*
*E-mail address k_usanee@sut.ac.th

Keywords: Austempering, Ductile Cast Iron, Ausferrite

The Austempered Ductile Iron has the advantages of high specific strength, high stiffness, and high wear resistance. The excellent properties are achieved by the heat treatment process applied to the ductile cast iron. The chemical compositions of ductile cast iron and as-cast microstructure also play roles on the formation ausferrite, the mechanical properties and thus the processing window. Research on ADI development including both the alternative controlling austempering cycle and the addition of alloying elements. In this work, recent research on ADI have been reviewed and future research have been suggested.

MET-O-017

Microstructure and Mechanical Properties of Sintered Fe-Cr-Mo-Si-C-(Ni) Alloys

A. Wanalerkngam[a,*], S. Boonmee[a], T. Yotkaew[b], M. Morakotjinda[b], R. Tongsri[b]

[a]*School of Metallurgical Engineering, Institute of Engineering, Suranaree University of Technology, 111 University Avenue, Suranaree Road, Muang, Nakhon Ratchasima 30000, Thailand*

[b]*Particulate Materials Processing Technology (PMPT) Laboratory, Thailand National Metal and Materials Technology Center, 114 Paholyothin Road, Khlong Nueng, Khlong Luang, Pathum Thani 12120 Thailand*

*E-mail address corresponding author: arisara.jane@gmail.com

Keywords: Sintered Fe-Cr-Mo-Si-C-(Ni) steel, nickel addition, bainite/martensite, mechanical property.

Previous research works revealed that sintered Fe-Cr-Mo-Si-C alloys, prepared from two different pre-alloyed powders, Fe-1.5Cr-0.2Mo and Fe-3.0Cr-0.5Mo, added with fixed 4.0 wt. % silicon carbide, had microstructures resembling that of a fully pearlitic ductile iron. In this work, it is motivated that the matrices of sintered Fe-Cr-Mo-Si-C alloys can be modified by altering phase transformations during post sintering cooling. Nickel, as austenite stabilizer, was selected to control austenite stability hence pearlite transformation was expected to be modified. Different nickel powder amounts (0.0, 1.0, 2.0, 3.0, and 4.0 wt. %) were added to sintered Fe-Cr-Mo-Si-C alloys. It was found that the matrices of sintered alloys was changed according to the added nickel contents. Bainite and martensite were observed to form in addition to pearlite in sintered Fe-3.0Cr-0.5Mo-Si-C alloys added with ≥ 1 wt. % nickel. By changing the sintered alloy matrix, the fractions of bainite and martensite in sintered Fe-1.5Cr-0.2Mo-Si-C-(Ni) alloys were lower. This indicates that the combined effect of Cr, Mo and Ni elements is important for bainite and martensite transformations in these sintered alloys. Flexural strength varied unsystematically with added nickel content. Macrohardness values increased slightly with increasing added nickel content.

MET-O-028

Effects of Heat Treatment and Equal Channel Angular Pressing on the Microstructure and Mechanical Properties of Al-Mg-Si Alloy with Erbium Addition

Mizuki Mikami[a], Chaiyasit Banjongprasert[a,b*]

[a] *Department of Physics and Materials Science, Faculty of Science, Chiang Mai University, Muang Chiang Mai, Chiang Mai, 50200, Thailand*

[b] *Center of Excellence in Materials Science and Technology, Faculty of Science, Chiang Mai University, Muang Chiang Mai, Chiang Mai, 50200, Thailand*

*chaiyasit.b@cmu.ac.th

Keywords: Al-Mg-Si alloy, Heat treatment, Equal Channel Angular Pressing, Erbium

Al-Mg-Si wrought alloy (6XXX) is one of the most common aluminium alloys used in industry. The 6XXX series have moderate strength and can be modified by minor elements such as scandium, strontium, manganese, and zirconium to achieve microstructural modification and improvement in mechanical properties. Moreover, the mechanical properties can be enhanced by ultrafine-grained structure, produced by Equal-Channel Angular Pressing (ECAP), one of the most effective techniques of Severe Plastic Deformation (SPD). In this work, the influence of Erbium (Er) addition, heat treatments, and ECAP on the microstructure and mechanical property of an Al-Mg-Si alloy has been investigated. Microstructure of as-cast, solutionized, peak-aged, and ECAPed samples with/without Er were characterized by Optical microscope (OM) and Scanning Electron Microscope (SEM). Elemental distribution in the microstructure was identified by Energy Dispersion X-ray Spectroscopy (EDS). Grain size and crystallographic information of α-Al were analyzed by Electron Back Scatter Diffraction (EBSD). Grain size and morphology of the Al-Mg-Si samples changed with an addition of Er. Homogenization at 570°C for 15 hours could dissolve the Er-rich intermetallics and Mg_2Si, with an incomplete dissolution of AlFeSi. The formation and refinement of intermetallics enhanced the hardness of the alloys. After ageing at 175°C, the hardness of the specimen increased until the peak age. Er addition has significant effect on the ageing response. The ECAP modified the microstructure through the accumulative strain in the samples. The synergetic effect of both heat treatment and ECAP could offer an opportunity for a high specific strength Al-Mg-Si alloys with an addition of Er.

MET-O-034

Mechanical Properties of Dual-Grained Cemented Tungsten Carbide

Chiraporn Auechalitanukul[a,*], Ryan McCuiston[a], Nisara Deswongsa[a], Nutchanart Phanlek[a], Vongsagon Changniam[a]

[a]King Mongkut's University of Tehnology Thonburi, Thungkru, Bangkok, 10140, Thailand

*chiraporn.aue@kmutt.ac.th

Keywords: Dual-grained microstructure, Cemented tungsten carbide, Powder metallurgy, Mechanical Property

Cemented carbides are widely used as cutting tool materials in many manufacturing processes due to their high hardness and durability. However, they can be brittle, and thus ways are sought to enhance their toughness. Cemented carbides with a dual-grain size microstructure, compared to a regular mono-grain size microstructure, have been shown to have higher toughness. In this study, a dual-grained tungsten carbide (WC) reinforced with cobalt (Co) was fabricated by powder metallurgy. The effects of the dual-grained microstructure on the mechanical properties of the WC-Co were investigated. A WC-20Co was made using coarse WC grains (6 μm), with fine WC grains (0.6 μm). The WC and Co powders were ball milled to blend them, compacted into specimens under 200 MPa, and sintered at 1340 ^{o}C for 1 hour in an Ar atmosphere. After sintering, the microstructures were observed. A decrease of the average WC grain size was found for increased fine grain content. The hardness increased with fine grain content up to 20 wt%. The strength was found to increase with fine grain content up to 15 wt%, but for 20 wt% there was a slight decrease of strength. In the 20 wt% specimen, the microstructure showed a thinning of the Co phase between the WC grains. It was observed that as the WC grain separation distance decreased due to the Co thinning, that the hardness increased, likely because the grains came into contact easier and limited the deformation. In tension or bending however, this deformation limit led to WC grain cracking and ultimately failure.

MET-O-041

Effects of Multiple Repair Welds at Rail Head to Serviceability

Thiraphong Nakthong[a,*], Bovornchok Poopat[a], Somporn Peansukmanee[a], Titinan Methong[a]

[a]Department of Production engineering, Faculty of Engineering, King Mongkut's University of Technology Thonburi, Bang Mod, Thung Khru, Bangkok 10140, Thailand

*thiraphong.n@mail.kmutt.ac.th

Keywords: Hardness Property / Microstructure / Multiple repair welding / R350HT

Generally, the welding procedure for restoration of damaged railhead is designed for single repairing. But the damages are always repeated at the same location. So, multiple repairs of the damaged railheads are needed. Nowadays, none of the research studies about the effect of multiple repairing welds on mechanical properties and microstructure on the railheads. The purpose of this study is to observe the effect of multiple from 1st to 4th repaired welding of R350HT rail steel by using Shielded Metal Arc Welding process. The hardness testing and metallography technique were done on the mechanical properties and microstructure to determine. The results are shown that macro-sections of weld were consisting of 3 main regions, weld metal, heat-affected zone, and base metal. The heat-affected zone was divided into a white heat-affected zone and a black heat-affected zone with a spheroidized carbides structure. The white heat-affected zone has a higher amount of spheroidized particles than the black heat-affected zone. The microstructure of black heat affected zone consists of lamella pearlite structure and spheroidized carbides structure which is a higher hardness property than a white heat-affected zone. Moreover, repeating welds caused the growth of the prior-austenite structure in the black heat-affected zone. It can be concluded that the multiple repaired welding affected both mechanical and metallurgical properties, and usability must be concerned.

MET-O-060

Railway Underfloor Chloride Deposition Rate Estimation from Atmospheric Corrosion Monitoring (ACM) Sensor and its Validation by ISO 16539 Accelerated Corrosion Test

Wanida Pongsaksawad[a, *], Benjawan Moonsri[a], Warut Butrassamee[a], Navin Innoy[a], Piya Khamsuk[a], Tawee Pogfay[b], and Pranpreeya Wangjina[a]

[a]National Science and Technology Development Agency, 111 Thailand Science Park, Phahonyothin Rd., Klong Nueng, Klong Luang, Pathum Thani, 12120, Thailand

[b]National Electronics and Computer Technology Center, 112 Thailand Science Park, Phahonyothin Rd., Klong Nueng, Klong Luang, Pathum Thani, 12120, Thailand

*E-mail address corresponding author: wanida.pon@nstda.or.th

Keywords: atmospheric corrosion monitoring (ACM) sensor, chloride deposition rate, railway underfloor, ISO 16539

Coastal railway is subjected to severe corrosion influenced by chloride ion from sea salt. The underfloor area has a long time of wetness with no washing from heavy rainfall. The components in this area commonly requires frequent maintenance during the service life. An atmospheric corrosion monitoring sensor (ACM sensor) was installed to monitor the time of wetness and total charge output at the underfloor structure of an in service-train. Meanwhile, representative coupons were exposed together with the sensor. After 3, 6, and 12 months, the sensor data and weight loss data were obtained. The results revealed linear correlation between corrosion loss vs. cumulative charge output. Therefore, corrosion loss can be estimated by ACM sensor. The atmosphere of underfloor environment can be simulated by ISO 16539 using actual chloride deposition rate data. To determine the amount of chloride deposition rate on the underfloor structure, ACM sensor output was calibrated with a stationary chloride monitoring station at the nearby train station and corresponding ACM sensor output data. A correlation between cumulative charge output from the two locations were observed. Thus, accelerated corrosion test according to ISO 16539 could be conducted based on estimated underfloor chloride level. A validation between ISO 16539 and actual corrosion loss was verified on carbon steel samples. The corrosion loss of this in-service railway line can be predicted from cumulative ACM sensor data. The atmosphere of underfloor condition can be simulated by ISO 16539 test such that similar approach can be conducted for other coastal routes to systematically plan for predictive maintenance.

MET-O-065

Compact Field Exposure Test of Hot-Dip Galvanized Steel and Zn-Al-Mg Coated Steel with and without Organic Coating Under Tropical Climate

Pranpreeya Wangjina[a], Piya Khamsuk[a], Benjawan Moonsri[a], Navin Innoy[a], Warut Butrassamee[a], Sikharin Sorachot[a], Pitichon Klomjit[b], and Wanida Pongsaksawad[a, *]

[a] *National Science and Technology Development Agency, 111 Thailand Science Park, Phahonyothin Rd., Klong Nueng, Klong Luang, Pathum Thani, 12120, Thailand*
[b] *National Center for Genetic Engineering and Biotechnology, 113 Thailand Science Park,Phahonyothin Rd., Klong Nueng, Klong Luang, Pathum Thani, 12120, Thailand*
*E-mail address corresponding author: wanida.pon@nstda.or.th

Keywords: Hot-dip galvanized steel, Zn-Al-Mg coated steel, Corrosion, tropical climate

Hot-dip galvanized coating (GI) and Zn-Al-Mg coating (ZAM) enhance corrosion resistance by zinc-based coating as cathodic protection for steel structures. In this study, GI and ZAM with and without organic coating were tested at 4 test stations under the tropical climate of Thailand. The test sites were located at Nakhon Ratchasima, Chon Buri, Samut Sakhon, and Prachuap Khiri Khan. Compact test racks were designed for 70x 70 mm coupons and attached to existing structures on sites. Test periods were 6, 12,and 18 months. Corrosion loss for specimens without organic coating was evaluated by weight loss method. Coating degradation behaviors were accessed by electrochemical impedance spectroscopy (EIS) and cyclic corrosion test for specimens with organic coating. Samut Sakhon and Prachuap Khiri Khan were right by the sea, but corrosion loss at Prachuap Khiri Khan was more aggressive than that at Samut Sakhon due to different chloride deposition rates. At all test sites, corrosion losses of GI were greater than that of ZAM. For organic coated samples, coating resistance tended to decrease with increasing exposure time. After 1000 hr. under cyclic corrosion test, some organic coating disbondment occurred on GI sample, while the organic layer on ZAM exhibited no noticeable change. The results from this work led to life time estimation of 60-micron thick coatings and recommended organic coating requirement in severe marine environment.

MET-O-098

A Study for Influence of PWHT on Sensitization Microstructure of AISI 316Ti Stainless Steel Weld Joints

Jade Wongsakul, Titinan Methong, and Bovornchok Poopat
Department of Production Engineering, Faculty of Engineering
King Mongkut's University of Technology Thonburi, Thung Khru, Bangkok, 10140, Thailand
E-mail: Jade.wskwelding@gmail.com

Keywords: sensitization, post weld heat treatment, inter-granular corrosion

The aim of this study was to investigate the influence of post weld heat treatment to microstructure of AISI 316Ti stainless steel. This study was started from welding 316Ti pipe with ER318Si filler metal, then the welded samples were post-weld heat treated at 800, 850, 900, 950, 1000, 1050 ºC for various times of 1, 4, 10 hours. Each specimen was analyzed the microstructure examination at base metal, heat affected zone, and welded area to study for volume, size, and distribution of TiC, TiCN. After that, the inter-granular corrosion testing (IGC test) was performed as per ASTM A262-15 Practice-E standard to find the appropriate heat treatment time and temperature. Selected specimens were performed tensile and bending test following ASME Section IX standard to prepare WPS and PQR. The results showed that, at the temperature above 950 ºC, no severe inter-granular corrosion was observed at heat affected zone, but severe corrosion was found at weldment area. Scanning electron microscopy (SEM) results showed that, at 1050 ºC heat treatment temperature, the corrosion was significantly decreased comparing to that of 1000 ºC. Also, the inter-granular corrosion tended to increase when post weld heat treatment time increased.

MET-O-120

Investigation of Surface Hardness and Roughness on Formability of Aluminum Alloy Sheet AA2024-T3 Subjected to the Shot Peening Process by Silica Shots

Jurarat Sawangpan[a], Sansot Panich[a,*], Tanakorn Jantarasricha[b], Anak Khantachawana

[a]*King Mongkut's University of Technology North Bangkok, Bangsue, Bangkok, 10800, Thailand*

[b]*Pibulsongkram Rajabhat University, Amphoe Mueang, Phitsanulok, 65000, Thailand*

[c]*King Mongkut's University of Technology Thonburi, Thung Khru, Bangkok, 10140, Thailand*

*sansot.p@eng.kmutnb.ac.th

Keywords: Shot Peening, Formability, Surface Hardness, AA2024-T3

In the aerospace-part manufacturing sector of the twenty-first century, lightweight materials have been utilizing and unsurprisingly replacing conventional steels in many applications. Aluminum alloys are among those light metals frequently used for making pivotal load-carrying components. Currently, the AA2024-T3 sheet aluminum alloy has established itself as a strong candidate in the market for the aerospace industry. Nevertheless, its biggest drawback from the manufacturing perspective is an insufficiency of formability. It fails shortly after the ultimate loading point at a room temperature. This reason induces to study how to improve the formability of the AA2024-T3 sheet aluminum alloy. Obviously, shot peening (SP) is one of a cold working process which produces a residual compressive stress layer on the material subsurface and improves material properties such as surface hardness and roughness. Plastic deformation happens by stretching surface layer of the base material when shots hit on the surface using compressed air. These results in an enhancement of their surface properties, which favorable properties can improve sheet material formability process that obtained prevent early failure during the sheet metal forming process.

This research work aims to improve surface properties, which reflect the enhanced material formability of aluminum alloy 2024-T3 sheet, having 1.2 mm of thickness by imparting surface residual compressive stress using the shot peening technique using silica particles of 0.1 mm in diameter. First, shot peening was carried out using compressed air in a nozzle with a pressure of 0.35 and 0.5 MPa, a nozzle to target distance of 150 and 250 mm, and a duration time ranging from 5 to 15 seconds. Based on the obtained peening sheet, the surface hardness and roughness tests were experimentally performed on the peened surface of material sheets. Additionally, the X-ray diffraction method is used for the calculation of residual stress induced in AA2024 T3 after the shot peening process. Consequently, the shot-peened and unpeened sheets were put through Hole expansion and Erichsen cupping tests to compare the results of the formability between the shot-peened and unpeened sheets. From the obtained results, it was found that peened sheets had a low surface roughness, increased surface hardness, which is better than the surface properties of no shot peening. Moreover, the result of compressive residual stresses is higher than the original material sheet. Lastly, the results of the formability tests show that the peened sheet on Hole expansion and Ericshen cupping tests are highly significant.

MET-O-127

Study of Intergranular Corrosion in 617-Ni Alloy Using Electrochemical Technique

Noppakorn Phuraya [a,*]
[a] *Department of Industrial Engineering, Faculty of Engineering, Mahidol University, Nakornprathom, 73170, THAILAND*
* noppakorn.phu@mahiol.edu.

Keywords: INCONEL 617, sensitization, intergranular corrosion, electrochemical reactivation (EPR)

INCONEL 617 is a creep-resisting material that can operate at high temperatures which affect to form M23C6 carbide along the grain boundaries and degrade the creep properties. Up to now, there is no quantitative investigation of this problem. Intergranular corrosion testing is, thus, introduced. Generally, the testing has two well-known methods, the acid etching test and electrochemical reactivation test. However, the acid etching method requires high concentrations of acid and takes long experimentation time. Moreover, it is not possible to quantitatively study intergranular corrosion. This research has been developed to study sensitization on intergranular corrosion in INCONEL 617 using electrochemical potentiokinetic reactivation (EPR) in base materials and creep rupture tests were conducted at 700, 750, 800 and 900 °C. The specimens were grouped to undergo three heat treatment conditions including 1) as-received specimens (AS-CR) 2) aged specimens (AG-CR) and 3) as-solutionized specimens (SO-CR). Then, specimens were subjected to electrochemical testing to indicate changes in the surface of the metal along with the intergranular corrosion (Pa value). The intergranular corrosion on specimen surface was characterized under Scanning Electron Microscopy (SEM). The EPR results showed that the Pa value of creep specimens was higher than base specimens. Pa value of the AG-base specimens has greater values than that of AS and SO-base specimens, respectively. This is because the Pa value contributes to the sludge of more $M_{23}C_6$ carbides at grain boundaries. For the creep specimens, it was also founded that Pa value at low temperature of AS-CR, AG-CR and SO-CR specimens is high, because the temperature and time to failure lead to the formation of high $M_{23}C_6$ carbides at grain boundaries through the intergranular corrosion easily. This is consistent with the characterization of intergranular corrosion through the electron images.

MET-P-062

Zn-Al Coatings Produced by Low Velocity Oxy-Fuel Technique with Different Powder Feed Rates

Duangrada Yuttakamthon[a,b], Hathaipat Koiprasert[c], Wanida Pongsaksawad[c], Chaiyasit Banjongprasert[b,*]

[a] Master's degree Program in Materials Science, Faculty of Science, Chiang MaiUniversity, Chiang Mai, Thailand

[b]Department of Physics and Materials Science, Faculty of Science, Chiang MaiUniversity

[c]Rail and Modern Transports Technology Research Center (RMT), National Science and Technology Development Agency

*Corresponding author's E-mail address: chaiyasit.b@cmu.ac.th

Keywords: Thermal spray coating, Flame spraying, Zn-Al alloy, Corrosion, Cathodic protection

Maintenance technology is very important for the railway industry in Thailand. Corrosion in steel railway components is one of the critical damages that lead to a premature maintenance. Thermal spray coating is a technique for corrosion protection. Low velocity oxygen fuel (LVOF) process or flame spraying is an on-site, flexible, and low-cost thermal spray technique. Moreover, it is also suitable for zinc and zinc alloys that can be used as a sacrificial anode to protect steel components in railway. This research focuses on the study of microstructure of the Zn pure and Zn- Al alloy coatings produced by LVOF. In addition, this research investigated the effect of feedstock powders and feed rates on the microstructure and corrosion behaviours of the coatings. The powder feed rates in flame spraying were varied. The electrochemical corrosion behaviors were observed by standard corrosion tests, including potentiodynamic polarization technique. The results showed that Zn-Al coatings by flame spraying could not produce a complete coating because the feedstock powder sizes were too small and resulted in a discontinuous powder feeding. Form polarization test of pure Zn coating, it was found that the coating, with a feed rate of 30 g/min had the lowest corrosion rate of 1.19 ± 0.92 mm/year with a porosity of 9.60 ± 1.87 vol%, while the coating with a feed rate of 45 g/min had a corrosion rate of 1.33 ± 0.92 with a porosity of 9.91 ± 1.66 vol%. Accordingly, a higher feed rate reduced corrosion resistance due to a higher porosity content in the coating. Therefore, the properties and corrosion resistance of both pure Zn and Zn-Al coatings are related to the amount of porosity of the coating, corresponding to a higher corrosion rate of the coating. When compared with LVOF coatings, arcsprayed Zn15Al shows better corrosion resistance and lower corrosion rate due to a lower amount of porosity.

MET-P-068

Identification of Martensitic Structures in Plastically Deformed 316L Stainless Steel by AFM/MFM

Pimsiri Rattanasopa[a], Pinit Kidkhonthod[b], Waraporn Piyawit[a,*]

[a]*School of Metallurgical Engineering, Suranaree University of Technology, Nakhon Ratchasima, 30000, Thailand*

[b]*Synchrotron Light Research Institute (Public Organization), Nakhon Ratchasima, 30000, Thailand*

*E-mail address corresponding author: wpiyawit@sut.ac.th

Keywords: 316L stainless steel; Martensitic transformation; AFM; MFM

Atomic force microscopy (AFM) is a particularly useful characterization technique in evaluating the microstructures and the surface topography of various materials at high spatial resolutions. Moreover, the AFM can be modified to the magnetic force microscopy (MFM) by inducing the magnetic field to the probe tip. The MFM can reveal the magnetic domain structure at a microscopic scale. The 316L stainless steel commonly has austenitic structures but it can be undergone martensitic transformation during loading applied. In the study, the compressive load was introduced to the 316L surface by using a vibrating cup mill machine. After deformation, the phase transformation from austenite to martensite and topographical changed had simultaneously occurred. Austenite is paramagnetic and becomes antiferromagnetic at room temperature. On the other hand, martensite is ferromagnetic. Due to their distinct magnetic properties, combining both AFM and MFM characterization methods may provide the chance to identify martensitic phase in deformed 316L structures. AFM/MFM micrographs showed the groove-like plastic deformation patterns. The deformed structures comprised of slips, mechanical twins, and/or shear bands. The martensite domain was found in the region of plastic deformation and at the intersection of those structures. The combination of AFM/MFM technique increases potentials to observe the deformation induced martensitic transformation (DIM). These findings were in a good agreement with the X-Ray diffraction analysis and color etching micrographs in order to confirm the existence of martensite and where the martensite formed. In conclusion, the combination of AFM/MFM technique can potentially provide the magnetic characteristics information under high resolution. Therefore, this technique can be applied to evaluate the dissimilarity between magnetic and non-magnetic structures in other materials.

MET-P-092

Thermal Stability of Al-Ni-Sc Alloy Fabricated by Equal Channel Angular Pressing

Sirinapa Shuecamlue[a], Phromphong Pandee[b,c], Ussadawut Patakham[d], Chaiyasit Banjongprasert[a,e,f,*]

[a]*Department of Physics and Materials Science, Faculty of Science, Chiang Mai University, Mueang Chiang Mai, Chiang Mai, 50200, Thailand*

[b]*Department of Production Engineering, King Mongkut's University of Technology Thonburi, Bang Mod, Thung Khru, Bangkok, 10140, Thailand*

[c]*Center for Lightweight Materials, Design and Manufacturing, King Mongkut's University of Technology Thonburi, Bang Mod, Thung Khru, Bangkok, 10140, Thailand*

[d]*National Metal and Materials Technology Center/NSTDA, Klong Luang, Pathum Thani, 12120, Thailand*

[e]*Center of Excellence in Materials Science and Technology, Chiang Mai University, Mueang Chiang Mai, Chiang Mai, 50200, Thailand*

[f]*Materials Science Research Center, Faculty of Science, Chiang Mai University, Mueang Chiang Mai, Chiang Mai, 50200, Thailand*

*Corresponding Author's E-mail: chaiyasit.b@cmu.ac.th

Keywords: Al-Ni alloy, ECAP, Al_3Ni microfiber, Scandium.

Improving the strength of Al alloys at elevated temperatures has been always the quest for metallurgists. Al-Ni alloys provide a high potential for applications at elevated temperatures. Moreover, equal channel angular pressing (ECAP) is one of severe plastic deformation (SPD) that can produce ultrafine-grained alloys with a high specific strength. This work presents the microstructure and thermal stability of Al-3Ni-0.4Sc alloy (wt.%) fabricated by ECAP. The ECAP process was repetitively carried out up to 5 passes (true strain ~5). The microstructure of ECAPed and heat-treated Al-Ni-Sc alloys were investigated by using scanning electron microscopy (SEM) and electron backscatter diffraction (EBSD) technique. Vicker's microhardness test was done to evaluate the mechanical property and thermal stability of the alloy. The ECAPed specimen shows an increase in fracture and refinement of Al_3Ni microfibers, resulting in more homogeneity of Al_3Ni phase in Al matrix. Al matrix grain size was also refined to 0.49 microns. Al_3Sc was formed during the heat treatment and thus increased the thermal stability of the microstructure. The hardness of the specimen with Sc remained at 925±26 MPa when heated at 300 ºC for 120 mins. The ultrafine grains and the Al_3Sc precipitates can help maintain the strength of the ECAPed specimen in long-term applications at elevated temperatures.

FUNCTIONAL POLYMERIC MATERIALS

POL-I-01

Polymeric Micellar Nanoreactors for Chemical Reactions in Water

Voravee P. Hoven[a,*], Wisanu Sombat[b], Panuwat Padungros[a]
[a]*Department of Chemistry, Faculty of Science, Chulalongkorn University, Bangkok 10330, Thailand*
[b]*Program in Petrochemistry and Polymer Science, Faculty of Science, Chulalongkorn University, Bangkok 10330, Thailand*
*vipavee.p@chula.ac.th

Keywords: Amphiphilic copolymer; Micelles, Post-polymerization Modification, Catalysis

Several chemical reactions are performed in organic solvents which are mostly toxic and eventually become problematic from both economical and environmental perspectives. To make chemical process "greener", this research aims to develop micellar nanoreactors that can accommodate chemical reactions in water, the most well-known and environmentally friendly media. Sequential post-polymerization modification of poly(pentafluorophenyl acrylate) (PPFPA), a hydrophobic and functionalizable polymer precursor with benzylamine and 1-amino-2-propanol yielded poly(benzylacrylamide)-*ran*-poly(*N*-(2-hydroxypropyl)acrylamide), PBzA-*ran*-PHPA. The random copolymers of controlled composition can self-assemble into well-dispersed nanoparticles in water having size in a range of 150-200 nm. These polymeric micellar nanoassemblies were used as nanoreactors for the Thia-Michael addition between various thiols and nitrostyrene derivatives. The nanoreactors of 0.5 wt% was found to increase the conversion up to 100% for all thiols at room temperature within 24 h in the absence of catalyst. Without the nanoreactors, the reaction conversion decreased with increasing alkyl chain length of thiol due to the solubility limitation in aqueous media. The micellar nanoreactors can be re-used for up to ten times while reasonably high reaction conversion was still maintained. On the other hand, post-polymerization modification of PPFPA with 1-amino-2-propanol and 1-(3-amipropyl)imidazole gave imidazolium-conjugated random copolymers that can self-assemble into water-dispersible micelles upon Cu coordination. Preliminary investigation suggested that the developed imidazolium-Cu micelles can serve as effective nanocatalysts for azide-alkyne click reactions. Since a wide range of chemical functionalities can be proportionally incorporated and varied as a function of selected nucleophilic modifiers, it is strongly believed that post-functionalization of polymer precursor to generate functional random copolymer followed by self-assembly would be a versatile route to customized nanoreactors/nanocatalysts for a variety of chemical and biochemical processes in aqueous media. This would not only comply well with "the 12 Principles of Green Chemistry" but also satisfy "the BCG economic model".

POL-I-02

Role of Chemistry in the Successful Development of Low Rolling Resistance Tires for Better Sustainability

Kannika Sahakaro[a,*], Wisut Kaewsakul[b], Chesidi Hayichelaeh[a], Wilma K. Dierkes[b], Anke Blume[b], and Jacques W.M. Noordermeer[b]

[a]Department of Rubber Technology and Polymer Science, Faculty of Science and Technology, Prince of Songkla University, Pattani Campus, Pattani 94000 Thailand

[b]Elastomer Technology and Engineering, Faculty of Engineering Technology, University of Twente, P.O.Box 217, 7500AE Enschede, The Netherlands

*E-mail address: kannika.sah@psu.ac.th

Keywords: Low rolling resistance tires; Silica-silane; Natural Rubber; Sustainability

Tire development is moving towards sustainability through various approaches, for example, by developing lower rolling resistance tire tread and by utilizing more sustainable raw materials including polymers, fillers, and additives. This presentation will highlight the development of silica-reinforced natural rubber (NR) for low rolling resistance or energy-saving tires. The successful use of silica with a silane coupling agent requires an optimum silanization reaction occurring during mixing. By understanding the chemistry involved and the mechanical process, compounds with high silica-rubber interaction, low filler-filler interaction, and fine filler dispersion can be achieved. Moreover, as the silanization can be catalyzed by diphenylguanidine (DPG) which is normally used as a secondary accelerator for vulcanization but the decomposition of DPG gives toxic aniline, various amine alternatives have been investigated. Different types of aliphatic amines having alkyl or cyclic structures and similar pKa were explored. Linear aliphatic amines that have better accessibility toward the silica surface and a shielding effect provide better performance than the cyclic ones. Among various types of amines studied, octadecylamine (OCT) provides the properties of silica-reinforced NR compounds closest to the reference with DPG, showing its potential as an alternative for DPG.

POL-O-024

Polydiacetylene/Zn^{2+}/Zinc Oxide Nanocrystal for Volatile Organic Compound Sensing Applications

Kawinphob Phetnam[a], Rakchart Traiphol[c], Nisanart Traiphol[a,b,*]

[a]*Laboratory of Advanced Chromic Materials, Department of Materials Science, Faculty of Science, Chulalongkorn University, Bangkok 10300, Thailand*

[b]*Center of Excellence on Petrochemical and Materials Technology, Chulalongkorn University, Bangkok 10330, Thailand*

[c]*Laboratory of Advanced Polymer and Nanomaterials, School of Materials Science and Innovation, Faculty of Science, Mahidol University at Salaya, Phuttamonthon 4 Road, Nakorn Pathom 73170, Thailand*

*Nisanart.T@chula.ac.th

Keywords: Nanocomposite, Polydiacetylene, Solvatochromism, Sensor

Polydiacetylene (PDA)/Zn^{2+}/zinc oxide (ZnO) nanocomposite is considered as a powerful material for colorimetric sensing applications. The color-transition occurs by external stimuli, for example temperature, acid-base, organic solvent, and biomolecule. When the π-π interactions in the backbone chain are disturbed, the color-transition from blue to red presents. From the previous study by our research group, the sensitivity of the nanocomposite increases when the size of ZnO nanoparticles decreases. Moreover, the shortening of PDA alkyl tail increases the sensitivity of nanocomposite materials. However, the length of alkyl segment adjacent to the PDA head group is difficult to apprise. In this work, the nanocomposite is prepared using ZnO nanocrystals of size 3.6 nm, which is much smaller than nanoparticles (65 nm) used in our previous works. The length of alkyl segment adjacent to the PDA head group is varied from 2 to 8 of methylene units while the alkyl tail is fixed at 10 methylene units. Ten types of volatile organic compounds (VOCs), including ethanol, n-butanol, methanol, n-propanol, tetrahydrofuran, 1,4 dioxane, acetone and, dimethyl sulfoxide, are used as stimuli. The color-transition behaviors are investigated by Ultraviolet–visible spectroscopy and digital camera. The molecular structure and interactions within the nanocomposites are explored by X-ray diffractometer and Fourier-transform infrared spectroscopy, respectively. We have found that, the shortening of PDA alkyl chain length systematically increases the sensitivity of the nanocomposite to VOCs. In addition, the sensitivity of PDA/ Zn^{2+}/ZnO sensors depends on the VOCs molecular structure. The linear molecules tend to disturb the nanocomposite structure at higher degree than the cyclic molecules. Our study provides the VOCs sensors with tuning sensitivity based on the PDA/ Zn^{2+}/ZnO nanocomposites.

POL-O-063

Development of the Organic Superhydrophobic Coating on Plastic Sheet for Food Packaging Applications

Pakjira Sirirutbunkajal*, Yolada Issaraseree, Pawarisa Wijaranakul, Bongkot Hararak, Charinee Winotapun*,
National Metal and Materials Technology Center (MTEC), Thailand Science Park (TSP), Pathum Thani, 12120, Thailand
*pakjira.sir@ncr.nstda.or.th and *charinew@mtec.or.th

Keywords: Superhydrophobic, Self-cleaning, Beeswax, Lignin

Currently, the organic superhydrophobic coating (OSC) is an interesting topic in the food packaging applications due to environmentally friendly, nontoxic, and inexpensive. This coating can prevent the waste of liquid foods adhered to the inside of containers. Therefore, this study focused on the development of OSC coated on plastic sheet for improving wetting property of the food packaging. Beeswax and lignin approved by U.S. Food and Drug Administration were used to prepare the OSC. The important parameters such as lignin content (0.15 and 0.3 g), beeswax content (0.15, 0.2, 0.25, and 0.3 g), organic solvent content (8, 14, 17 and 19 ml), and mixing process (hot plate stirrer and ultrasonic probe) were varied. The OSC was coated on the polyethylene terephthalate (PET) sheet using spray coating. The micro/nanostructure of coating surface, water contact angle (WCA), sliding angle (SA), self-cleaning, mechanical robustness of the sample surface were investigated. From these results, it was found that lignin content of 0.15 g, beeswax 0.3 g, the solvent content of 14 ml, and mixing with the ultrasonic probe for 2 min is the optimal condition to improve all properties. The micro/nanoscale structure was observed on the coating surface using confocal laser scanning microscopy. The high WCA of approximately 159.2 ± 6.0 degrees and low SA of 5 degrees were achieved while the low WCA of the neat PET sheet were 73.4 ± 2.2 degrees and the drop of water did not move on the neat PET sheet at 5 degrees. For food packaging applications, the OSC was coated on the PET cups. The various liquid foods such as sauce and honey were used to investigate the wetting property of the packaging. The cups were filled with the variety of liquid foods. After pouring out of liquid foods from the container, there was no residues in the cup covered with the super-hydrophobic coating. Form overall results, this study demonstrates that the developed OSC coated on plastic surface has a high potential for food packaging application in reducing the residue of liquid foods form the container avoiding the food wastes.

POL-O-078

Development of an International Standard for Rubber Sheets for Livestock – Dairy Cattle – Specification

Chayapha Nimsuwan*, Pairote Jittham, Pongdhorn Sae-Oui
National Metal and Materials Technology Center, Pathum Thani, 12120, Thailand

Keywords: International standard, Rubber sheet, Livestock, Dairy cattle

A rubber sheet for dairy farming is generally used to provide comfort and reduce lameness or pain from long standing, lying, and getting up on a hard surface. Despite the worldwide usage, there was no international standard indicating the specification for this product. This project was therefore proposed as a new work item proposal (NWIP) to the International Organization for Standardization (ISO) under the purview of technical committee 45 (ISO/TC45), on behalf of Thailand, to develop an international standard (ISO) for rubber sheets for dairy cattle. Extensive research was conducted regarding to physical properties and product performances. The standard draft was established and subsequently circulated to ISO members for gathering comments and suggestions. After being discussed amongst ISO members, the specification of the rubber sheet is summarized as follows: hardness range of 50-80 shore A, tensile strength $\geq$ 3 MPa, elongation at break $\geq$ 80%, and volume loss $\leq$ 300 mm^3. The product shall be non-slippery (coefficient of friction under wet and dry conditions $\geq$ 0.40) and its deformability under specific conditions shall be 1.0-9.0 mm for rubber sheets intended to be used in walking area and shall not less than 5.0 mm for those intended to be used in lying area. The final draft standard was finally approved and published in September 2021 as ISO 22941:2021 Rubber sheets for livestock – Dairy cattle – Specification.

POL-O-095

Effect of Glucose as Pore Former on Physical and Morphological Properties of High Ammonia Natural Rubber Latex Film

Jedsada Rueangsen[a,*], Weeradech Kiratitanavit[a]
[a]Department of Mining and Materials Engineering, Faculty of Engineering, Prince of Songkla University, Hat Yai, Songkhla, 90110, Thailand
*jrdtc21@hotmail.com

Keywords: High Ammonia Natural Rubber Latex, Glucose, Pore Former

High ammonia natural rubber latex (HANR) concentrate is an important agricultural product in Thailand, particularly in the south. It has been utilized in a number of applications, including gloves, tubes, and adhesives. In this research, this type of latex has been used to develop porous films, which maybe further used in agricultural and coating applications. To make the porous film, HANR was mixed with glucose, which acted as a pore-forming agent, in varying concentrations of 0, 5, 10, 15, and 20 parts per hundred of rubber (phr). The films were then prepared by casting, followed by drying and glucose leaching to form a porous structure by immersing the films in water. The physical and morphological characteristics of the films were then used to determine the effect of the pore former. By analyzing the characteristic peak of glucose, the spectroscopic technique as FTIR was employed to determine the remaining glucose. According to the preliminary findings, the glucose and other organic substances containing within HANR were eliminated from the films. Consequently, as the glucose content of the film increased, its optical properties improved, becoming increasingly translucent to nearly transparent. The morphological studies by using the Scanning Electron Microscope (SEM) technique and water absorption were conducted to determine the porosity of latex films. Surprisingly, a latex film prepared with a high glucose loading has been found to have a dense structure with a lower ability for water absorption. The reason will be discussed in more detail in this research work.

POL-O-097

Study on Microperforated Biodegradable Films for Fresh Produce Packaging Applications

Charinee Winotapun[a,*], Yolada Issaraseree[a] and *Pattarin* leelaphiwat[b,*]
[a]*National Metal and Materials Technology Center, National Science and Technology Development Agency, Thailand Science Park, Pathum Thani, 12120, Thailand*
[b]*Department of Packaging and Materials Technology Faculty of Agro-Industry, Kasetsart University 50 Ngam Wong Wan Rd. Ladyao District, Chatuchak, Bangkok 10900*
*E-mail address: charinew@mtec.or.th and *pattarin*.le@*ku*.ac.th.

Keywords: microperforated film, biodegradable film, laser perforation, fresh produce packaging

This study focused on the development of microperforated biodegradable film fabricated using CO_2 laser with infrared wavelength of 10.2 μm. The polylactic acid (PLA) and polybutylene succinate (PBS) films were produced via blown film extrusion. These films were perforated using various laser pulse fluence. From the results, it was found that the microhole formation on PLA and PBS film was firstly observed at laser fluence of 147.9 J/cm^2 and 129.4 J/cm^2, respectively. The size and shape of holes on the film were observed by optical microscope. The re-solidified rim surrounding microhole was noticed. The area and diameter of microhole increased with increasing laser fluence. From mechanical testing, it was noticed that the *tensile failure* of microperforated film did not occur at microhole position. The Young's modulus, tensile strength, and elongation at break of microperforated films were almost the same value as the neat film without microhole. Besides, microperforated film showed a significant improvement in oxygen transmission rates (OTR) and carbon dioxide transmission rates (CO_2TR) over than that of the neat film. The gas transmission rates can be tailored by the hole diameter and number of microholes. Very high OTR film of ~100,000 cc/m^2.d could be achieved for microperforated film. To demonstrate the microperforated film applications, banana was packed in microperforated PBS bag and stored at 25 °C. The bag size was 12 x 22 cm corresponding to the film surface area of 528 cm^2. The O_2 concentration inside the PBS packaging without microhole decreased rapidly to 1% while CO_2 generated up to 40% within storage time for 1 d. Microperforated film with OTR and CO_2TR of approximately 4,800 and 6,000 cm^3/528 cm^2.d, respectively, was clearly shown to create modified atmosphere condition in the package. The steady state level of 6% O_2 and 16% CO_2 was achieved. Overall results clearly demonstrated that CO_2 laser perforation process can create the equilibrium modified atmosphere inside the packaging for keeping the freshness quality of banana for 6 d.

POL-O-111

Characterization of Nanocellulose Extracted from Used Papers

Weeradech Kiratitanavit[a,b*]
[a]*Department of Mining and Materials Engineering, Faculty of Engineering, Prince of Songkla University, Hat Yai, Songkhla, 90110, Thailand*
[b]*Center of Excellence in Metal and Materials Engineering (CEMME), Prince of Songkla University, Hat Yai, Songkhla, 90110, Thailand*
*kweeradech@eng.psu.ac.th

Keywords: Characterization, Nanocellulose, Ultrasonic Extraction, Used Papers

Paper is considered an environmentally friendly product because it is made from cellulose-rich wood as naturally occurring material. Even though the paper has excellent biodegradability under appropriate conditions and can be reused and recycled, used paper has become the predominant waste product due to the difficult in collecting and sorting used paper products. Used papers, including office paper and paper bag, are used as raw materials for nanocellulose extraction in this study to address the issue of paper waste. To obtain pure cellulose, the research began with a study and analysis of the effect of paper preparation (deinking and bleaching processes). The effect of ultrasonic extraction times of 0, 15, 30, and 60 minutes on the extraction of nanocellulose from used paper was then determined. Finally, the extracted nanocellulose was analyzed to compare their chemical structure and morphological properties using FTIR and SEM, respectively. The preliminary results indicated that nanocellulose in fibrillary form with a diameter of 50 nm could be extracted from both types of paper sources at 60 minutes of extraction time. However, nanocellulose extracted from paper bag demonstrated more distinct fiber separation properties than nanocellulose extracted from office paper. FTIR analysis of the chemical structure of nanocellulose prepared from used office paper revealed the characteristic peak of amorphous cellulose, whereas the dominant peaks indicating inter-hydrogen bonding can be observed in the nanocellulose extracted from paper bag. These help confirm that the cellulosic chain has been shortened as a result of this extraction method.

POL-O-112

Enhanced Mechanical Properties and Improving Wetting Ability of Polypropylene/Cassava Pulp Composites

Natcha Prakymoramas[a,*], Sanya Keawket[a] Jareenuch Rojsatean[a], Kawin Keeratipinit [a], Bongkot Hararak[a], Wuttipong Rungseesantivanon[a], Charinee Winotapun[a,*]

[a]National Metal and Materials technology Center (MTEC), Klong Nueng, Klong Luang Pathum Thani, 12120, Thailand

*E-mail address: natchap@mtec.or.th and and charinew@mtec.or.th

Keywords: Cassava pulp, Polypropylene, Mechanical properties, Wetting properties

Natural cassava pulp was selected as a bio-based reinforcement in polymer composites to enhance mechanical and wetting properties of ubiquitous plastic for eco-friendly products. Therefore, this study focused on the development of reinforcement of polypropylene composites with cassava pulp to improve mechanical properties and wetting ability. The cassava pulp was milled to obtain an average particle size of 284.48 $\pm$ 16.46 µm. The obtained cassava pulp was pre-dried at 80 °C for 3 hrs prior to melt-extrusion process. The composites consisting of polypropylene, 10 wt% cassava pulp and 3 phr compatibilizer (PP-gMA) were fabricated via a twin screw extrusion and injection molding. The effects of cassava pulp blended with polypropylene on the mechanical and wetting properties were investigated. Tensile and bending test were performed using universal testing machine. The wetting properties were characterized using contact angle goniometer. From the results, incorporation cassava pulp can enhance tensile strength (4.85 %) and Young's modulus (14.38 %), and flexural modulus (23.30 %) compared with those of neat polypropylene. These indicate higher stiffness of the natural fiber-filled composites. However, it was observed that the water contact angle of the polypropylene/cassava pulp composite surface was lower than that of neat polypropylene (approximately 12.85%). To solve this problem, the surface microstructure patterns were successfully fabricated via hot-embossing technique. The fabricated microstructure could enhance surface hydrophobicity. By comparing the composites surface with and without microstructure patterns, the water contact angle of neat-polypropylene and polypropylene/cassava pulp composite with microstructure obviously increased by 29.74% and 41.86 %, respectively. From overall results, the relationship between the cassava pulp, polypropylene and surface microstructure can be used to develop materials with high mechanical and wetting properties.

POL-O-123

Possibility Epoxidized Natural Rubber Replacement Acrylonitrile Butadiene Rubber Gasket

Karnda Sengloyluan[a,*], Apissara Komkay[a], Nattapon Uthaipan[a]
[a]*International College, Prince of Songkla University, Songkhla, 90110, Thailand*
*karnda.s@psu.ac.th

Keywords: Epoxidized natural rubber, seal, gasket, acrylonitrile butadiene rubber

The investigation of the effect of epoxidized natural rubber (ENR) to replace some acrylonitrile butadiene rubber (NBR) in gasket formulation is presented in this work. Most gasket and seal formulations are produced based on NBR compounds which are indicated by their polarity characteristics. ENR is a modified natural rubber (NR) with presenting of epoxy groups on its structure leading to improving the polarity of NR. Moreover, NR is produced from a renewable source while NBR is produced from a petrochemical product. ENR with 50 mol% epoxide (ENR50) is blended with NBR containing 80 phr of carbon black (N550). The ENR50/NBR blends were varied from 100/0, 90/10, 80/20, 70/30, 60/40, 50/50, 40/60, 30/70, 20/80, 10/90, and 0/100 to study cure characteristics and mechanical properties. Mooney viscosities of the blends are interestingly shown that viscosities of the blends dramatically decreased with an increasing amount of ENR50 content which is the same trend with scorch time and cure time. Moduli at 100% and 300% strain are not significantly different, but reinforcement index and tensile strength increase with an increasing amount of ENR50 in the blends. These results must be influenced by superior blend compatibility and the interaction between carbon black and epoxy groups of ENR50 together with acrylonitrile groups of NBR. At the low amount of ENR50 at 10-30 phr, tensile strengths of the blends are not different, but it tends to increase when the use of ENR50 above 40 phr. Tear strength of NBR vulcanizates is higher than that of ENR50 vulcanizates. However, the tear strength of ENR50/NBR blends at 30/70, 40/60, and 50/50 shows the same level with NBR result. Swelling test of the blends in an engine oil shows the same level with NBR pure even though ENR50 was used up to 80 phr or blend ratio of ENR50/NBR at 80/20 and it is slightly increased at the blend ratio of 90/10 and pure ENR50 vulcanizates, respectively. However, the swelling test of overall samples are considerably low because the %swelling is lower than 1%. Aging resistance of ENR50/NBR blends was studied at 100˚C and 120˚C for 72 hr. It is found that the aging properties of the blends are poorer when increasing the aging temperature. ENR50 vulcanizate shows surprisingly higher aging resistance than NBR vulcanizate, while the aging properties of the blends are in between ENR50 and NBR properties. From the overall results, it can be concluded that ENR50 shows a positive potential to replace some of NBR content for gasket applications and the amount of ENR50 in the blends can be used up to 50 phr without inferior mechanical properties and swelling resistance.

POL-O-129

Improving Dispersion of Conductive Carbon Black in Natural Rubber Latex using Methyl Cellulose and Carboxymethyl Cellulose

Natsaporn Butsri*, Sasitorn Srisawadi, Siwaporn Srimongkol, PanithiWiroonpochit, Kittaporn Utra,
National Metal and Materials Technology Centre (MTEC), National Science and Technology Development Agency (NSTDA), Pathum Thani, 12120, Thailand
* natsaporn.but@ncr.nstda.or.th

Keyword: Cellulose, Conductive carbon black, Conductive natural rubber, Strainsensor

Flexible strain sensors are getting wide attention because they can be used in a variety of applications such as electronic skin, health monitoring sensors, wearable strain sensors, etc. Typically, natural rubber (NR) has excellent flexibility and fatigue resistance. Hence, it has a great potential to be used as a matrix of conductive polymer composite for the flexible strain sensors. Our previous study successfully prepared the conductive NR latex using conductive carbon black (CCB.) However, when adding more volume of the CCB to the latex, it was found that the CCB was not well dispersed. In this research, novel conductive natural rubber was prepared with an addition of cellulose to effectively improve the dispersion of the CCB in the latex. Effects of types and concentrations of the cellulose on the dispersion of the CCB network in the conductive NR and its electromechanical properties were studied. The fact that electrical resistances on the top and bottom surfaces of the specimens were measured approximately the same is strong evidence of the effective conductive network that was formed by an excellent CCB dispersion. Morphology of the specimen was studied using transmission electron microscopy (TEM) and it confirmed that both methyl cellulose and carboxymethyl cellulose can help disperse the CCB in the latex. In addition, a relative resistance change ($\Delta R/R_0$), which reflects the electromechanical sensitivity of the sample, increased as the cellulose content increased. It was found that the carboxymethyl cellulose at 1.2 phr had the largest gauge factor of 616.14 (at 80-100% strain range) and had a good reproducibility of at least 300 cycles. This indicates that the conductive natural rubber filled with the CCB and the carboxymethyl cellulose could be further developed as the flexible strain sensors for applications with high sensitivity requirements.

POL-P-071

Fabrication of Thermo-Responsive Rhodamine Derivatives/Polymer Blend Films for Optical Temperature Indicator Label Applications

Sanguansak Sriphalang [a,b,*], Kannika Putho [e], Sutthikan Auttaphan [e], Chatthai Kaewtong [d] and Datchanee Pattavarakorn [a,c,*]

[a] *Department of Industrial Chemistry, Faculty of Science, Chiang Mai University, Chiangmai, 50200, Thailand*

[b] *Graduate School, Chiang Mai University, 50200, Chiang Mai, Thailand*

[c] *Center of Excellence in Materials Science and Technology, Faculty of Science, Chiang Mai University, Muang, Chiang Mai, 50200, Thailand*

[d] *Nanotechnology Research Unit and Supramolecular Chemistry Research Unit, Department of Chemistry and Center of Excellence for Innovation in Chemistry, Faculty of Science, Mahasarakham University, Maha Sarakham, 44150, Thailand*

[e] *Program of Chemistry, Faculty of Science, Ubon Ratchathani Rajabhat University, Ubon Ratchathani 34000, Thailand*

* sanguansak.s@ubru.ac.th * datchanee.p@cmu.ac.th

Keywords: Rhodamine B, Thermochromic dyes, Thermo-responsive, Polymer film

This research, the synthesis and properties of rhodamine B derivatives to be used as an easy-to-use optical temperature indicator label have been studied. The color change of the rhodamine solution, filter paper dipped in rhodamine solution and rhodamine/polymer blend film were tested. It was found that the solution and the filter paper changed from colorless to pink after heat treatment. For the rhodamine/polymer blend films, it was also found that all films exhibited a colorless to pink color change when taken from room temperature to 80 °C. Moreover, the films turned orange when observing the color change under UV light. FT-IR (Fourier Transform Infrared Spectroscopy) and UV-Vis spectroscopy were used to study the color change mechanism. The FT-IR spectra of Open and closed structures of rhodamine B showed broadband at 3450-3250 cm^{-1} which attributed to O-H stretching of the carboxylic group of Open structure of Rhodamine B and a sharp band at 1725 cm^{-1} was attributed to C=O stretching of the carbonyl group. A strong peak appearing at 1067 cm^{-1} was attributed to C-O stretching and C-O stretching at 1067 cm^{-1} slightly shifted to 1066 cm^{-1} after synthesized. In addition, it was observed that FT-IR spectra of two structures of rhodamine were different, indicates that the structure has been changed in which open structure has completed change to a closed structure. The UV-Vis Spectroscopy results showed the absorbance at wavelength of 530-580 nm in which the open structure Rhodamine B had higher absorbance intensity than the closed structure. From the experimental results, it can be concluded that Rhodamine B/Polymer blend film can be developed and applied as an optical temperature indicator label material.

POL-P-076

Development of a National Standard for Tactile Rubber Flooring for Visually Impaired Persons

Chayapha Nimsuwan* and Pongdhorn Sae-Oui
National Metal and Materials Technology Center, Pathum Thani, 12120, Thailand

Keywords: National standard, Tactile rubber flooring, Visually impaired persons

Tactile rubber flooring is a rubber product that has distinguishable tactility and color from the surrounding surface, specially designed for visually impaired persons. Despite its widespread use in Thailand, there was no national standard for quality control of this product. This project was therefore carried out to establish Thai Industrial Standard for the tactile rubber flooring for visually impaired persons by gathering information from the existing international standards and the involved parties, e.g., manufacturers, users, and academic experts. Nine tactile rubber flooring samples from four makers were collected from the market and tested. By analyzing the test data, the standard draft was made and the product specification was considered and approved by the involved parties. According to the study, this product shall have a hardness ranging from 65 Shore A to 94 Shore A with a minimum tensile strength of 6 MPa and 10 MPa for indoor and outdoor applications, respectively. It shall be durable (volume loss after abrasion resistance test ≤ 400 mm^3), non-slippery (wet skid resistance ≥ 24), and flame-resistant for indoor applications (HB Class according to UL-94). In addition, it shall have sufficiently high visual contrast, compared to adjacent surface, and possess high weathering resistance for outdoor applications with a maximum ΔL and ΔE using CIE L*a*b of 10% and 25%, respectively. The approved standard draft was subsequently submitted to the Thai Industrial Standards Institute (TISI) for consideration and implementation. Finally, the standard draft was published in the Royal Gazette as TIS 3011-2562 Tactile rubber flooring for visually impaired persons in March 2020.

POL-P-079

Assessment of Fresh Natural Rubber Latex Putrefaction Using Resazurin Reduction Test

Chayanoot Kositanont*, Preeyawis Na Ubol, Panthakan Taengkhiaw, Chaveewan Kongkaew
National Metal and Materials Technology Center, Pathum Thani, 12120, Thailand
*chayanoot.kos@mtec.or.th

Keywords: Natural Rubber Latex, Resazurin, Putrefaction

Fresh natural rubber latex tapped from the *Hevea Brasiliensis* tree is spoiled by micro-organism activity and can remain liquid for not over 6-8 hours. The Resazurin reduction test was applied to estimate an ease of the fresh latex putrefaction. The observed color at a specific temperature and time after mixing latex with the dye was related to the number of micro-organisms in the latex and then the latex quality could be determined. Moreover, the latex samples with VFA (Volatile fatty acid) numbers higher than the threshold value could be specified by using this method. This new latex putrefaction assessment method is aimed to use at fresh latex collection centers in the community. The method is less complicated and takes less time when compared to the conventional total plate count and VFA number methods.

POL-P-084

Effect of Crosslinking Agents on Properties and Oil-Painting Cleaning Efficacy of Poly(vinyl alcohol) Gel

Watsachon Leksomboon[a], Duangdao Aht-Ong[b,c], Pichayada Katemake[a], Kamonwan Pacaphol[a*]

[a]*Department of Imaging and Printing Technology, Faculty of Science, Chulalongkorn University, Pathumwan, Bangkok, 10330, Thailand*

[b]*Department of Materials Science, Faculty of Science, Chulalongkorn University, Pathumwan, Bangkok, 10330, Thailand*

[c]*Center of Excellence on Petrochemical and Materials Technology, ChulalongkornUniversity, Pathumwan, Bangkok, 10330, Thailand*

*Kamonwan.p@chula.ac.th

Keywords: Cultural Heritage, Cleaning Gels, Poly(vinyl alcohol), Crosslinking Agents.

Artifacts created by our ancestors are irreplaceable, that should be preserved for future generations. The professionalized management of cultural heritage has not seriously occurred in underdeveloped countries until relatively recently. Oil-painting cleaning in these countries simply uses cotton swabs with liquid solvents; however, the liquid causes swelling of the art surface, resulting in permanent damage to the artwork. In this research, 4 wt% of poly(vinyl alcohol) (PVA) with an average molecular weight of about 146,000 $g.mol^{-1}$ was selected based on suitable viscoelasticity of gel to produce polymer gel as a cleaning material. Three different crosslinking agents, *i.e.*, sodium tetraborate (borax), borax plus polyethylene glycol (borax-PEG), and glutaraldehyde (GA), at various concentrations were used to determine the optimal formulation of PVA gel. Firstly, the formulation of PVA gel providing the highest degree of water swelling from each kind of crosslinking agent was selected for studying methods of gel formation. Secondly, three formation methods, I. conventional casting, II. casting plus freeze-thawing, and III. casting plus freeze-thawing and solvent, were employed to study the effect of the formation methods on morphology, crystallinity, and viscoelasticproperties (storage and loss modulus) of the PVA gel. These properties of the gel are essential for the application of the cleaning gel and the final cleaning efficacy on a substrate. According to morphology results, two PVA gels crosslinked with borax and borax-PEG showed a significant increase in porosity after freeze-thawing by method II and had a high absorption of polar solvent according to swollen structures by method
III. The best formulation of these two gels was 10 wt% borax and 5 wt% borax plus 0.5 wt% PEG, respectively. In contrast, low porosity and poor swelling were found on the PVA gel crosslinked with GA. Interestingly, the freeze-thawing process significantly improved the crystallinity of the PVA gels which increased in all samples formed by method II, especially in the borax sample where the crystallinity increased from 32 to 51%. However, the borax-PEG sample displayed a more suitable storage modulus (in the range of 1-10 kPa) and tanδ(in the range of 0.2-0.7) under 0.1-10 Hz than the borax sample. These property ranges are typically required for the cleaning gel application due to easily peeling, without the gel residue being left on a substrate. The cleaning efficacy of the PVA gels was evaluated by Infrared False Color photography (IRFC), a part of technical photography, to detect a stain of artificial soil left on the oil- painting surface after cleaning. The borax-PEG sample was more effective in cleaning efficacy on oil (alkyd) painting than other gels. These findings show the feasibility of the use of PVA crosslinked with 5 wt% borax plus 0.5 wt% PEG and formed by the casting plus freeze-thawing and solvent as a cleaning gel for oil-painting conservation.

MATERIALS TESTING AND RELIABILITY

TES-I-01

Nanoscale Stress Distribution and Crack Propagation in Rubber-Based Nano-Composites under Stretching

Hiroshi Jinnai[a,*]

[a]*Institute of Multidisciplinary Research for Advanced Materials, Tohoku University, 2-1-1 Katahira, Aoba-ku, Sendai, Miyagi 980-8577, Japan*

*E-mail address: hiroshi.jinnai.d4@tohoku.ac.jp

Keywords: Nanoparticle-filled rubber, Tensile deformation, Tensile strain, Stress pathway, Transmission electron microscopy, Nanoscale observation, FEM simulation

Nanoparticle-filled cross-linked rubber under tensile deformation was observed in situ by transmission electron microscopy (TEM), and the spatial distributions of the local maximum and minimum principal strains (ε_{max} and ε_{min}) under tensile deformation were experimentally determined. The local ε_{max} showed that deformation behavior depends heavily on the local structures and their spatial arrangements. Additionally, significantly deformed rubbery regions appeared along a network consisting of silica aggregates (silica-aggregate network). The finite element method (FEM) was applied to a series of TEM images under tensile deformation to simulate the structural changes, principal strains, and von Mises stress. The simulated morphology and ε_{max} were in excellent agreement with the experimentally-obtained morphology and strain. The simulated von Mises stress distribution, obtainable only from the experimentally-results-based-FEM, revealed that significant stress propagates along the silica-aggregate network parallel to the tensile direction. This result suggests that the silica-aggregate network may be primarily responsible for providing mechanical strength to the nanoparticle-filled rubber under deformation. Because the stress concentrates along the silica-aggregate networks, cavities appeared along these "stress pathways." The present study would pave the way to understanding the microscopic factors determining the macroscopic mechanical properties of rubber nanocomposites mainly used for automobile tires and seismic isolation rubber.

TES-I-02

Probing Micro Nano and Atomic Structures of Material with Synchrotron X-Rays

Supagorn Rugmai[a,*], Siriwat Soontaranon[a], Nuntaporn Kamonsutthipaijit[a], Sirinart Chio-Srichan[a], Cateleya Rojviriya[a], Phakkhananan Pakavanit[a]
[a]Synchrotron Light Research Institute (Public Organization), Mueang, Nakhon Ratchasima, 30000, Thailand
*supagorn@slri.or.th

Keywords: Synchrotron radiation, Small angle x-ray scattering, Wide angle x-ray scattering, X-ray Tomographic Microscopy

Synchrotron radiation provides high intensity photons covering wide range of energies from infrared to x-ray. High intensity x-rays from a synchrotron light source is particularly useful for multi-level structural studies of various types of material. Micro structures can be probed using X-ray Tomographic Microscopy (XTM) technique, which utilization of synchrotron x-ray enables high resolution 3-dimentional x-ray images of the sample. In nano scale synchrotron Small Angle X-ray Scattering (SAXS) is one of the important techniques used to investigate material structures. SAXS can give valuable information ranging from shape and size distribution of nano particles and macro molecules to molecular arrangement in polymeric materials. Combining with an efficient optimization code, SAXS data can be used to model molecular arrangement and nano structures of wide range of systems. With the same instrument, synchrotron Wide Angle X-ray Scattering (WAXS) gives atomic scale information related to crystalline or semi-crystalline structures in materials, soft matter and biological samples. Simultaneous SAXS/WAXS setup at a synchrotron beamline can therefore yield structural information from nano to atomic scale in a single measurement. Combining XTM, SAXS/WAXS can therefore give structural information covering micro nano and atomic scale. Flexibility of synchrotron experimental station also enables various in-situ studies in which dynamic structural changes can be probed.

TES-O-010

Optimizing Process Conditions and Ensuring End Product Requirements of Polymers with Rheological Analysis

Fabian Meyer[a,*], **Nate Crawford**[a]
[a]*ThermoScientific, Karlsrule, 76227, Germany*
*fabian.meyer@thermofisher.com

Keywords: Polymers, Viscoelasticity, Processing, Extensional test

A good knowledge of the viscoelastic properties of a polymer material is essential to optimizing formulations and blends as well as to adapt a process to the properties of a given material. To understand how polymer melts deform and flow. The different rheological tests can explain how the obtained results relate to different processing condition and final product properties. Rheological tests can be utilized to investigate the viscoelastic behavior of polymers from the melt-state to the solid-state. It can be used not only to optimize processing conditions and the final product performance, but also to establish structure property relationships. This is the reason why rheological test are commonly used in analytics for polymeric fluids in industry as well as academia.

TES-O-011

Introduction of JEOL Latest Ultrahigh Resolution FESEM and Its Capability of Chemical State Analysis

Tan Teck Siong
JEOL Asia Pte Ltd, 2 Corporation Road, #01-12 Corporation Place, 618494, Singapore
Tel: +65-65659989, Mobile: +65-96701794
Email: tstan@jeolasia.com.sg

The unique features of JEOL latest FESEM, JSM-IT800SHL will be introduced and presented. These features include 3 years warranty of emitter, low vacuum mode to handle non-conductive specimens, magnetic samples handling, full integration of FESEM and EDX, etc. In addition, with the attachment of soft X-ray spectrometer, the performance of the FESEM is further enhanced to provide chemical state analysis and Lithium element detection. An analysis report that identify if Silicon is present in crystalline or amorphous states is presented.

TES-O-050

Characterization of 3D Printed-Part and AISI 316L Conventional Stainless Steel Pipe Jointed by TIG Welding

Niwat Kunawong[a,*], Bovornchok Poopat[a], Viboon Saetang[a]
[a]*Department of Production Engineering, Faculty of Engineering, King Mongkut's University of Technology Thonburi, Bangkok, 10140, Thailand*
*niwat.kun@kmutt.ac.th

Keywords: Additive Manufacturing, WAAM, Dissimilar Welding, Pipe Welding

Wire and arc additive manufacturing (WAAM) is a 3D metal printing based on arc welding process which can reduce part cost and produce complex shape that cannot be obtained by conventional processing. Sometimes the joining of 3D printed parts with other 3D printed parts or conventionally produced parts is required and control the characteristics of the welded components that may affect the service requirements is very importance. In this work, circular wall 3D printed was prepared by welding electrode ER316L stainless steel wire based on arc welding, then welded to wrought pipe AISI 316L with same thickness by manual TIG welding. The microstructure and mechanical properties of welded joint were investigated according to ASME IX for verify compatibility of materials and techniques able to produce welded components have acceptable mechanical properties. For the welding conditions is used, the fracture occurred at 3D printed part with tensile strength met acceptance criteria.

TES-O-054

Synthesis and Characterization of Cesium Iodide Thin Film for Radiation Detection

Pariwat Limthanameteekul[1] , Phannee Saengkaew[1*], Mati Horprathum[2], Tossaporn Lertvanithphol[2*] and Tuksadon Wutikhun[3]

[1]Department of Nuclear Engineering, Faculty of Engineering, Chulalongkorn University, Bangkok, 10330, Thailand

[2]National Electronic and Computer Technology Center (NECTEC), National Science and Technology Development Agency, Ministry of Science and Technology, Pathumthani, Thailand

[3]National Nanotechnology Center (NANOTEC), National Science and Technology Development Agency, Ministry of Science and Technology, Pathumthani, Thailand

[*]E-mail address corresponding author**:** phannee.s@chula.ac.th

Keywords: CsI thin films, Optoelectronic devices, Radiation detector, Sputtering deposition

To develop Cesium Iodide (CsI) -based optoelectronic devices on Si substrates, CsI films were investigated for good crystalline quality and suitable optical and electrical properties. Under an optimized growth condition by RF-magnetron sputtering technique, the CsI films were grown at a pressure of 10 mTorr in argon atmosphere and a variation of a sputtering power of 10, 30 and 50 W in order to achieve an optimized sputter power for the deposition of the CsI films without extra post-annealing. At the sputter power of 50 W for 1 hour, the shiny films were deposited on both Si-substrate and glass substrate with yellowish mirror-like surfaces. To characterize the crystal structure and quality, XRD measurements were performed in a grazing incidence mode showing the typical XRD pattern of BCC-structure of CsI crystal as the reflection planes as (110), (200), (211), (220), (310) and (222), the most dominant reflection of (110) and (211) for the second one and having a lattice constant of 4.567±0.001 Å with a very small strain. By cross-sectional SEM measurements to exhibit the morphology and examine the thickness of grown CsI thin films, it found that the film layer with a thickness of about 200 nm was fully deposited covering the Si substrate by growing at the sputtering power of 50 W. Meanwhile, the CsI film was obtained with very thin and low crystalline quality at the power of 30 W. But the CsI film could not be observed and many CsI islands or clusters could be found at the power of 10 W. Furthermore, the optical properties of grown CsI films will be analyzed by UV-Vis spectrophotometry and Photoluminescence measurements to find out the emission wavelength of these grown films. Finally, to develop CsI-based optoelectronic or diode-structure devices, the n-type CsI and p-type CsI films will be investigated and characterized by Hall-Effect measurements to evaluate the electrical properties of the CsI films in further experiments.

.

TES-O-130

Influence of Stabilization Heat Treatment on Sensitization Microstructure of ASTM A 312 TP316Ti Stainless Steel Welded Joints

Niwat Kunawong[a,*], Bovornchok Poopat[a], Somporn Peansukmanee[a]
[a]Department of Production Engineering, Faculty of Engineering, King Mongkut's University of Technology Thonburi, Bangkok, 10140, Thailand
*niwat.kun@kmutt.ac.th

Keywords: 316Ti, Sensitization, Stabilization, Chromium Carbide Precipitation

Austenitic stainless steels tend to form chromium depleted zones at the grain boundaries during welding and heat treatment to produce an area depleted in chromium and becomes susceptible to intergranular corrosion. Some stabilizing elements were used in extreme conditions, such as oil refineries and petrochemical plants industrial furnaces operating at high temperatures. Welding following solution treatment and stabilization is an optional welding procedure that is adopted only when attention to avoid sensitization during welding fabrication or service in sensitizing temperature range. An experimental study was carried out to study the susceptibility to the intergranular corrosion of stabilization post weld heat treatment and as-welded condition by gas tungsten arc welded (GTAW) 316Ti stainless steel (SS) joints. Both of as-weld and stabilized condition were sensitized when aged between sensitizing temperature range 600, 700, 800, 900 °C and held soaking times for 1,000 hours. Microstructure evaluations of the sensitized sample has been investigated by optical microscope and SEM analysis were used for assessment the precipitate of chromium carbide at grain boundary in heat affected zone (HAZ) of welded joint.

TES-O-132

Investigation of Bond Strength of Welded Coatings using Scratch Test Technique

H. Koiprasert*, P. Kunsuwan, C. Sukhonkhet, P. Sheppard, E. Viyanit
Rail and Modern Transports Technology Research Center (RMT), National Science and Technology Development Agency
*Corresponding author's E-mail address: Hathaipat.koi@nstda.or.th

Scratch test technique is widely used for an evaluation of bond strength of thin coatings. Scratch indenter is drawn on the coating surface with increasing load. Several research suggested the scratch test according to ISO/WD 27307 for investigated bond strength of thermal spray coating. They expect to use the scratch test to replace pull-off test. Scratch test was simpler experimental set-up, and a special glue was unnecessary for this method. The scratch indenter was dragged with constant load along the cross-section of the coating. This testing is a comparative method. A cone area and crack in the coating defined cohesion and crack at substrate-coating interface defined adhesion. A welded coatings had higher bond strength which could not be measured for the bond strength with pull-off test. Scratch test became an alternative bond strength testing method. This research used scratch test to investigate bond strength of Fe-based materials coated on high carbon steel. Shielded Metal Arc Welding (SMAW), Flux-Cored Arc Welding (FCAW) and Laser Cladding were used as the coating techniques. The scratch test was performed on the cross-sectional of a specimen under variable level of constant loads of 15, 30, 45 and 90 N. Without visible crack at the substrate-coating interface and inside the scratch track which indicated that adhesion strength at the substrate-coating interface could not be destroyed with the scratch load 15-90N. SMAW coating had the highest cone area value which means the lowest cohesion strength of these coatings. The scratch load lower than 45 N, the FCAW coating, and laser cladding coating had the similar cone area value. At the load 45N onwards, the FCAW coating had lowest cone area value.

Conference Seretariat

National Metal and Materials Technology Center
114 Thailand Science Park, Pahonyothin Rd., Khlong Neung,
Khlong Luang, Pathum Thani 12120, Thailand
Tel. +66-2564-6500 ext.4680
E-mail: tpr-hms@mtec.or.th

www.mtec.or.th/msat-11